arXiv:hep-th/9902103v2 17 Feb 1999

# INAUGURAL-DISSERTATION

**zur**
**Erlangung der Doktorwürde**
**der**
**Naturwissenschaftlich-Mathematischen**
**Gesamtfakultät**
**der**
**Ruprecht-Karls-Universität**
**Heidelberg**

vorgelegt von
**Dipl.-Phys. Elena Gubankova**
aus Moskau

Tag der mündlichen Prüfung: 1. Juli 1998

# FLOW EQUATIONS
# FOR THE QUANTUM ELECTRODYNAMICS
# ON THE LIGHT-FRONT

**Gutachter: Prof. Dr. Franz Wegner**
**Prof. Dr.Hans-Christian Pauli**

## Abstract

The method of flow equations is applied to QED on the light front. Requiring that the particle number conserving terms in the Hamiltonian are considered to be diagonal and the other terms off-diagonal an effective Hamiltonian is obtained which reduces the positronium problem to a two-particle problem, since the particle number violating contributions are eliminated.

Using an effective electron-positron Hamiltonian, obtained in the second order in coupling, we analyze the positronium bound state problem analytically and numerically. The results obtained for Bohr spectrum and hyperfine splitting coincide to a high accuracy with experimental values. The rotational invariance, that is not manifest symmetry on the light-front, is recovered for positronium mass spectrum.

Except for the longitudinal infrared divergences, that are special for the light-front gauge calculations, no infrared divergences appear. The ultraviolet renormalization in the second order in coupling constant is performed simultaneously. To preserve boost invariance we take into account the diagrams arising from the normal ordering of instantaneous interactions. Using flow equations and coupling coherence we obtain the counterterms for electron and photon masses, which are free from longitudinal infrared divergences.

## Abstrakt

In dieser Arbeit wird die Methode von Flußgleichungen im Lichtkegel-Formalismus auf die QED angewandt. Wir konstruieren einen effektiven, block-diagonalen Hamiltonian, wobei wir fordern, daß diejenigen Terme, welche die Teilchenzahl erhalten, diagonal sind, während alle anderen Terme nichtdiagonal sind. Dieser effektive Hamiltonian vereinfacht das Positronium-Problem auf ein Zweikörper-Problem, weil die Anteile, die eine Teilchenzahländerung verursachen, eliminiert sind.

Mittels des effektiven Elektron-Positron-Hamiltonians, der in der elektromagnetischen Kopplung von zweiter Ordnung ist, werden die Bindungszustände des Positroniums analytisch und numerisch untersucht. Unsere Resultate für das Bohr-Spektrum und die Hyperfeinaufspaltung stimmen sehr gut mit den experimentellen Werten überein. Die Rotationsinvarianz, welche auf dem Lichtkegel nicht mehr gewährleistet ist, kann für das Massenspektrum wieder hergestellt werden.

Außer longitudinalen Infrarot-Divergenzen, die für die Lichtkegel-Eichung spezifisch sind, treten bei den Rechnungen keine Infrarot-Divergenzen auf. Die Renormierung der Ultraviolet-Divergenzen bis zur zweiten Ordnung in der Kopplungskonstanten erhält man mit der Konstruktion des Hamiltonians automatisch. Um die Invarianz des renormierten Hamiltonian unter Boosts sicherzustellen, berücksichtigen wir auch die Diagramme, welche aus der Normalordnung von instantanen Wechselwirkungen entstehen. Die aus den Flußgleichungen und der Kopplungskohärenz resultierenden Counterterme der Photon- und Elektronmasse erhalten dann keine longitudinalen Infrarot-Divergenzen.

# Contents

**1 Introduction 6**

**2 Flow equations 8**
2.1 Flow equations for Hamiltonian matrices . . . . . . . . 8
2.2 Similarity transformation . . . . . . . . 9
2.3 Flow equations for solid state physics . . . . . . . . 11
2.4 Flow equations in field theory . . . . . . . . 11

**3 Light-front field theory 14**
3.1 Introduction . . . . . . . . 14
3.2 Preceding work . . . . . . . . 15
3.2.1 Models and methods in the light-front field theory . . . . . . . . 15
3.2.2 Results for light front $QED_{3+1}$ . . . . . . . . 16
3.3 Canonical QED Hamiltonian . . . . . . . . 18
3.3.1 Canonical light-front $QED_{3+1}$ Hamiltonian . . . . . . . . 18
3.3.2 QED Hamiltonian in second quantization . . . . . . . . 21

**4 Hamiltonian bound state problem on the light-front 23**
4.1 Introduction . . . . . . . . 23
4.2 Flow equations in the perturbative frame . . . . . . . . 24
4.3 Effective low-energy Hamiltonian . . . . . . . . 26
4.3.1 Effective electron-positron interaction . . . . . . . . 26
4.3.2 Positronium model (general computational strategy) . . . . . . . . 31
4.3.3 Effective, renormalized QED Hamiltonian . . . . . . . . 32

**5 Positronium spectrum (analytically) 35**
5.1 Bound state perturbative theory (BSPT) . . . . . . . . 35
5.2 Effective electron-positron interaction in light-front and instant frames . . . . . 38
5.3 Positronium's ground state spin splitting . . . . . . . . 40

**6 Positronium spectrum (numerically) 45**
6.1 Light-front bound state equation . . . . . . . . 45
6.2 Brodsky-Lepage prescription of the light-front dynamics: effective electron-positron interaction . . . . . . . . 47
6.2.1 First and second order solutions of the flow equations . . . . . . . . 47
6.2.2 Effective electron-positron interaction . . . . . . . . 49
6.3 Mass spectrum and wave functions of positronium . . . . . . . . 55

**7 Renormalization in the light-front QED 58**
7.1 Introduction. . . . . . . . . . . . . . . . . . . . . . . . . . . . . . . . . . . . . 58
7.2 Flow equations for renormalization issues . . . . . . . . . . . . . . . . . . . . . 61
7.3 Mass renormalization . . . . . . . . . . . . . . . . . . . . . . . . . . . . . . . . 68

**8 Conclusions and outlook 70**

**A Calculation of the commutator $[\eta^{(1)}(l), H_{ee\gamma}]$ in the electron-positron sector 72**

**B Matrix elements of the effective interaction.Exchange channel 76**
B.1 The general helicity table. . . . . . . . . . . . . . . . . . . . . . . . . . . . . . 77
B.2 The helicity table for arbitrary $J_z$. . . . . . . . . . . . . . . . . . . . . . . . . . 79

**C Fermion and photon self energy terms 81**

**Bibliography 85**

**List of Figures 88**
Figure 1: Block-diagonalization of Hamiltonians . . . . . . . . . . . . . . . . . . 89
Table 1: Effective light-front QED Hamiltonian . . . . . . . . . . . . . . . . . . . 90
Figure 2: Matrix elements of the effective Hamitonian . . . . . . . . . . . . . . . . 91
Figure 3: Effective electron-positron interaction . . . . . . . . . . . . . . . . . . . 93
Figure 4: Effective electron-positron interaction (another choice of coordinates) . . . . 94
Figure 5: Positronium spectrum . . . . . . . . . . . . . . . . . . . . . . . . . . . 95
Figure 6: Stability of positronium spectrum . . . . . . . . . . . . . . . . . . . . . 96
Figure 7: Deviation of corresponding eigenvalues for $J_z = 0$ and $J_z = 1$ . . . . . . . . 97
Figure 8: Electron self energy . . . . . . . . . . . . . . . . . . . . . . . . . . . . 98
Figure 9: Photon self energy . . . . . . . . . . . . . . . . . . . . . . . . . . . . . 99

**Acknowledgments 100**

# Chapter 1

# Introduction

Quantum chromodynamics (QCD) is widely accepted as the microscopic theory of strong interaction, where quarks and gluons are considered as the elementary degrees of freedom. But we are still unable to solve this theory on the macroscopic level (in the low energy domain) and to obtain an accurate description of the structure of hadrons, which are the strongly interacting particles observed in nature.

A central goal of modern theoretical particle physics is to build a bridge between microscopic (high energy) and macroscopic (low energy) domains of QCD.

At the microscopic level the theory is defined completely, and no further development seems to be necessary. On the other side, when it comes to the macroscopic hadron world, there is no rigorous way to calculate hadron properties immediately from QCD. One still has to resort to different phenomenological methods and QCD-inspired models of covariant field theory to calculate the hadron mass spectrum, form factors, wave functions, *etc.* Also lattice calculations serving as a model-independent method in covariant field theory improved our understanding of the hadronic structure. However, besides different problems, this approach is still strongly limited by the available computer power.

In this work we use the light-front formulation of field theory, which is best suited for solving relativistic bound state problems in QCD [1], because of the simplified vacuum structure. We believe that light-front field theory together with the renormalization group approach for Hamiltonians [2],[3] provides a good strategy to reach the above mentioned goal. The physical idea behind this approach is to use the renormalization concept for Hamiltonians on the light-front to get an effective, low-energy Hamiltonian.

Recently, Glazek and Wilson suggested the renormalization scheme for Hamiltonians, called similarity renormalization by the authors, where they developed a renormalization group and the basic elements of renormalization group calculations for Hamiltonians on the light-front [3]. An alternative approach for Hamiltonian renormalization, the method of flow equations, was proposed by Wegner [2]. It is common for both methods that they renormalize the canonical Hamiltonian of light-front field theory to a given order of perturbation theory. A basic advantage of the method of flow equations in comparison to the similarity renormalization scheme is that one obtains an effective, renormalized Hamiltonian for a limited (truncated) Fock space.

The method of flow equations is based on the following idea: performing a set of infinitesimal unitary transformations, with the condition that the particle number conserving terms in the Hamiltonian are considered to be diagonal and the other terms off-diagonal, it is possible to get the block-diagonal effective Hamiltonian, where the particle number in each block is conserved. This reduces the bound state problem to a few-body problem, since the particle number violating contributions are eliminated. This procedure is similar to the Tamm-Dancoff space truncation [33] in the sense that also in this truncation particle number changing interactions are eliminated. The effective Hamiltonian constructed by flow equations is automatically renormalized to the given order in the coupling constant, since an elimination of particle number changing sectors can not be achieved in one step but rather sequently for transition amplitudes from large to small energy differences.

Low-energy QCD is challenging and explicit calculations become complicated due to the nonperturbative nature of this theory. To test and to illustrate our approach we consider $QED_{3+1}$ in the light-front dynamics and investigate the corresponding positronium bound state problem.

This work is organized as follows: In chapter 2 we outline the theoretical framework by giving the key ingredients of the flow equation method and by enumerating their applications to problems of solid state physics and statistical mechanics done so far. The approach of similarity renormalization is also considered. In chapter 3 we review the methods and results known for light-front $QED_{3+1}$. To second order in the coupling constant we obtain the effective, renormalized QED Hamiltonian (chapter 4), which reduces the positronium problem to a two-particle problem to be analyzed further analytically (chapter 5) and numerically (chapter 6) for positronium bound states. The renormalization issues of light-front QED are considered in chapter 7.

# Chapter 2

# Flow equations

In this section we give the key ingredients of flow equations method and set up the framework to use flow equations for the problems of high-energy physics.

Flow equations are introduced in order to bring Hamiltonians closer to diagonalization. The method is based on the numerical recipe by Jacobi, consisting of unitary transformations between two states which makes the connecting off-diagonal matrix elements vanishing. If this is repeated for all off-diagonal matrix elements again and again then the off-diagonal matrix elements will become arbitrarily small. It is characteristic for these equations that matrix elements between degenerate or almost degenerate states do not decay or decay very slowly. In the next section we follow the original work of Wegner [2] to introduce flow equations for Hamiltonian matrices.

## 2.1 Flow equations for Hamiltonian matrices

The aim is to find continuous unitary transformation, that brings Hamiltonian to diagonalization. Continuous unitary transformation depend on the flow parameter $l$. We call it $U(l)$. In what follows we assume that $U(0) = 1$ is valid and that $U(\infty)$ brings the given Hamiltonian operator $H$ or the given matrix $H$ to the diagonal form. The operator $H$ acquires the $l$-dependence through the unitary transformation $U(l)$

$$H(l) = U^{+}(l) H U(l) \tag{2.1}$$

If the transformation $U(l)$ were known, one would find $H(\infty)$ and the problem would be solved. Generally, one does not know the transformation, which diagonalizes the given matrix. Therefore the transformation is formulated in infinitesimal form

$$\frac{dH(l)}{dl} = [\eta(l), H(l)] \tag{2.2}$$

Here $\eta$ is the generator of transformation; $\eta$ is antihermitian $\eta^{+} = -\eta$. The connection between the unitary transformation and its generator is given

$$U(l) = exp\left(\int_0^l \eta(l')dl'\right) \tag{2.3}$$

where the ordering along 'l-axis' is imposed. One has for the matrix elements

$$\frac{dh_{k,q}(l)}{dl} = \sum_p (\eta_{k,p}(l) h_{p,q}(l) - h_{k,p}(l)\eta_{p,q}(l)) \tag{2.4}$$

The generator $\eta$ must be chosen in a way, that the matrix $H$ is more and more diagonal as $l$ increases. We demand, that $\sum_{k\neq q} h_{k,q}^2$ falls monotonously. We separate $H = H_d + H_r$ and use that use that $TrH^2$ is invariant under the unitary transformation

$$TrH_d^2 + TrH_r^2 = TrH^2 = const \tag{2.5}$$

$\sum_{k\neq q} h_{k,q}^2 = TrH_r^2$ monoton falls when $TrH_d^2$ increases. One has

$$\frac{dTrH_d^2}{dl} = \frac{d}{dl}\sum_q h_{q,q}^2 = 2\sum_q h_{q,q}\sum_p(\eta_{q,p}h_{p,q} - h_{q,p}\eta_{p,q}) = 2\sum_{p,q}\eta_{p,q}h_{p,q}(h_{p,p} - h_{q,q}) \tag{2.6}$$

The right hand side must be negative. The possible choice for the generator is $\eta_{p,q} = h_{p,q}(h_{p,p} - h_{q,q})$ or

$$\eta = [H_d, H_r] \tag{2.7}$$

We have

$$\begin{aligned}
\frac{dh_{k,q}(l)}{dl} &= \sum_p (h_{k,k}(l) + h_{q,q}(l) - 2h_{p,p}(l))h_{k,p}(l)h_{p,q}(l) \\
\frac{d}{dl}\sum_{k\neq q} h_{k,q}^2 &= -\frac{d}{dl}\sum_k h_{k,k}^2 = -2\sum_{k,q}(h_{k,k} - h_{q,q})^2 h_{k,q}^2 = -2\sum_{k,q}\eta_{k,q}^2
\end{aligned} \tag{2.8}$$

Since $\sum_{k\neq q} h_{k,q}^2$ falls monotonously and is restricted from below, the derivative must vanish in the limit $l \to \infty$. Therefore one has

$$\eta(l) = [H_d, H] \to_{l\to\infty} 0 \tag{2.9}$$

Practically we have reached the aim, the matrix commute with its diagonal part as $l \to \infty$. The eqs. (2.2) and (2.9) are called flow equations for Hamiltonians and are the basis for the work presented further.

## 2.2 Similarity transformation

Another method to diagonalize Hamiltonians continuously was suggested independently by Glazek and Wilson [3], which has been called similarity transformation by the authors. In this subsection we follow the original work of Glazek and Wilson [3] to give the key ingredients of this scheme.

We define the unitary transformation, that brings the Hamiltonian operator in a form, where no transitions between the states with energy difference larger than $\lambda$ are present. The role of 'flow parameter' plays $\lambda$, which corresponds to the ultraviolet (UV)-cutoff (see chapter 7) and is changed continuously.

The Hamiltonian operator $H_\lambda$ (and other quantities) depend then on the continuous parameter $\lambda$. The Hamiltonian is given as a sum $H_\lambda = H_{0\lambda} + H_{I\lambda}$, where $H_{0\lambda}$ is the free Hamiltonian and $H_{I\lambda}$ contains (not renormalized) interactions and counterterms.

We separate each matrix $M$ into two parts, $M = D(M) + R(M)$. Let $E_{i\lambda}$ are the eigenvalues of $H_{0\lambda}$, and

$$\begin{aligned}
x_{ij\lambda} &= \frac{|E_{i\lambda} - E_{j\lambda}|}{E_{i\lambda} + E_{j\lambda} + \lambda} \\
u_{ij\lambda} &= u(x_{ij\lambda}), \quad r_{ij\lambda} = 1 - u_{ij\lambda} = r(x_{ij\lambda})
\end{aligned} \tag{2.10}$$

and $u(x)$ is the function, which is 1 for small arguments and vanishes for large arguments. Explicit one can choose for $u(x)$

$$\begin{aligned}
&u(x) = 1 \ \ for \ \ 0 \leq x \leq \frac{1}{3} \\
&u(x) \ falls \ monotonously \ from \ 1 \ to \ 0 \ for \ \frac{1}{3} \leq x \leq \frac{2}{3} \\
&u(x) = 0 \ \ for \ \ \frac{2}{3} \leq x \leq 1
\end{aligned} \tag{2.11}$$

We define $D(M)_{ij} = u_{ij\lambda} M_{ij}$ and corresponding $R(M)_{ij} = r_{ij\lambda} M_{ij}$. As we introduce $u_{ij\lambda}$ and $r_{ij\lambda}$, we have the continuous transition between $D(M)$ and $R(M)$. It is important in order to avoid the divergences in renormalization equations. When one chooses $u(x) = \theta(x_0 - x)$, then one has the original definition for $D(M)$ and $R(M)$. The continuous transformation for Hamiltonian operator can be written as before in the form

$$\frac{dH_\lambda}{d\lambda} = [\eta_\lambda, H_\lambda] \tag{2.12}$$

The generator $\eta_\lambda$ is chosen in a way that $D(H_\lambda) = H_\lambda$. For practical purpose to distinguish in the calculations between the Hamiltonian operator $H_\lambda$ and its 'D'-part, it is useful to introduce the operator $Q$, such that

$$H_\lambda = D(Q_\lambda) \tag{2.13}$$

Then one has for the matrix elements

$$\frac{du_{ij\lambda}}{d\lambda} Q_{ij\lambda} + u_{ij\lambda} \frac{dQ_{ij\lambda}}{d\lambda} = \eta_{ij\lambda}(E_{j\lambda} - E_{i\lambda}) + [\eta_\lambda, H_{I\lambda}]_{ij} \tag{2.14}$$

One is not able to find $Q_\lambda$ and $\eta_\lambda$ from this equation. The reason is, that for the given $\lambda$ the Hamiltonian operator $H_\lambda$ can be additionally transformed unitary without breaking the condition $D(H_\lambda) = H_\lambda$. Thus one has one more condition. We rewrite the above equation in the form

$$u_{ij\lambda} \frac{dQ_{ij\lambda}}{d\lambda} - \eta_{ij\lambda}(E_{j\lambda} - E_{i\lambda}) = G_{ij\lambda} \tag{2.15}$$

where we define

$$G_{ij\lambda} = [\eta_\lambda, H_{I\lambda}]_{ij} - \frac{du_{ij\lambda}}{d\lambda} Q_{ij\lambda} \tag{2.16}$$

Now let

$$u_{ij\lambda} \frac{dQ_{ij\lambda}}{d\lambda} = D(G_\lambda)_{ij} \tag{2.17}$$

and

$$\eta_{ij\lambda}(E_{j\lambda} - E_{i\lambda}) = -R(G_\lambda)_{ij} \tag{2.18}$$

Now all functions are defined. One has

$$\eta_{ij\lambda} = \frac{r_{ij\lambda}}{E_{i\lambda} - E_{j\lambda}} \left( [\eta_\lambda, H_{I\lambda}]_{ij} - \frac{du_{ij\lambda}}{d\lambda} \frac{H_{ij\lambda}}{u_{ij\lambda}} \right) \tag{2.19}$$

and

$$\frac{dH_{ij\lambda}}{d\lambda} = u_{ij\lambda} [\eta_\lambda, H_{I\lambda}]_{ij} + r_{ij\lambda} \frac{du_{ij\lambda}}{d\lambda} \frac{H_{ij\lambda}}{u_{ij\lambda}} \tag{2.20}$$

There are no small energy denominators in these equations. These equations should be solved iteratively.

## 2.3 Flow equations for solid state physics

Flow equations were successfully applied to different systems in solid state physics. Unitary transformation in the form of exact diaginalization of Hamiltonian operator has been tested in
(1) model of impurity in the electron band [5];
(2) dissipative quantum systems, in particular for spin-boson problem [6];
(3) Lipkin model [7];
(4) problem of interacting electrons and phonons in a solid (referred to as BCS-theory) [10].
In all these models a system of interest couples to its environment Hamiltonian (for example, in (1) single impurity couples to the band of electrons; in (2) a small quantum system couples to the thermodynamical bath). The aim is then to decouple 'small' system from its 'large' environment to find a behavior of the system. It is different from what is usually done: most theoretical work starts off by tracing out the bath degrees of freedom and then using suitable approximation schemes for the time evolution of the reduced density matrix of the small quantum system. In general the approach of Hamiltonian diagonalization is particularly suited for studying low-energy properties of the system, thereby being complementary to most other approximation schemes.

In some cases the aim to get the diagonal Hamiltonian operator for $l \to \infty$ can not be reached. It was shown in the original work of Wegner [2] for the model of interacting fermions in one dimension, that a literal use of the concept of Hamiltonian diagonalization can lead to convergency problems. In the case discussed there the divergences appeared as $l \to \infty$. The way out, as proposed by Wegner [2], is to bring Hamiltonian operator instead of diagonal to the block-diagonal form, where the number of quasiparticles is conserved in each block.

In many cases it is enough to transform the given Hamiltonian to the block-diagonal form. In particular it is so, when the block, which describes the states of interest, can be treated further with other methods. There are many known transformations, that construct in this way from the initial Hamiltonian operator an effective Hamiltonian operator, acting in a smaller Hilbert space and which is simpler to consider. Flow equations, where block-diagonalization is performed, have been compared with the following transformations
(1) the Schrieffer-Wolff transformation, which reduces the Anderson model with single magnetic impurity to the Kondo problem [8];
(2) the Foldy-Wouthuysen transformation, which decouples the Dirac equation into two two-component equations, one of which gives in the nonrelativistic limit the known Pauli equation [9];
(3) the Fröhlich transformation, which constructs from the electron-phonon interaction an effective electron-electron interaction [10]. In all these cases flow equations re-examine the transformations used before.

## 2.4 Flow equations in field theory

In this section we set up the framework to use flow equations for the problems of high-energy physics. We remind, that flow equations perform the unitary transformation, which brings the Hamiltonian to a block-diagonal form with the number of particles (or Fock state) conserving in each block. In what follows we distinguish between the 'diagonal' (here Fock state conserving) and 'rest' (Fock state changing) sectors of the Hamiltonian. We break the Hamiltonian as

$$H = H_{0d} + H_d + H_r \tag{2.21}$$

where $H_{0d}$ is the free Hamiltonian; and the indices 'd','r' correspond to 'diagonal','rest' parts of the Hamiltonian, respectively. The flow equation for the Hamiltonian eq. (2.2) and the generator of unitary transformation eq. (2.7) are written [2]

$$\begin{aligned} &\frac{dH}{dl} = [\eta, H_d + H_r] + [[H_d, H_r], H_{0d}] + [[H_{0d}, H_r], H_{0d}] \\ &\eta = [H_{0d}, H_r] + [H_d, H_r] \end{aligned} \tag{2.22}$$

In the basis of the eigenfunctions of the free Hamiltonian

$$H_{0d}|i >= E_i|i > \tag{2.23}$$

one obtains for the matrix-elements between the many-particle states

$$\begin{aligned} &\frac{dH_{ij}}{dl} = [\eta, H_d + H_r]_{ij} - (E_i - E_j)[H_d, H_r]_{ij} - (E_i - E_j)^2 H_{rij} \\ &\eta_{ij} = (E_i - E_j)H_{rij} + [H_d, H_r]_{ij} \end{aligned} \tag{2.24}$$

The energy differences are given by

$$E_i - E_j = \sum_{k=1}^{n_2} E_{i,k} - \sum_{k=1}^{n_1} E_{j,k} \tag{2.25}$$

where $E_{i,k}$ and $E_{j,k}$ are the energies of the created and annihilated particles, respectively. The generator belongs to the 'rest' sector, i.e. $\eta_{ij} = \eta_{rij}, \eta_{dij} = 0$. In what follows we use

$$\begin{aligned} &[\hat{O}_r, \hat{H}_d]_d = 0 \\ &[\hat{O}_r, \hat{H}_d]_r \neq 0 \end{aligned} \tag{2.26}$$

where $\hat{O}_r$ is the operator from the 'rest' sector (for example $\hat{H}_r$ or $\hat{\eta}_r$) and $\hat{H}_d$ is the diagonal part of Hamiltonian.

For the 'diagonal' ($n_1 = n_2$) and 'rest' ($n_1 \neq n_2$) sectors of the Hamiltonian one has correspondingly

$$\begin{aligned} &\frac{dH_{dij}}{dl} = [\eta, H_r]_{dij} \\ &\frac{dH_{rij}}{dl} = [\eta, H_d + H_r]_{rij} - (E_i - E_j)[H_d, H_r]_{rij} + \frac{du_{ij}}{dl}\frac{H_{rij}}{u_{ij}} \end{aligned} \tag{2.27}$$

where we have introduced the cutoff function $u_{ij}(l)$

$$u_{ij}(l) = \mathrm{e}^{-(E_i - E_j)^2 l} \tag{2.28}$$

The energies $E_i(l)$ start to depend on the flow parameter $l$ in the second order of perturbation theory, that is taken into account by the renormalization of single-particle electron and photon energies (see chapter 7).

The main difference between these two sectors is the presence of the third term in the 'rest' sector $\frac{du_{ij}}{dl}\frac{H_{rij}}{u_{ij}}$, which insures the band-diagonal structure for the 'rest' part

$$H_{rij} = u_{ij}\tilde{H}_{rij} \tag{2.29}$$

i.e. in the 'rest' sector the matrix elements with the energy differences larger than $1/\sqrt{l}$ are suppressed. In the similarity renormalization scheme [3] the width of the band corresponds to the UV cutoff $\lambda$. The connection between the two quantities is given

$$l = \frac{1}{\lambda^2} \tag{2.30}$$

The matrix elements of the interactions, which change the Fock state, are strongly suppressed,if the energy difference exceeds $\lambda$, while for the Fock state conserving part of the Hamiltonian the matrix elements with all energy differences are present. As the flow parameter $l \to \infty$ (or $\lambda \to 0$) the 'rest' part is completely eliminated, except maybe for the matrix elements with $i = j$. One is left with the block-diagonal effective Hamiltonian.

Generally, the flow equations are written

$$\begin{aligned}
\frac{dH_{ij}}{dl} &= [\eta, H_d + H_r]_{ij} - (E_i - E_j)[H_d, H_r]_{ij} + \frac{du_{ij}}{dl}\frac{H_{ij}}{u_{ij}} \\
\eta_{ij} &= [H_d, H_r]_{ij} + \frac{1}{E_i - E_j}\left(-\frac{du_{ij}}{dl}\frac{H_{ij}}{u_{ij}}\right)
\end{aligned} \tag{2.31}$$

where the following condition on the cutoff function in 'diagonal' and 'rest' sectors, respectively, is imposed

$$\begin{aligned}
u_{dij} &= 1 \\
u_{rij} &= u_{ij}
\end{aligned} \tag{2.32}$$

One recovers with this condition the flow equations eq. (2.27) for both sectors. Other unitary transformations, which bring the Hamiltonian to the block-diagonal form, with the Fock state conserving in each block are used [3]

$$\begin{aligned}
\frac{dH_{ij}}{d\lambda} &= u_{ij}[\eta, H_d + H_r]_{ij} + r_{ij}\frac{du_{ij}}{d\lambda}\frac{H_{ij}}{u_{ij}} \\
\eta_{ij} &= \frac{r_{ij}}{E_i - E_j}\left([\eta, H_d + H_r]_{ij} - \frac{du_{ij}}{d\lambda}\frac{H_{ij}}{u_{ij}}\right)
\end{aligned} \tag{2.33}$$

and [4]

$$\begin{aligned}
\frac{dH_{ij}}{d\lambda} &= u_{ij}[\eta, H_d + H_r]_{ij} + \frac{du_{ij}}{d\lambda}\frac{H_{ij}}{u_{ij}} \\
\eta_{ij} &= \frac{1}{E_i - E_j}\left(r_{ij}[\eta, H_d + H_r]_{ij} - \frac{du_{ij}}{d\lambda}\frac{H_{ij}}{u_{ij}}\right)
\end{aligned} \tag{2.34}$$

where $u_{ij} + r_{ij} = 1$; and the constrain eq. (2.32) on the cutoff function in both sectors is implied. One can choose the sharp cutoff function $u_{ij} = \theta(\lambda - |\Delta_{ij}|)$.

# Chapter 3

# Light-front field theory

## 3.1 Introduction

The development of light-front field theory dates back to the work of Dirac [11], where he introduced the light-front coordinates (the coordinate vector is $x = (x^+, x^-, x_\perp)$ with $x^\pm = x^0 \pm x^3$ and $x_\perp = (x_1, x_2)$) and the concept of front form dynamics for Hamiltonians. Dirac suggested, that a Hamiltonian operator can 'propagate' a physical system either in the usual time $x^0$ (instant form dynamics) or in the light-front time $x^+$ (front form dynamics). The latter form of relativistic dynamics combines "the restricted principle of relativity with the Hamiltonian formulation of dynamics" [11].

Later the rules for front form perturbation theory were formulated [12], and the equivalence of this theory with the Feynman rules of covariant perturbation theory was established [13],[14].

Recent interest in light-front coordinates is driven mainly by two topics: low-energy bound state problem in QCD, where light-front coordinates offer a scenario in which a constituent picture of hadron structure can emerge from QCD, because of the simplified vacuum on the light-front [20], [31], [22]; and high-energy scattering processes, where light-front coordinates are the natural coordinates of the system [49], [22]. For an extensive list of light-front references through the early $1990's$ see [1], for the list of recent reviews see [21], [22] and references within.

Below we give briefly an introduction to light-front field theory (for introduction see also [23]).

Light-Front (LF) quantization is very similar to canonical equal time (ET) quantization (here we closely follow Ref. [15]). Both are Hamiltonian formulations of field theory, where one specifies the fields on a particular initial surface. The evolution of the fields off the initial surface is determined by the Lagrangian equations of motion. The main difference is the choice of the initial surface, $x^0 = 0$ for ET and $x^+ = 0$ for the LF respectively. In both frameworks states are expanded in terms of fields (and their derivatives) on this surface. Therefore, the same physical state may have very different wave functions[1] in the ET and LF approaches because fields at $x^0 = 0$ provide a different basis for expanding a state than fields at $x^+ = 0$. The reason is that the microscopic degrees of freedom — field amplitudes at $x^0 = 0$ versus field amplitudes at $x^+ = 0$ — are in general quite different from each other in the two formalisms.

From the purely theoretical point of view, various advantages of LF quantization derive from properties of the ten generators of the Poincaré group (translations $P^\mu$, rotations $\vec{L}$ and boosts $\vec{K}$) [15]. Those generators which leave the initial surface invariant ($\vec{P}$ and $\vec{L}$ for ET and $P_-$, $\vec{P}_\perp$, $L_3$ and $\vec{K}$ for LF) are "simple" in the sense that they have very simple representations in terms of the fields (typically just sums of single particle operators). The other generators, which include the "Hamiltonians" ($P_0$, which is conjugate to $x^0$ in ET and $P_+$, which is conjugate to the LF-time $x^+$ in LF quantization) contain interactions among the fields and are typically very complicated. Generators which leave the initial surface invariant are also called *kinematic* generators, while the others are called *dynamic* generators. Obviously it is advantageous to have as many of the ten generators kinematic as possible. There are seven kinematic generators on the LF but only six in ET quantization.

---

[1] By "wave function" we mean here the collection of all Fock space amplitudes.

The fact that $P_-$, the generator of $x^-$ translations, is kinematic (obviously it leaves $x^+ = 0$ invariant!) and positive has striking consequences for the LF vacuum[15]. For free fields $p^2 = m^2$ implies for the LF energy $p_+ = \left(m^2 + \vec{p}_\perp\right)/p_-$. Hence positive energy excitations have positive $p_-$. After the usual re-interpretation of the negative energy states this implies that $p_-$ for a single particle is non-negative [which makes sense, considering that $p_- = p_0 - p_3$]. $P_-$ being kinematic means that it is given by the sum of single particle momenta $p_-$. Combined with the non-negativity of $p_-$ this implies that, even in the presence of interactions, the physical vacuum (ground state of the theory) differs from the Fock vacuum (no particle excitations) only by so-called *zero-mode* excitations, i.e. by excitations of modes which are independent of the longitudinal LF-space coordinate $x^-$. Due to this simplified vacuum structure, the LF-framework seems to be the only framework, where a constituent quark picture in a strongly interacting relativistic field theory has a chance to make sense [16, 17, 18, 19]. This is the most attractive feature of LF-frame to approve constituent quark model desription for QCD.

## 3.2 Preceding work

As far as progress is concerned, the light-front approach is not so far along; most research effort has occurred since late $1980's$ [1]. Progress is currently limited by conceptual issues, mainly by problems in renormalization program.

Further the methods available in the light-front field theory to solve the bound state problem are discussed. Then the results for positronium problem on the light-front follow.

### 3.2.1 Models and methods in the light-front field theory

The ultimate goal of the light-front field theory is to start with QCD Lagrangian and, with a minimum of approximation, calculate the hadron spectrum. The basic idea behind this approach is to use Hamiltonian techniques in the coordinate system best suited for relativistic dynamics. For light-front field theory, physically interesting observables are quite easily calculated then from the bound state wave-functions.

Further we review several methods to solve the bound state problem in the light-front field theory.

There are several attempts to solve for QCD bound states in the light-front approach, based on simplification of initial $QCD_{3+1}$ Lagrangian. Instead of real $QCD_{3+1}$ different models, resembling QCD and having its main properties (confinement, asymptotic freedom as in transverse lattice model, and also chiral symmetry breaking as in collinear model) are solved.

Collinear (tube) QCD model is a phenomenological model for light-front QCD, where the transverse momenta of all constituents are neglected. This reduces the $QCD_{3+1}$ Lagrangian to an effective $1 + 1$ dimensional theory, which is then solved for the spectrum, distribution amplitudes and form factors of mesons [25].

In the transverse lattice QCD approach one formulates an effective light-front Hamiltonian for $SU(N)$ Yang Mills theory in $2+1$ [26] ($(3+1)$ [27]) dimensions using two continuous space-time dimensions with the remaining transverse space dimension (two transverse dimensions) discretized on a lattice. In the case of $(2+1)$ - dimensional theory the reduction to a $(1+1)$ - dimensional theory takes place, that enables to investigate the string tension and the glueball spectrum.

The goal of such toy model studies is to build intuition which one can hopefully apply to $QCD_{3+1}$. However, while these models have been very useful for studing nonperturbative renormalization in $1+1$ dimesional LF field theories, it is not clear to what extend these results can be generalized to sufficiently nontrivial theories in $3+1$ dimensions.

In other approaches one reduces the initial Hamiltonian of light-front field theory to an effective, low-energy Hamiltonian, which can be solved for bound states. Different methods are used to construct such an effective Hamiltonian on the light-front.

First group of methods, known as Tamm-Dancoff approach, is based on Tamm-Dancoff truncation [33] and projection technique in Fock space (Bloch-Fleshbach technique). By Tamm-Dancoff truncation one simply restricts the full Fock space to several lowest Fock sectors of interest. The problem of renormalization arises in this approach, since in a limited Fock space the diagrams, needed for renormalization but containing more Fock components in intermediate state as allowed, inspite of it must be thrown away. The method of iterative resolvents developed by Pauli, together with discretized light cone quantization (DLCQ) approach is the synthesis of the methods from the first group [28], [29]. In this approach one repeats projecting high Fock components upon the lower in sequence several times. Thus constructed few-body effective Hamiltonian describes most adequately low-lying bound states. Application of this method to QED is discussed below.

Second group of methods uses renormalization group concept to construct low-energy Hamiltonian. Similarity renormalization scheme [3], formulated by Glazek and Wilson, develops a renormalization group and the basic elements of renormalization group calculations for Hamiltonians on the light-front. In this method continuous unitary transformation, similarity transformation, is performed to bring the Hamiltonian operator $H_{ij}$ to a band-diagonal form $|E_i - E_j| \leq \lambda$. It turns out, that the width of the band $\lambda$ corresponds to the energy scale and plays the role of UV cutoff, changing of which gives rise to renormalization group running of Hamiltonian. Also new interactions, not present in canonical theory Hamiltonian, appear through this scaling.

The alternative approach for Hamiltonian renormalization, the method of flow equations [2], was proposed independently by Wegner. One performs a set of infinitesimal unitary transformations to get the block-diagonal effective Hamiltonian, with the particle number conserving in each block. This reduces the bound state problem to a few-body problem, since the particle number violating contributions are eliminated.

There is a need for an effective formalism for gauge theories: nobody ever has solved rigorously a relativistic many-body theory in $3+1$ dimensions.

### 3.2.2 Results for light front $QED_{3+1}$

In this section we review the results obtained by others on positronium problem in the light front dynamics. First we discuss the first group of methods based on Tamm-Dancoff approach (Tamm-Dancoff truncation and projection technique in Fock space). The numerical recipes are well elaborated there.

Brodsky, Pauli, and Tang [32] showed how to set up the positronium bound state problem in DLCQ (discretized light cone quantization) with a Tamm-Dancoff truncation [33] to two sectors of Fock space: (i) the electron-positron sector, and (ii) the electron-positron-photon sector. In order to solve the associated eigenvalue problem, the diagonalization of the discretized Hamiltonian, and variational methods were used. The leading results for the triplet ground state of positronium were obtained not quit satisfactory. To produce significant results by diagonalizing the Hamiltonian matrix, one would have had to include much more Fock states or to improve the numerical convergence of the method applied.

Krautgärtner, Pauli, and Wölz [34] derived the continuum limit in the positronium model discussed above for the calculation analytically, and with a prescription for handling an infrared divergence they showed that to leading order the binding energy for positronium results. They have used an effective interaction, obtained from a projecting of the $|e\bar{e}\gamma>$-sector onto the $|e\bar{e}>$-sector. The corresponding effective integral equation was solved numerically using the method of Coulomb counterterms, introduced to improve numerical convergence. The results obtained for Bohr spectrum and hyperfine splitting show an excellent convergence and coincide with the expected values. For the first time the relativistic effects as fine structure could be investigated (numerically) in the light-front Hamiltonian approach.

Kaluza and Pauli [35] showed that reasonably accurate numerical results can be obtained with proper renormalization of the Hamiltonian, although logarithmic 'divergences' remain in their calculations. These divergences are not a serious problem if one uses a sufficiently small cutoff and weak coupling. For calculation of fine structure the diagonalization technique was improved to enlarge the Fock space feasible with the computer. But the convergence of spectra was rather poor, since no proper counterterms for the Coulomb singularity of the relativistic problem were taken.

Kaluza and Pirner extended the work in [34] through the fine structure [36].

Pauli formulated the method of iterative resolvents [28], which enables, in general, to take into account infinite many high Fock states by projecting in sequence high Fock sectors unto the lower Fock sectors. The main advantage of the method is, that it requires the inversion of the effective sector Hamiltonians, corresponding to the given Fock sectors, at each step of iteration, instead of inversion of the full Hamiltonian matrix, standing in the bound state equation. To avoid in the leading order the infrared divergences (collinear singularities) the full energy appeared in the interaction kernel for the electron-positron bound state was replaced with a free energy. In the physical amplitudes the collinear singularities are exactly cancelled by the dynamical terms [45]. Pauli and Trittmann have solved numerically the corresponding light-front integral equation for positronium bound state in the continuum limit [30], including the Coulomb counterterm technique in the computer code. The results show excellent convergence and coincide to a high degree of accuracy with the expected values.

Renormalization program for positronium in the light-front QED was performed using similarity renormalization scheme (similarity transformation and coupling coherence) by several authors. Perry has shown [37] that the resultant effective Hamiltonian leads to standard lowest order bound state results, with the Coulomb interaction emerging naturally.

For the first time Jones,Perry, and Glazek [39] presented using similarity renormalization a systematic analytic calculation in a light-front Hamiltonian approach of the singlet-triplet spin splitting in the ground state of positronium through order $\alpha^4$. The standard singlet-triplet splitting of positronium was obtained with degeneracy of triplet state, that recovers rotational symmetry that is non-manifest symmetry in the light-front field theory.

Jones, and Perry have calculated also the Lamb shift in the same approach [40]. The dominant part of the splitting between the $2S_{\frac{1}{2}}$ and $2P_{\frac{1}{2}}$ energy levels in hydrogen was obtained.

All calculations in similarity renormalization approach were done within the perturbative theory and results for spectrum were obtained with several approximations analytically.

We do not mention here applications of both methods, Tamm-Dancoff approach [41] and similarity renormalization [20], to bound state problem for light-front QCD.

## 3.3 Canonical QED Hamiltonian

In this section we write the canonical $QED_{3+1}$ Hamiltonian in the light-front gauge and also give briefly its derivation from Lagrangian density, following the original work of Zhang and Harindranath [24]. The QED Hamiltonian in the secondary quantization is given further, which is used in the main part of the work (in the chapters 4,5,7).

### 3.3.1 Canonical light-front $QED_{3+1}$ Hamiltonian

Starting with the QED Lagrangian density

$$\mathcal{L} = -\frac{1}{4}F_{\mu\nu}F^{\mu\nu} + \overline{\psi}(i\not{\partial} + e\not{A} - m)\psi, \tag{3.1}$$

in a fixed gauge, $A^+ = A^0 + A^3 = 0$,[2] the constrained degrees of freedom, $A^-$ and $\psi_-$ ($\psi = \psi_+ + \psi_-, \psi_\pm = \Lambda_\pm \psi$; see all definitions below), are removed explicitly, producing a canonical QED Hamiltonian, defined through the independent physical fields $A_\perp$ and $\psi_+$. Details of derivation follow below. The resulting canonical Hamiltonian $H_{can}$ is given as a sum of the free Hamiltonian and the interacting term

$$P^- = H_{can} = \int dx^- d^2x^\perp (\mathcal{H}_0 + \mathcal{H}_I) \ . \tag{3.2}$$

where each term in eq. (3.2) is written [24]

$$\mathcal{H}_0 = \frac{1}{2}(\partial^i A^j)(\partial^i A^j) + \xi^+ \left(\frac{-\partial_\perp^2 + m^2}{i\partial^+}\right)\xi \ , \tag{3.3}$$

$$\mathcal{H}_I = \mathcal{H}_{ee\gamma} + \mathcal{H}^{inst}_{ee\gamma\gamma} + \mathcal{H}^{inst}_{eeee} \tag{3.4}$$

and

$$\mathcal{H}_{ee\gamma} = e\xi^\dagger \left[-2(\frac{\partial^\perp}{\partial^+}\cdot A^\perp) + \sigma\cdot A^\perp \frac{\sigma\cdot\partial^\perp + m}{\partial^+} + \frac{\sigma\cdot \overleftarrow{\partial}^\perp + m}{\overleftarrow{\partial}^+}\sigma\cdot A^\perp\right]\xi \ , \tag{3.5}$$

$$\mathcal{H}^{inst}_{ee\gamma\gamma} = -ie^2\left[\xi^+\sigma\cdot A^\perp \frac{1}{\partial^+}(\sigma\cdot A^\perp \xi)\right] \ , \tag{3.6}$$

$$\mathcal{H}^{inst}_{eeee} = 2e^2\left[\left(\frac{1}{\partial^+}(\xi^+\xi)\right)\left(\frac{1}{\partial^+}(\xi^+\xi)\right)\right] \ , \tag{3.7}$$

where $\{\sigma^i\}$ are the standard $2\times 2$ Pauli matrices, $i = 1, 2$ only, e.g., $\sigma\cdot\partial^\perp = \sigma^i\partial^i = \sigma^1(-\frac{\partial}{\partial x^1}) + \sigma^2(-\frac{\partial}{\partial x^2})$, and $\partial^+ = 2\partial_- = 2\frac{\partial}{\partial x^-}$. Formally one can write the last term eq. (3.7) in the form

$$\mathcal{H}^{inst}_{eeee} = -\frac{1}{2}J^+ \frac{1}{(\partial^+)^2}J^+ \ . \tag{3.8}$$

---

[2] This derivation will not include a discussion of the gauge field zero-modes. In this work we drop zero-modes. For a treatment that incorporates these gauge field zero-modes from the start in QED, see [43] and references within; (see also footnote at the end of this section).

where $J^+ = -2e\xi^\dagger\xi$. We have used the two-component representation for fermion fields introduced by Zhang and Harindranath [24][3]

Now the details of the derivation of the canonical Hamiltonian are presented. Given $\mathcal{L}$ of Eq. (3.1), the equations of motion are

$$\begin{aligned} \partial_\mu F^{\mu\nu} &= J^\nu \ , && (3.12)\\ (i \not\partial + e \not A - m)\psi &= 0 \ , && (3.13) \end{aligned}$$

where $J^\mu = -e\overline{\psi}\gamma^\mu\psi$. The physical gauge $A^+ = 0$ is chosen and the projection operators $\Lambda_+$ and $\Lambda_-$ are inserted into the equations of motion. Note $\psi_- = \Lambda_-\psi$ and $\psi_+ = \Lambda_+\psi$. Two of the equations are seen to be constraint equations:

$$-\frac{1}{2}\partial^+\partial^+ A^- + \partial^i\partial^+ A^i = J^+ \ , \tag{3.14}$$

$$i\partial^+\psi_- = \left(i\alpha^i\partial^i + e\alpha^i A^i + \frac{m\gamma^+}{2}\right)\psi_+ \tag{3.15}$$

The fact that these are constraints can be seen from the fact that no time derivatives $\partial^-$ appear. Note $\alpha^i = \gamma^0\gamma^i$. Inverting the space derivative $\partial^+$ gives

$$A^- = \frac{-2}{(\partial^+)^2}J^+ + 2\frac{\partial^i}{\partial^+}A^i \ , \tag{3.16}$$

$$\psi_- = \frac{1}{i\partial^+}\left[\left(i\alpha^i\partial^i + e\alpha^i A^i + \frac{m\gamma^+}{2}\right)\psi_+\right] \ . \tag{3.17}$$

The gauge singularities in light-front QED (QCD) that arise when one tries to eliminate the unphysical gauge degrees of freedom by solving the constraint equations can be seen clearly

---

[3] In the two-component representation the fermion fields are given

$$\begin{aligned} \psi_+ &= \begin{pmatrix} \xi \\ 0 \end{pmatrix} \\ \psi_- &= \begin{pmatrix} 0 \\ \frac{1}{i\partial^+}\left\{\left[\sigma^i\left(i\partial^i + eA^i\right) + im\right]\xi\right\} \end{pmatrix} \ , \end{aligned} \tag{3.9}$$

where $\xi$ is expressed through the two-component spinors $\chi_s$ as follows

$$\begin{aligned} \xi(x) &= \sum_{s\pm\frac{1}{2}}\chi_s\int\frac{dp^+d^2p^\perp}{2(2\pi)^3}\theta(p^+)(b_{p,s}e^{-ipx} + d^\dagger_{p,\bar{s}}e^{ipx}) \\ &\qquad \chi(\uparrow) = \frac{1}{\sqrt{2}}\begin{pmatrix} 1 \\ 0 \end{pmatrix} \qquad \text{and} \qquad \chi(\downarrow) = \frac{1}{\sqrt{2}}\begin{pmatrix} 0 \\ 1 \end{pmatrix} \end{aligned} \tag{3.10}$$

and $\bar{s} = -s$.

For completness we give the representation for the physical gauge field (transverse component) through the polarization vectors $\varepsilon(\lambda)$

$$\begin{aligned} A^i(x) &= \sum_\lambda\int\frac{dq^+d^2q^\perp}{2(2\pi)^3}\frac{\theta(q^+)}{\sqrt{q^+}}(a_{q,\lambda}\varepsilon^i_\lambda e^{-iqx} + a^+_{q,\lambda}\varepsilon^{*i}_\lambda e^{iqx}) \\ &\qquad \varepsilon(\uparrow) = \frac{-1}{\sqrt{2}}(1, i) \qquad \text{and} \qquad \varepsilon(\downarrow) = \frac{1}{\sqrt{2}}(1, -i) \ , \end{aligned} \tag{3.11}$$

in momentum space. In momentum space, the constraint eq. (3.14) and eq. (3.15) cannot determine the dependent fields in terms of physical fields for the single longitudinal momentum $k^+ = 0$. In coordinate space, this implies that the $A^+ = 0$ gauge has a singularity at longitudinal boundary. A careful treatment of the definition of $1/\partial^+$ is necessary. A suitable definition of $(1/\partial^+)$ (and consequently $(1/\partial^+)^2$), which determines uniquely the initial value problem at $x^+ = 0$, is given [24]

$$\begin{aligned}
&\left(\frac{1}{\partial^+}\right) f(x^-) = \frac{1}{4}\int_{-\infty}^{+\infty} dy^- \epsilon(x^- - y^-)\, f(y^-) + g_1 \ , \\
&\left(\frac{1}{\partial^+}\right)^2 f(x^-) = \frac{1}{8}\int_{-\infty}^{+\infty} dy^- |x^- - y^-|\, f(y^-) + g_2 + x^- g_3 \ , \\
&\partial^+ = 2\partial_- = 2\frac{\partial}{\partial x^-} \ , \\
&\partial_- \epsilon(x^- - y^-) = 2\delta(x^- - y^-) \ , \\
&\epsilon(x) = \theta(x) - \theta(-x) \ .
\end{aligned}$$

where $f(x)$ is an arbitrary field with $x^\perp$ and $x^+$ being implicitly in the argument of it. The functions $g_1$, $g_2$ and $g_3$ are arbitrary fields independent of $x^-$. For a discussion on these boundary terms see [24]. Notice that this inverse longitudinal derivative is non-local.

In practice, we define the inverse longitudinal derivative in momentum space. We explicitly put the momentum representation of the field operators into the respective terms of the Hamiltonian, multiply the fields out explicitly, and then replace the inverse derivatives by appropriate factors of longitudinal momentum with the restriction $|p^+|/\mathcal{P}^+ \geq \epsilon = 0_+$ [$\mathcal{P}^+$ is the total longitudinal momentum of the physical state of interest]. The absolute value sign on $|p^+|$ is required for the instantaneous interactions. For example, a product of two fields gives

$$\frac{1}{i\partial^+} \exp[-i(p-k)\cdot x] \longrightarrow \frac{1}{p^+ - k^+}\theta\left(|p^+ - k^+| - \epsilon\mathcal{P}^+\right) \exp[-i(p-k)\cdot x] \ . \tag{3.18}$$

The dynamical degrees of freedom are $A^i$ and $\psi_+$. The canonical Hamiltonian density is defined in terms of these dynamical degrees of freedom

$$\mathcal{H} = \frac{\partial\mathcal{L}}{\partial(\partial^- A^i)}\partial^- A^i + \frac{\partial\mathcal{L}}{\partial(\partial^-\psi_+)}\partial^-\psi_+ - \mathcal{L} \ . \tag{3.19}$$

Taking these derivatives of the Lagrangian density and combining terms, the Hamiltonian density takes the following simple form

$$\mathcal{H} = \frac{1}{2}(\partial^i A^j)^2 + \psi_-^\dagger i\partial^+\psi_- - 2\left(\frac{1}{\partial^+}\frac{J^+}{2}\right)^2 + \frac{J^+}{2}A^- \ , \tag{3.20}$$

where the constraints of eq. (3.14),eq. (3.15) are assumed to be satisfied. In our $\gamma$-matrix representation, only two of the components of the 4-spinor $\psi_+$ are nonzero. Writing these as the 2-spinor $\xi$,[4] and inserting the constraints of eq. (3.16),eq. (3.17), $H_{can}$ takes on the form written earlier in Eqs. (3.2)–(3.7), where surface terms such as in

$$\int d^2x^\perp dx^- \left(\frac{1}{\partial^+}J^+\right)\left(\frac{1}{\partial^+}J^+\right) = -\int d^2x^\perp dx^- J^+ \left(\frac{1}{\partial^+}\right)^2 J^+ + \text{surface terms} \ , \tag{3.21}$$

are dropped [5].

---

[4] In other words, we are defining $\psi_+ = \Lambda_+\psi = (\psi_1, \psi_2, 0, 0) \equiv (\xi, 0)$

[5] A set of boundary integrals (as the first term in eq. (3.21)), arising from elimination of unphysical gauge degrees of freedom, is associated with the light-front infrared singularity, $k^+ = 0$. Using the above definition

### 3.3.2 QED Hamiltonian in second quantization

In this work we use the matrix elements of canonical Hamiltonian $H_{can}$, given in Eqs. (3.2)–(3.7), calculated in the free basis of $H_0$. Below we write the canonical Hamiltonian $H_{can}$ in the form of second quantization.

We use the following momentum-space representation for the field operators, [44] and [24], (see footnote in the previous section)

$$\begin{aligned} \xi(x) &= \sum_s \chi_s \int \frac{dp^+ d^2p^\perp}{2(2\pi)^3} \theta(p^+)(b_{p,s}e^{-ipx} + d^\dagger_{p,\bar{s}}e^{ipx}) \\ A^i(x) &= \sum_\lambda \int \frac{dq^+ d^2q^\perp}{2(2\pi)^3} \frac{\theta(q^+)}{\sqrt{q^+}} (\varepsilon^i_\lambda a_{q,\lambda} e^{-iqx} + h.c.) \; , \end{aligned} \tag{3.22}$$

where spinors are $\chi_{1/2} = (1,0)$, $\chi_{-1/2} = (0,1)$, with $\bar{s} = -s$ and polarization vectors $\varepsilon^i_1 = \frac{-1}{\sqrt{2}}(1,i)$, $\varepsilon^i_{-1} = \frac{1}{\sqrt{2}}(1,-i)$; the integration running over the $p^+ \geq 0$ only these states, that are allowed the light-front theory.

The corresponding (anti)commutation relations are

$$\begin{aligned} \{b_{p,s}, b^+_{p',s'}\} = \{d_{p,s}, d^+_{p',s'}\} = \delta_{p,p'}\delta_{ss'} \\ [a_{q,\lambda}, a^+_{q',\lambda'}] = \delta_{q,q'}\delta_{\lambda,\lambda'} \qquad\qquad , \end{aligned} \tag{3.23}$$

where

$$\delta_{p,p'} \equiv 2(2\pi)^3 \delta(p^+ - p'^+)\delta^{(2)}(p^\perp - p'^\perp) \; . \tag{3.24}$$

The light-front vacuum has trivial structure for both boson and fermion sectors, namely $a_q|0>= 0$; $b_p|0>= 0$, simplifying the analytical calculations. The normalization of states is according to

$$< p_1, s_1|p_2, s_2 >= \delta_{p_1,p_2}\delta_{s_1,s_2} \; , \tag{3.25}$$

where $b^+_{p,s}|0>= |p,s>$.

Making use of the field representation eq. (3.22), we have the following Fourier transformed for
the **free** Hamiltonian

$$H_0 = \sum_s \int \frac{dp^+ d^2p^\perp}{2(2\pi)^3} \theta(p^+) \frac{p^{\perp 2} + m^2}{p^+} (b^+_{p,s}b_{p,s} + d^+_{p,s}d_{p,s}) + \sum_\lambda \int \frac{dq^+ d^2q^\perp}{2(2\pi)^3} \theta(q^+) \frac{q^{\perp 2}}{q^+} a^+_{q,\lambda}a_{q,\lambda} \; , \tag{3.26}$$

the leading order $O(e)$-**the electron-photon coupling**

$$\begin{aligned} H_{ee\gamma} &= \sum_{\lambda s_1 s_2} \int d^3p_1 d^3p_2 d^3q \; e \; [\varepsilon^i_\lambda \tilde{a}_q + \varepsilon^{i*}_\lambda \tilde{a}^+_{-q}](\tilde{b}^+_{p_2}\tilde{b}_{p_1} + \tilde{b}^+_{p_2}\tilde{d}^+_{-p_1} + \tilde{d}_{-p_2}\tilde{b}_{p_1} + \tilde{d}_{-p_2}\tilde{d}^+_{-p_1}) \\ &\quad \times \chi^+_{s_2}\Gamma^i(p_1,p_2,-q)\chi_{s_1}\delta_{q,p_2-p_1} \; , \end{aligned} \tag{3.27}$$

where

$$\Gamma^i(p_1,p_2,q) = 2\frac{q^i}{q^+} - \frac{\sigma \cdot p^\perp_2 - im}{p^+_2}\sigma^i - \sigma^i \frac{\sigma \cdot p^\perp_1 + im}{p^+_1} \; , \tag{3.28}$$

---

eq. (3.18) in the boundary integrals, the singularity at $k^+ = 0$ is removed; the surface terms (as the second term in eq. (3.21)) vanish from the LFQED (LFQCD) Hamiltonian and the light-front linear infrared divergences cancel in all physical amplitudes [24]. The problem of 'zero modes' (the singularity of $A^+ = 0$ gauge at $k^+ = 0$) is hidden now in the nontrivial asymptotic behavior of the transverse (physical) gauge degrees of freedom at longitudinal infinity, see the first reference of [24]. In this work we do not consider this problem.

We have for the **instantaneous** interactions of the order $O(e^2)$

$$H^{inst}_{eeee} = \sum_{s_1 s_2 s_3 s_4} \int d^3p_1 d^3p_2 d^3p_3 d^3p_4 \; e^2 \; (\tilde{b}^+_{p_3} + \tilde{d}_{-p_3})(\tilde{b}^+_{p_4} + \tilde{d}_{-p_4})(\tilde{b}_{p_1} + \tilde{d}^+_{-p_1})(\tilde{b}_{p_2} + \tilde{d}^+_{-p_2})$$
$$\times \chi^+_{s_3}\chi^+_{s_4} \frac{4}{(p_1^+ - p_3^+)^2} \chi_{s_1}\chi_{s_2}\delta_{p_3+p_4,p_1+p_2}$$
$$\chi^+_{s_3}\chi^+_{s_4} \quad \mathbb{1} \quad \chi_{s_1}\chi_{s_2} = \delta_{s_1 s_3}\delta_{s_2 s_4} + \delta_{s_1 s_4}\delta_{s_2 s_3} \tag{3.29}$$

and

$$H^{inst}_{ee\gamma\gamma} = \sum_{s_1 s_2 \lambda_1 \lambda_2} \int d^3p_1 d^3p_2 d^3q_1 d^3q_2 \; e^2 \; (\varepsilon^{i*}_{\lambda_1}\tilde{a}^+_{q_1} + \varepsilon^{i}_{\lambda_1}\tilde{a}_{-q_1})(\varepsilon^{j}_{\lambda_2}\tilde{a}_{q_2} + \varepsilon^{j*}_{\lambda_2}\tilde{a}^+_{-q_2})(\tilde{b}^+_{p_2} + \tilde{d}_{-p_2})(\tilde{b}_{p_1} + \tilde{d}^+_{-p_1})$$
$$\times \chi^+_{s_2} \frac{\sigma^j \sigma^i}{(p_1^+ - q_1^+)} \chi_{s_1}\delta_{p_1+q_2,q_1+p_2}$$
$$\chi^+_{s_2} \quad \mathbb{1} \quad \chi_{s_1} = \delta_{s_1 s_2} \; ; \tag{3.30}$$

here

$$\tilde{a}_q \equiv a_{q,\lambda}\frac{\theta(q^+)}{\sqrt{q^+}}, \qquad \left[\tilde{a}_{-q} \equiv a_{-q,\lambda}\frac{\theta(-q^+)}{\sqrt{-q^+}}\right] \; ,$$
$$\tilde{b}_p \equiv b_{p,s}\theta(p^+), \qquad \tilde{d}_p \equiv d_{p,\bar{s}}\theta(p^+) \; , \tag{3.31}$$

and the $\delta$-symbol stands for the function defined in eq. (3.24), the short notation for the integral is

$$\int d^3p \equiv \int \frac{dp^+ d^2p^\perp}{2(2\pi)^3} \; . \tag{3.32}$$

# Chapter 4

# Hamiltonian bound state problem on the light-front

In this chapter we outline the program we follow to solve the bound state problem on the light-front. This includes two issues: the derivation of effective Hamiltonian and solving the corresponding bound state equation. The first point is discussed here explicitly in application to positronium bound state problem. The methods to solve bound state equation (analytically and numerically) are discussed in the next chapters.

## 4.1 Introduction

We use the method of flow equations to construct an effective Hamiltonian starting from the light-front formulation which can be used to solve the bound state problem. The physical idea behind this approach is to use renormalization concept for Hamiltonians to get an effective, low-energy Hamiltonian for a limited Fock space. The bound state problem is reduced then to a few-body problem with the effective Hamiltonian acting on the energy scale of bound state formation.

The key to renormalization of Hamiltonians is to diagonalize the Hamiltonian operator [3]. We have discussed briefly in chapter 2 the methods to diagonalize Hamiltonians continuously, suggested by Wegner [2] and Glazek and Wilson [3], which have been called flow equations and similarity renormalization by the authors, resp.

It is common to both methods that they eliminate by means of a unitary transformation initially the off-diagonal matrix elements between states with large energy differences and continue with states closer and closer in energy, so that off-diagonal matrix elements between states of energy difference larger than $\lambda$ are eliminated or strongly suppressed. The final aim is to eliminate them completely ($\lambda \to 0$) and to obtain a diagonalized Hamiltonian.

We have mentioned in chapter 3, that a literal use of this concept can lead to convergence problems [2]. As was suggested by Wegner [2], one may leave the idea of diagonalizing immediately in favor of block-diagonalizing. If matrix-elements between states of equal particle number are considered diagonal, then the procedure brings the Hamiltonian into a block-diagonal form. Application of flow equations to an $n$-orbital model has shown, that procedure of block-diagonalizing works much better, where block-diagonalization with respect to the quasiparticle number (number of electrons above the Fermi edge plus number of holes below the Fermi edge) is performed [2].

It becomes apparent from the calculations by Jones, Perry and Glazek [39] on the basis of the similarity transformation, that this scheme works well down to energy differences of the order of Rydberg, but if one goes below, then contributions in higher orders in the coupling become important.

Indeed it seems to be rather difficult to obtain bound states from plane waves by continuous unitary transformations. In eliminating only the terms which do not conserve the number of particles one postpones the diagonalization, but reduces the problem to one in the space of fixed particle number [46]. Thus for the positronium problem it is sufficient to determine the one- and two-particle contribution of the Hamiltonian for electrons and positrons.

Basically the procedure is very similar to that of the elimination of the electron-phonon interaction [10] which yields an effective attractive interaction between electrons responsible for superconductivity. Both the method of flow equations and the similarity remormalization [10] (the ref. to A. Mielke) yield results different from Fröhlich's original ones [52] but in very good agreement with more sophisticated methods. In QED it is the interaction of the electrons with the photons instead of the phonons which has to be eliminated.

A basic advantage of the methods of similarity renormalization and flow equations in comparison to conventional perturbation theory is, that one obtains normally less singular effective interactions.

This procedure is similar to the Tamm-Dancoff Fock space truncation [33, 30] in the sense that also in this truncation particle number changing interactions are eliminated.

We define an effective Hamiltonian

$$H^{eff} \to UHU^{+} \tag{4.1}$$

where $H$ is the bare Hamiltonian and the unitary transformation U is determined by the flow equations below.

## 4.2 Flow equations in the perturbative frame

In chapter 2 we have set up the framework to use flow equations in the field theory. In this section we formulate the equations, obtained in chapter 2, for a canonical QED Hamiltonian in the perturbative frame.

Flow equations read

$$\begin{aligned} \frac{dH(l)}{dl} &= [\eta(l), H(l)] \\ \eta(l) &= [H_d(l), H_r(l)] \end{aligned} \tag{4.2}$$

where the Hamiltonian is given $H = H_d + H_r$, with $H_d$ and $H_r$ including all the terms from the 'diagonal' and the 'rest' sectors, resp.

Our goal is to transform the Hamiltonian into blocks with the same number of (quasi)-particles. This means, that we define the 'diagonal' part $H_d$ as the part of the interaction which conserves the number of particles (electrons, positrons, photons), and the 'rest' $H_r$ as the particle number changing part. In the case of QED(QCD), where the electron-photon (quark-gluon) coupling is present, the number of photons (gluons) is conserved in each block of the final effective Hamiltonian.

As a result of the unitary transformation new interactions are induced (see below). They are absent at $l = 0$ and are generated as $l$ increases. They also give rise to new terms in the generator of transformation $\eta(l)$. This in its turn generates new interactions again.

To be able to perform the calculations analytically we proceed in a perturbative frame and truncate the series assuming the coupling constant is small. In the case of QED on the light-front one has for any finite value of $l$

$$H(l) = H_d^{(0)} + H_r^{(1)} + H_d^{(2)} + H_r^{(2)} + ... \tag{4.3}$$

where the superscript denotes the order in the bare coupling constant, $H^{(n)} \sim e^n$; the indices 'd' and 'r' indicate the diagonal and the rest parts correspondingly. The part $H_d^{(0)}$ is the free Hamiltonian, corresponding to the single particle energies with the structure in secondary quantization $a^+a, b^+b, d^+d$, where $a, b, d$ are the annihilation operators of the photons, electrons and positrons correspondingly; $H_r^{(1)}$ denotes the electron-photon coupling (of the type $a^+b^+b$); $H_d^{(2)}$ is the second order diagonal part of the Hamiltonian, having the structure $b^+d^+bd, b^+b^+bb, d^+d^+dd$ (in the light front they correspond to the canonical instantaneous (seagull) and to newly generated interactions in the diagonal sector in second order). Note, that the diagonal part in the flow equations is not only the free Hamiltonian but the full particle number conserving part of the effective Hamiltonian. The choice of only $H_d^{(0)}$ as the diagonal part gives rise to the band-diagonal structure of the effective Hamiltonian in each 'particle number' sector in the similarity renormalization scheme [53]. However, this makes a difference for the diagonal part only if one goes beyond third order in $e$.

The generator of the transformation is

$$\eta(l) = [H_d, H_r] = [H_d^{(0)}, H_r^{(1)}] + [H_d^{(0)}, H_r^{(2)}] + ... = \eta^{(1)} + \eta^{(2)} + ... \tag{4.4}$$

Up to second order the flow equation reads

$$\frac{dH(l)}{dl} = [\eta, H] = [[H_d^{(0)}, H_r^{(1)}], H_d^{(0)}] + [[H_d^{(0)}, H_r^{(1)}], H_r^{(1)}] + [[H_d^{(0)}, H_r^{(2)}], H_d^{(0)}] + ... \tag{4.5}$$

Also terms of higher orders in $e$ are generated by the flow equations.

In the basis of the eigenfunctions of the free Hamiltonian $H_d^{(0)}$

$$H_d^{(0)}|i >= E_i|i > \tag{4.6}$$

one obtains for the matrix-elements between the many-particle states

$$\begin{aligned} \eta &= (E_i - E_j)H_{rij}^{(1)} + (E_i - E_j)H_{rij}^{(2)} + ... \\ \frac{dH_{ij}}{dl} &= -(E_i - E_j)^2 H_{rij}^{(1)} + [\eta^{(1)}, H_r^{(1)}]_{ij} - (E_i - E_j)^2 H_{rij}^{(2)} + ... \end{aligned} \tag{4.7}$$

The energy differences are given by

$$E_i - E_j = \sum_{k=1}^{n_2} E_{i,k} - \sum_{k=1}^{n_1} E_{j,k} \tag{4.8}$$

where $E_{i,k}$ and $E_{j,k}$ are the energies of the created and annihilated particles, respectively.

The energy $E_i$ depends on the flow parameter $l$ only in second order in the coupling. Therefore one has

$$\begin{aligned} \frac{dH_{rij}^{(1)}}{dl} &= -(E_i - E_j)^2 H_{rij}^{(1)} \\ H_{rij}^{(1)}(l) &= H_{rij}^{(1)}(l=0)\mathrm{e}^{-(E_i-E_j)^2 l} = H_{rij}^{(1)}(\lambda = \Lambda \to \infty)\mathrm{e}^{-\frac{(E_i-E_j)^2}{\lambda^2}} \end{aligned} \tag{4.9}$$

Here we have used the physical meaning of the flow parameter $l$; $l = \frac{1}{\lambda^2}$, where $\lambda$ is UV-cutoff (see chapter 2, eq. (2.30)).

In the flow equations $\lambda$ defines the smooth UV-cutoff. This fact insures the analytical behavior of the effective Hamiltonian with $\lambda$, that helps in numerical calculations.

In second order one has to distinguish between the behavior of the 'diagonal' and the 'rest' term. For the 'rest' part one has

$$\frac{dH^{(2)}_{rij}}{dl} = [\eta^{(1)}, H^{(1)}]_{rij} - (E_i - E_j)^2 H^{(2)}_{rij}, \tag{4.10}$$

where index 'r' by $[\eta^{(1)}, H^{(1)}]_r$ defines the particle number changing part of the commutator. Introduce

$$H^{(2)}_{rij}(l) = \mathrm{e}^{-(E_i-E_j)^2 l}\tilde{H}^{(2)}_{rij}(l). \tag{4.11}$$

Then the solution reads

$$\tilde{H}^{(2)}_{rij}(l) = \tilde{H}^{(2)}_{rij}(l=0) + \int_0^l dl' \mathrm{e}^{(E_i-E_j)^2 l'}[\eta^{(1)}(l'), H^{(1)}(l')]_{rij}. \tag{4.12}$$

For the 'diagonal' part one has

$$\frac{dH^{(2)}_{dij}}{dl} = [\eta^{(1)}, H^{(1)}]_{dij} \tag{4.13}$$

and the solution is

$$H^{(2)}_{dij}(l) = H^{(2)}_{dij}(l=0) + \int_0^l dl'[\eta^{(1)}(l'), H^{(1)}(l')]_{dij}. \tag{4.14}$$

Note, that though in general the commutator $[[H^{(0)}_d, H^{(2)}_d], H^{(0)}_d]$ is not zero, it is not present in the flow equation due to the definition of the diagonal part. The corresponding commutator $[[H^{(0)}_d, H^{(2)}_r] H^{(0)}_d]$ in the 'non-diagonal' sector insures the band-diagonal form for the 'rest' interaction and also gives rise to the different structure of the generated interaction (the integral term) in the 'rest' and 'diagonal' sectors.

The commutator $[\eta^{(1)}, H^{(1)}]$ gives rise to new terms in second order in the bare coupling $e$. In the case of QED it induces new types of interactions and generates the renormalization group corrections to the electron (photon) masses. The coupling constant starts to run in third order in $e$.

## 4.3 Effective low-energy Hamiltonian

### 4.3.1 Effective electron-positron interaction

In this section we follow mainly the work [53]. We calculate by means of flow equations the effective interaction between electron and positron, generated in the second order in coupling $e$ by elimination of electron-photon vertex. We use the canonical QED Hamiltonian on the light-front in second quantization, given in chapter 3.

The term for electron-photon vertex by finite $l$ is given

$$\begin{aligned} H_{ee\gamma} = \sum_{\lambda s_1 s_2} \int & d^3p_1 d^3p_2 d^3q (g^*_{p_i p_f}(l)\varepsilon^i_\lambda \tilde{a}_q + g_{p_i p_f}(l)\varepsilon^{i*}_\lambda \tilde{a}^+_{-q})(\tilde{b}^+_{p_2}\tilde{b}_{p_1} + \tilde{b}^+_{p_2}\tilde{d}^+_{-p_1} + \tilde{d}_{-p_2}\tilde{b}_{p_1} + \tilde{d}_{-p_2}\tilde{d}^+_{-p_1}) \\ & \times \chi^+_{s_2}\Gamma^i_l(p_1, p_2, -q)\chi_{s_1}\delta_{q,p_2-p_1} \ , \end{aligned} \tag{4.15}$$

and

$$\Gamma^i_l(p_1,p_2,q) \;=\; 2\frac{q^i}{q^+} - \frac{\sigma\cdot p_2^\perp - im_{p_ip_f}(l)}{p_2^+}\sigma^i - \sigma^i\frac{\sigma\cdot p_1^\perp + im_{p_ip_f}(l)}{p_1^+}\ , \tag{4.16}$$

where $l$-dependence comes from the unitary transformation performed. Also we write explicitly the momentum dependence of the coupling constant and the mass as long as $l \neq 0$, here $p_i$ and $p_f$ stand for the set of initial and final momenta,resp. The initial conditions for the coupling constant and the mass are defined at the value of bare cutoff $\Lambda \to \infty$ $(l_\Lambda = 0)$

$$\begin{aligned}\lim_{\Lambda\to\infty} g(l_\Lambda) &= e\\ \lim_{\Lambda\to\infty} m(l_\Lambda) &= m\end{aligned} \tag{4.17}$$

Following the procedure outlined in the previous section, the leading order generator of the unitary transformation is

$$\begin{aligned}\eta^{(1)}(l) = \sum_{\lambda s_1 s_2}\int & d^3p_1 d^3p_2 d^3q(\eta^*_{p_ip_f}(l)\varepsilon^i_\lambda \tilde{a}_q + \eta_{p_ip_f}(l)\varepsilon^{i*}_\lambda \tilde{a}^+_{-q})(\tilde{b}^+_{p_2}\tilde{b}_{p_1} + \tilde{b}^+_{p_2}\tilde{d}^+_{-p_1} + \tilde{d}_{-p_2}\tilde{b}_{p_1} + \tilde{d}_{-p_2}\tilde{d}^+_{-p_1})\\ &\times\chi^+_{s_2}\Gamma^i_l(p_1,p_2,-q)\chi_{s_1}\delta_{q,p_2-p_1}\ ,\end{aligned} \tag{4.18}$$

$$\eta_{p_ip_f}(l) = -\Delta_{p_ip_f} g_{p_ip_f} = \frac{1}{\Delta_{p_ip_f}}\cdot\frac{dg_{p_ip_f}}{dl}\ . \tag{4.19}$$

where we have introduced $\Delta_{p_ip_f} = \sum p_i^- - \sum p_f^-$, and the light-front fermion energy is $p^- = \frac{p^{\perp 2}+m^2}{p^+}$, the photon one $q^- = \frac{q^{\perp 2}}{q^+}$. Further we calculate the bound states of positronium. In what follows we consider in the $|e\bar{e}>$ sector
the **generated interaction** to the first nonvanishing order

$$H^{gen}_{e\bar{e}e\bar{e}} = \sum_{s_1\bar{s}_2 s_3\bar{s}_4}\int d^3p_1 d^3p_2 d^3p_3 d^3p_4 V^{gen}_{p_ip_f}(l) b^+_{p_3} d^+_{p_4} d_{p_2} b_{p_1}\chi^+_{s_3}\chi^+_{\bar{s}_4}\chi_{\bar{s}_2}\chi_{s_1}\delta_{p_1+p_2,p_3+p_4}\ , \tag{4.20}$$

with the initial condition $\lim_{\Lambda\to\infty} V^{gen}_{p_ip_f}(l_\Lambda) = 0$,
and the **instantaneous interaction**

$$H^{inst}_{e\bar{e}e\bar{e}} = \sum_{s_1\bar{s}_2 s_3\bar{s}_4}\int d^3p_1 d^3p_2 d^3p_3 d^3p_4 V^{inst}_{p_ip_f}(l) b^+_{p_3} d^+_{p_4} d_{p_2} b_{p_1}\chi^+_{s_3}\chi^+_{\bar{s}_4}\chi_{\bar{s}_2}\chi_{s_1}\delta_{p_1+p_2,p_3+p_4}\ , \tag{4.21}$$

where

$$\begin{aligned}V^{inst}_{p_ip_f}(l) &= g^{inst}_{p_ip_f}(l)\frac{4}{(p_1^+ - p_3^+)^2},\\ \lim_{\Lambda\to\infty} g^{inst}_{p_ip_f}(l_\Lambda) &= e^2\ .\end{aligned} \tag{4.22}$$

where the initial (bare) value of instantaneous interaction (its matrix element in $|e\bar{e}>$ sector eq. (4.22)) is defined by the instantaneous term $\mathcal{H}^{inst}_{eeee}$ eq. (3.7),eq. (3.8) of the canonical light-front QED Hamiltonian. The order of the field operators in both interactions satisfies the prescription of standard Feynmann rules in the $|e\bar{e}>$ sector.

We note, that generated interaction eq. (4.20) is a new interaction, induced by flow equations in the second order in coupling, and corresponds to the dynamical photon exchange; while the instantaneous term eq. (4.21) enters the canonical light-front QED Hamiltonian and describes the instant photon exchange. Instantaneous term is special for the light-front calculations [1].

To the leading (second) order we neglect the $l$ dependence of the energies (which start to run in the second order in coupling constant, see chapter 7) in the interactions, that enables to write the flow equations for the corresponding couplings.

The flow equations to the first (for the electron-photon coupling) and second (for the instantaneous and generated interactions) orders are

$$\begin{aligned}\frac{dg_{p_ip_f}(l)}{dl} &= -\Delta_{p_ip_f}^2 g_{p_ip_f}(l)\\ \frac{dg_{p_ip_f}^{inst}(l)}{dl} &= 0 \\ \frac{dV_{p_ip_f}^{gen}(l)}{dl} &= <[\eta^{(1)}(l),H_{ee\gamma}]>_{|e\bar{e}>}\ ,\end{aligned}\tag{4.23}$$

where

$$\Delta_{p_ip_f}=\sum p_i^- - \sum p_f^- \tag{4.24}$$

The second and the third equations are written for the 'diagonal' sector. The matrix element $<[\eta^{(1)}(l),H_{ee\gamma}]>_{|e\bar{e}>}$ is understood as the corresponding commutator between the free electron-positron states, namely $<p_3s_3,p_4\bar{s}_4|...|p_1s_1,p_2\bar{s}_2>$. In the order $O(e^2)$ there is also the contribution of the commutator $<[\eta^{(1)},H_{ee\gamma}]>$ to the free Hamiltonian in one-electron and one-photon sectors, that defines the renormalization of electron and photon masses, resp., (see chapter 7). Renormalization group running of both (instantaneous and generated) interactions starts in the order $O(e^4)$, and the electron-photon coupling starts to run in the order $O(e^3)$.

Neglecting the dependence of the light-front energies on the flow parameter $l$ (that is the corrections of higher orders), the solution of eq. (4.24) reads

$$\begin{aligned}g_{p_ip_f}(l) &= f_{p_ip_f}\cdot e+O(e^3)\\ g_{p_ip_f}^{inst}(l) &= g_{p_ip_f}^{inst}(l_\Lambda=0)=e^2+O(e^4)\\ V_{p_ip_f}^{gen}(l) &= \int_0^l dl'<[\eta^{(1)}(l'),H_{ee\gamma}(l')]>_{|e\bar{e}>}+O(e^4)\\ f_{p_ip_f} &= \mathrm{e}^{-\Delta_{p_ip_f}^2 l}=\mathrm{e}^{-\frac{\Delta_{p_ip_f}^2}{\lambda^2}}\ ,\end{aligned}\tag{4.25}$$

where the subscript $|e\bar{e}>$ means, that the commutator is considered in the electron-positron sector. The electron-photon interaction exists in the band of size $\lambda$ ($|\Delta_{p_ip_f}|<\lambda$), whereas the matrix elements of instantaneous and generated interactions in $|e\bar{e}>$ sector are defined for all energy differences.

We give below the explicit expressions for the generated interaction, and details of calculations can be found in Appendix A. In what follows we use the notations of this Appendix.

The matrix elements of the commutator $[\eta^{(1)},H_{ee\gamma}]$ in the exchange and annihilation channels are

$$<[\eta^{(1)},H_{ee\gamma}]>=\left\{\begin{array}{l} M_{2ii}^{(ex)}\frac{1}{(p_1^+-p_3^+)}\left(\eta_{p_1,p_3}g_{p_4,p_2}+\eta_{p_4,p_2}g_{p_1,p_3}\right)\ ,\\ \\ -M_{2ii}^{(an)}\frac{1}{(p_1^++p_2^+)}\left(\eta_{p_1,-p_2}g_{p_4,-p_3}+\eta_{p_4,-p_3}g_{p_1,-p_2}\right)\ ,\end{array}\right.\tag{4.26}$$

---

[1] The analogous problem, interacting electrons and phonons in a solid, was considered by Wegner and Lenz [10]. They used 'equal time' canonical electron-phonon Hamiltonian known from BCS-theory. The elimination of electron-phonon interaction by the flow equations generates a new interaction between electrons, that defines an effective electron-electron interaction. This effective interaction leads to the leading Coulomb behavior.

where

$$\begin{aligned}
&\eta_{p_1,p_2}(l) = e \cdot \frac{1}{\Delta_{p_1 p_2}} \frac{df_{p_1,p_2}(l)}{dl} \\
&g_{p_1,p_2}(l) = e \cdot f_{p_1,p_2}(l) \\
&\Delta_{p_1,p_2} = p_1^- - p_2^- - (p_1 - p_2)^-
\end{aligned} \tag{4.27}$$

and the conservation of "+" and "⊥" components of the total momentum is implied, i.e. $p_1^+ + p_2^+ = p_3^+ + p_4^+$ and $p_1^\perp + p_2^\perp = p_3^\perp + p_4^\perp$. The matrix elements $M_{2ii}$ between the corresponding spinors in both channels are given

$$\begin{aligned}
M_{2ij}^{(ex)} &= [\chi_{s_3}^+ \Gamma^i(p_1, p_3, p_1 - p_3)\chi_{s_1}]\,[\chi_{\bar{s}_2}^+ \Gamma^j(-p_4, -p_2, -(p_1 - p_3))\chi_{\bar{s}_4}] \\
M_{2ij}^{(an)} &= [\chi_{s_3}^+ \Gamma^i(-p_4, p_3, -(p_1 + p_2))\chi_{\bar{s}_4}]\,[\chi_{\bar{s}_2}^+ \Gamma^j(p_1, -p_2, p_1 + p_2)\chi_{s_1}]
\end{aligned} \tag{4.28}$$

where

$$\Gamma^i(p_1, p_2, q) = 2\frac{q^i}{q^+} - \frac{\sigma \cdot p_2^\perp - im}{p_2^+}\sigma^i - \sigma^i \frac{\sigma \cdot p_1^\perp + im}{p_1^+} \tag{4.29}$$

This equation, eq. (4.29), defines the spin structure of the generated interaction.

We combine the formulas for commutator $[\eta^{(1)}, H_{ee\gamma}]$ together with the generator $\eta(l)$ and coupling constant $g(l)$, expressed through the similarity function $f(l)$. The generated interactions eq. (4.25) are given then in both channels

$$\begin{aligned}
V_{gen}^{(ex)}(\lambda) &= -e^2 M_{2ii}^{(ex)} \frac{1}{(p_1^+ - p_3^+)} \left( \frac{\int_\lambda^\infty \frac{df_{p_1,p_3,\lambda'}}{d\lambda'} f_{p_4,p_2,\lambda'} d\lambda'}{\Delta_{p_1,p_3}} + \frac{\int_\lambda^\infty \frac{df_{p_4,p_2,\lambda'}}{d\lambda'} f_{p_1,p_3,\lambda'} d\lambda'}{\Delta_{p_4,p_2}} \right) \\
V_{gen}^{(an)}(\lambda) &= e^2 M_{2ii}^{(an)} \frac{1}{(p_1^+ + p_2^+)} \left( \frac{\int_\lambda^\infty \frac{df_{p_1,-p_2,\lambda'}}{d\lambda'} f_{p_4,-p_3,\lambda'} d\lambda'}{\Delta_{p_1,-p_2}} + \frac{\int_\lambda^\infty \frac{df_{p_4,-p_3,\lambda'}}{d\lambda'} f_{p_1,-p_2,\lambda'} d\lambda'}{\Delta_{p_4,-p_3}} \right) \\
&.
\end{aligned} \tag{4.30}$$

where in the integral we have neglected the dependence of light-front energies on the cutoff $\lambda$ (that is the correction of the order $O(e^2)$), and the connection between flow parameter and cutoff, $l = 1/\lambda^2$, is used. We use the explicit form for similarity function

$$f_{p_1,p_2,\lambda} = \mathrm{e}^{-\frac{\Delta_{p_1 p_2}^2}{\lambda^2}} \; . \tag{4.31}$$

that gives for the generated interaction in both channels fig.(2), fig.(3)

$$\begin{aligned}
V_{gen}^{(ex)}(\lambda) &= -e^2 M_{2ii}^{(ex)} \frac{1}{(p_1^+ - p_3^+)} \frac{\Delta_{p_1,p_3} + \Delta_{p_4,p_2}}{\Delta_{p_1,p_3}^2 + \Delta_{p_4,p_2}^2} \cdot (1 - f_{p_1,p_3,\lambda} f_{p_4,p_2,\lambda}) \\
V_{gen}^{(an)}(\lambda) &= e^2 M_{2ii}^{(an)} \frac{1}{(p_1^+ + p_2^+)} \frac{\Delta_{p_1,-p_2} + \Delta_{p_4,-p_3}}{\Delta_{p_1,-p_2}^2 + \Delta_{p_4,-p_3}^2} \cdot (1 - f_{p_1,-p_2,\lambda} f_{p_4,-p_3,\lambda}) \; ,
\end{aligned} \tag{4.32}$$

For finite values of $l$ the solutions of the flow equations have no divergences in the form of small energy denominators, present in perturbation theory. The divergent contribution in the generated interaction as $\Delta_{p_1,p_3} \sim \Delta_{p_4,p_2} \sim 0$ is effectively cancelled by the factor in bracket containing similarity functions $(1-f_{p_1,p_3,\lambda}f_{p_4,p_2,\lambda})$ (the same for annihilation channel). One has for the generated interaction in the exchange channel

$$\frac{\Delta_{p_1,p_3}+\Delta_{p_4,p_2}}{\Delta^2_{p_1,p_3}+\Delta^2_{p_4,p_2}}=\frac{\Delta_{p_1,p_3}+\Delta_{p_4,p_2}}{\Delta^2_{p_ip_f}+2\Delta_{p_1,p_3}\Delta_{p_4,p_2}} \tag{4.33}$$

where

$$\Delta_{p_ip_f}\equiv p_1^-+p_2^--p_3^--p_4^-=\Delta_{p_1,p_3}-\Delta_{p_4,p_2}=\Delta_{p_1,-p_2}-\Delta_{p_4,-p_3} \tag{4.34}$$

due to the total momentum conservation in $'+'$ and 'transversal' directions. The matrix elements with any energy differences (i.e. $\forall\Delta_{p_ip_f}$) are present in 'diagonal' sector.

The effective Hamiltonian is defined in the limit $\lambda\to 0$. In this limit the electron-photon coupling, present in generated interaction through the similarity functions $f_{p_ip_f}$, is completely eliminated $f_{p_ip_f}(\lambda\to 0)=0$ for $\Delta_{p_ip_f}\neq 0$, and generated interaction is given by the expression that does not depend explicitly on the cutoff $\lambda$.

The resultant **generated interactions** in both channels are given fig.(2),fig.(3)

$$\begin{aligned}
\tilde{V}^{(ex)}_{gen} &= -e^2N_{1,\lambda}\,\frac{\tilde{\Delta}_1+\tilde{\Delta}_2}{\tilde{\Delta}_1^2+\tilde{\Delta}_2^2}\\
\tilde{V}^{(an)}_{gen} &= e^2N_{2,\lambda}\,\frac{M_0^2+M_0'^2}{M_0^4+M_0'^4}\ ,
\end{aligned} \tag{4.35}$$

where we have introduced

$$\begin{gathered}
P^{+2}M^{(ex)}_{2ii,\lambda}=-N_1\quad;\qquad P^{+2}M^{(an)}_{2ii,\lambda}=N_2\\
\Delta_{p_1p_3}=\tfrac{\Delta_1}{P^+}=\tfrac{\widetilde{\Delta}_1}{(x'-x)P^+}\quad;\qquad \Delta_{p_4p_2}=\tfrac{\Delta_2}{P^+}=\tfrac{\widetilde{\Delta}_2}{(x'-x)P^+};\\
\Delta_{p_1,-p_2}=\tfrac{M_0^2}{P^+}\quad;\qquad \Delta_{p_4,-p_3}=\tfrac{M'^2_0}{P^+}
\end{gathered} \tag{4.36}$$

(see Appendix A for the explicit definition of these quantities in the light-front frame).

The expression eq. (4.35) is written for the rescaled value of the potential, i.e. $V_\lambda=\tilde{V}_\lambda/P^{+2}$, and the cutoff is defined in units of the total momentum $P^+$, i.e. $\lambda\to\frac{\lambda^2}{P^+}$, with $l=1/\lambda^2$. The spin structure of the interaction is carried by the matrix elements $M_{2ii}$, defined in Appendix A.

We summarize the **instantaneous interactions** in both channels in the order $\mathbf{O(e^2)}$ fig.(2),fig.(3)

$$\begin{aligned}
V^{(ex)}_{inst} &= -\frac{4e^2}{(p_1^+-p_3^+)^2}\ \delta_{s_1s_3}\delta_{s_2s_4}\\
V^{(an)}_{inst} &= \frac{4e^2}{(p_1^++p_2^+)^2}\ \delta_{s_1\bar{s}_2}\delta_{s_3\bar{s}_4}\ ,
\end{aligned} \tag{4.37}$$

where we have used $\chi^+_{s_3}\chi^+_{\bar{s}_2}1\!\!1\chi_{s_1}\chi_{\bar{s}_4}=\delta_{s_1s_3}\delta_{s_2s_4}+\delta_{s_1\bar{s}_2}\delta_{s_3\bar{s}_4}$. For the rescaled potential in the light-front frame Appendix A eq. (A.14) we have

$$\begin{aligned}
\tilde{V}^{(ex)}_{inst} &= -\frac{4e^2}{(x-x')^2}\ \delta_{s_1s_3}\delta_{s_2s_4}\\
\tilde{V}^{(an)}_{inst} &= 4e^2\ \delta_{s_1\bar{s}_2}\delta_{s_3\bar{s}_4}\ .
\end{aligned} \tag{4.38}$$

In the second order in coupling the effective electron-positron interaction, calculated in the light-front dynamics, is given as a sum of interactions, generated by the flow equations eq. (4.35), and instantaneous interactions eq. (4.38), that are present in the light-front gauge calculations;i.e.

$$V^{eff} = \tilde{V}^{gen} + \tilde{V}^{inst} = \sum_{(i)=ex,ann} (\tilde{V}^{(i)}_{gen} + \tilde{V}^{(i)}_{inst}) \tag{4.39}$$

where we sum over exchange and annihilation channels.

In the chapters 5 and 6 we use the effective electron-positron interaction eq. (4.39) to calculate positronium mass spectrum.

In the next section we outline the general computational strategy to solve for bound states of positronium using an effective Hamiltonian.

### 4.3.2 Positronium model (general computational strategy)

In this section we give the program to solve positronium bound state problem in the light-front dynamics. This approach can be applied also to the other systems.

Required that the particle number (Fock state) conserving terms in the Hamiltonian were considered to be diagonal and the other terms off-diagonal an effective Hamiltonian was obtained which is block-diagonal in particle number (Fock) space. This means, that the 'diagonal' sectors are decoupled, since the particle number (Fock state) violating contributions are eliminated, and one is able then to truncate the full Fock space in the effective Hamiltonian to the lowest Fock sectors of interest. The bound state problem is reduced then to a few-particle Hamiltonian problem. Sure, this is true to the given order of perturbation theory. This is the idea of the approach.

Below we illustrate schematically this procedure for the case of light-front QED, where the positronium bound state problem is reduced to a two-particle problem.

We start with the light front Schrödinger equation for the positronium model

$$H_{LC}|\psi_n >= M_n^2|\psi_n > \tag{4.40}$$

where $H_{LC} = P^\mu P_\mu$ is the invariant mass (squared) operator, referred for convenience to as the light front Hamiltonian of positronium and $|\psi_n >$ being the corresponding eigenfunction; $n$ labels all the quantum numbers of the state.

The canonical Hamiltonian of the system $H_{LC}$ contains infinitely many Fock sectors (i.e. one has for the positronium wave function $|\psi_n >= c_{e\bar{e}}|(e\bar{e})_n > +c_{e\bar{e}\gamma}|(e\bar{e}\gamma)_n > +c_{e\bar{e}\gamma\gamma}|(e\bar{e}\gamma\gamma)_n > +...$) and each Fock sector contains states with arbitrarily large energies. We now

(1) introduce the bare cutoff (regularization) with the result $H^B(\Lambda)$ - the bare Hamiltonian;

(2) perform the unitary transformation by means of flow equations with the result $H^{eff}$ - the effective renormalized Hamiltonian (table 1 for finite value of $\lambda$);

(3) truncate the Fock space to the lowest Fock sector ($|e\bar{e} >$) with the result $\tilde{H}^{eff}$ - the effective, renormalized Hamiltonian acting in the electron-positron sector.

Then the eigenvalue equation reads

$$\tilde{H}^{eff}|(e\bar{e})_n >= M_n^2|(e\bar{e})_n > . \tag{4.41}$$

The effective light front Hamiltonian consists of the free (noninteracting) part and the effective electron-positron interaction

$$\tilde{H}^{eff} = H^{(0)} + V^{eff} \tag{4.42}$$

The light front equation eq. (4.41) is then expressed by the integral equation (the coordinates are given in fig.(4)

$$\left(\frac{m^2+\vec{k}_\perp'^2}{x'(1-x')}-M_n^2\right)\psi_n(x',\vec{k}_\perp';s_3,s_4)$$
$$+\quad\sum_{s_1,s_2}\int_D\frac{dxd^2k_\perp}{2(2\pi)^3}<x',\vec{k}_\perp';s_3,s_4|V^{eff}|x,\vec{k}_\perp;s_1,s_2>\psi_n(x,\vec{k}_\perp;s_1,s_2)=0 \tag{4.43}$$

The kernel of this equation, the effective electron-positron interaction $V^{eff}$, was obtained in the previous section, eq. (4.39). Note, that the effective interaction $V^{eff}$, present in eq. (4.43), is boost invariant (i.e. does not depend on $P^+$). The integration domain $D$ in eq. (4.43) is restricted by the covariant cutoff condition [45]

$$\frac{m^2+\vec{k}_\perp^2}{x(1-x)}\leq\Lambda^2+4m^2 \tag{4.44}$$

which allows for states which have a kinetic energy below the cutoff $\Lambda$.

In the chapter 5 we solve eigenvalue equation eq. (4.41) analytically, using the bound state perturbation theory. In the chapter 6 we solve the corresponding integral equation eq. (4.43) numerically, using the numerical methods elaborated in Tamm-Dancoff approach and discussed in the section 3.2.2.

We have considered here $|e\bar{e}>$-sector. In the next section we consider extended Fock space to give diagrammatic representation of the effective Hamiltonian, obtained in the second order in $e$.

### 4.3.3 Effective, renormalized QED Hamiltonian

In this section we review diagrammatic rules for the effective Hamiltonian, obtained by flow equations in the second order in $e$. It is useful to represent Hamiltonian matrix elements in the form of table, consisting of different Fock blocks, each of them has infinite many matrix elements describing the transition between corresponding Fock states and with infinite many energy differences (Table 1). In this representation the canonical field theory Hamiltonian on the light-front has definite structure, that is simpler than that in equal-time formalism. On the light-front the vacuum 'does not fluctuate'. This means, that only one- and two-particle transitions are possible, three- and more-particle transitions are absent. In the case of QED on the light-front one-particle transitions are defined by the electron-photon interaction and two-particle transitions are given by the instantaneous interactions. Kinetic energy term is diagonal in Fock space representation, also there are instantaneous terms that does not change particle number. The canonical QED Hamiltonian has therefore pentadiagonal structure in this representation [28].

Now consider the effective QED Hamiltonian. We do not include instantaneous diagrams, since the flow equations do not change them to the second order in coupling. We start with the situation, when the 'rest' (Fock state changing) sector consists of matrix elements of electron-photon vertex, and the 'diagonal' (Fock state conserving) sector has matrix elements of kinetic terms for electron and photon. We perform the unitary transformation to eliminate the 'rest' sector. In the second order in $e$ the elimination of electron-photon vertex generates one- and two-particle operators. The elimination of 'rest' sector in the next orders in $e$ generates many-particle operators.

The matrix elements of the effective Hamiltonian, obtained by flow equations in the second order in $e$, namely the diagrams in different Fock sectors are depicted in Table 1. Dot denote the zero in the second order matrix elements. Corresponding analytic expressions for the matrix elements in 'diagonal' and 'rest' sectors are listed in fig.(2). The diagrammatic rules are obtained by direct calculation of matrix elements between free particle states. We consider the situation with finite $\lambda$. The matrix elements of the 'rest' sectors are squeezed in the energy band $\Delta_{p_ip_f} = |\sum p_i^- - \sum p_f^-| < \lambda$; there are matrix elements with all energy differences in 'diagonal' sector. As $\lambda \to 0$ the 'rest' sector is completely eliminated to the given order of perturbation theory. One ends up with the block-diagonal effective Hamiltonian, where in each block the Fock state is conserved.

For completenes we give below the matrix elements of effective interactions in different Fock sectors, generated by the flow equations in the second order in coupling constant. The transitions between Fock states and corresponding matrix elements are given, resp.,
in the **'diagonal' sectors**

$$
\begin{aligned}
& |e\bar{e}> \to |e\bar{e}>, |e\bar{e}e\bar{e}> \to |e\bar{e}e\bar{e}>, ... \\
& -e_\lambda^2 M_{2ij,\lambda}\delta^{ij}\frac{1}{[p_1^+ - p_3^+]}\left(\frac{\int_\lambda^\infty \frac{df_{p_1p_3\lambda'}}{d\lambda'}f_{p_4p_2\lambda'}d\lambda'}{\Delta_{p_1p_3\lambda}} + \frac{\int_\lambda^\infty \frac{df_{p_4p_2\lambda'}}{d\lambda'}f_{p_1p_3\lambda'}d\lambda'}{\Delta_{p_4p_2\lambda}}\right) \\
& |e\bar{e}\gamma> \to |e\bar{e}\gamma>, |e\bar{e}\gamma\gamma> \to |e\bar{e}\gamma\gamma>, ... \\
& e_\lambda^2 \tilde{M}_{2ij,\lambda}\varepsilon^{i*}\varepsilon^j\left(\frac{\int_\lambda^\infty \frac{df_{p_1k_1\lambda'}}{d\lambda'}f_{p_2k_2\lambda'}d\lambda'}{\Delta_{p_1k_1\lambda}} + \frac{\int_\lambda^\infty \frac{df_{p_2k_2\lambda'}}{d\lambda'}f_{p_1k_1\lambda'}d\lambda'}{\Delta_{p_2k_2\lambda}}\right) \ ,
\end{aligned}
\tag{4.45}
$$

in the **'rest' sectors**

$$
\begin{aligned}
& |e\bar{e}> \to |e\bar{e}e\bar{e}>, |e\bar{e}e\bar{e}> \to |e\bar{e}>, ... \\
& -e_\lambda^2 f_{p_ip_f\lambda} M_{2ij,\lambda}\delta^{ij}\frac{1}{[p_1^+ - p_3^+]}\left(\frac{\int_\lambda^\infty \frac{1}{f_{p_ip_f\lambda'}}\frac{df_{p_1p_3\lambda'}}{d\lambda'}f_{p_4p_2\lambda'}d\lambda'}{\Delta_{p_1p_3\lambda}} + \frac{\int_\lambda^\infty \frac{1}{f_{p_ip_f\lambda'}}\frac{df_{p_4p_2\lambda'}}{d\lambda'}f_{p_1p_3\lambda'}d\lambda'}{\Delta_{p_4p_2\lambda}}\right) \\
& |e\bar{e}> \to |\gamma\gamma>, |\gamma\gamma> \to |e\bar{e}>, ... \\
& e_\lambda^2 f_{p_ip_f\lambda}\tilde{M}_{2ij,\lambda}\varepsilon^{i*}\varepsilon^j\left(\frac{\int_\lambda^\infty \frac{1}{f_{p_ip_f\lambda'}}\frac{df_{p_1k_1\lambda'}}{d\lambda'}f_{p_2k_2\lambda'}d\lambda'}{\Delta_{p_1k_1\lambda}} + \frac{\int_\lambda^\infty \frac{1}{f_{p_ip_f\lambda'}}\frac{df_{p_2k_2\lambda'}}{d\lambda'}f_{p_1k_1\lambda'}d\lambda'}{\Delta_{p_2k_2\lambda}}\right) \ ,
\end{aligned}
\tag{4.46}
$$

where 'dots' denote the higher Fock sectors; one obtains the next higher Fock sector, when in the given Fock state an additional $(e\bar{e})$-pair or $\gamma$-photon are created. Note, that in eq. (4.45),eq. (4.46) the order of momenta is given for $|e\bar{e}>$ channel, fig.(2). We use the similarity function

$$
\begin{aligned}
& f_{p_ip_f\lambda} = \mathrm{e}^{-\frac{\Delta_{p_ip_f}^2}{\lambda^2}} \\
& \Delta_{p_ip_f} = \sum p_i^- - \sum p_f^- \ ,
\end{aligned}
\tag{4.47}
$$

in eq. (4.45),eq. (4.46) to get the explicit form of interactions in both sectors listed in fig.(2). 'Rest' diagrams are drawn schematically to show the difference between the interactions in 'diagonal' and 'rest' sectors. Namely, for the 'rest' sectors we imply, that the corresponding momentum exchange must be done in the diagrams of fig.(2) to get analytical expressions for diagrams depicted in Table 1.

In the second order flow equations give rise to the mass corrections in one-particle sector. It turns out that the electron, photon mass corrections are equal, but have the opposite sign, to the standard electron, photon self energy terms, obtained in the light-front perturbation theory. We consider this explicitly in the chapter 7. In order to make the diagrammatic rules complete we include mass diagram for the photon in the table (sector $|\gamma>\to|\gamma>$). After the unitary transformation is performed the electron (photon) mass depends on the cutoff

$$m_\lambda^2 = m_0^2 - \delta\Sigma_\lambda \ , \tag{4.48}$$

where $\delta\Sigma_\lambda$ is the self energy term ($m_0 = 0$ for a photon), and subscript 0 denotes the bare mass. In the third order the coupling constant gets the cutoff dependence, i.e. $e_\lambda = e_0(1 + O(e_\lambda^2))$, that is beyond our consideration.

The two-component LF theory, introduced by Zhang and Harindranath [24], as compared to four-component formalism of Brodsky and Lepage, is formulated purely in terms of physical degrees of freedom; so that each term in the effective, renormalized Hamiltonian corresponds to a real dynamical process (or give renormalization term). Different 'diagonal' sectors of the effective Hamiltonian contribute to: in $|\gamma>$ sector - to self energy photon operator, in $|e\bar{e}>$ sector - to electron-positron bound state (or corresponding scattering process), in $|\gamma\gamma>$ sector - to light-light scattering, in $|e\bar{e}\gamma>$ sector - to Compton scattering, *et. cetera* (see Table 1).

In the previous section we considered this formalism in application to the positronium bound state problem.

# Chapter 5

# Positronium spectrum (analytically)

In this chapter we solve an effective eigenvalue equation for positronium, obtained in the previous chapter, analytically. We perform the bound state calculations perturbatively. The idea of calculations is the following. We split an effective Hamiltonian $H^{eff}$ into $H^{(0)}$, a part which is solved nonperturbatively, and $\delta V$, the difference between the original Hamiltonian and $H^{(0)}$. The effects of $\delta V$ are to be computed using bound state perturbation theory. The criteria for choosing $H^{(0)}$ is that it approximates the physics relevant for the given bound states (positronium in our case) as closely as possible. As a consequence, $H^{(0)}$ contributes the dominant term to the mass spectrum and the bound state perturbation theory converges with respect to $\delta V/H^{(0)}$. For QED, where the analytic answer is known, the leading order solution $H^{(0)}$ is simply given by a sum of kinetic terms and the Coulomb potential. This result arise straightforward from the form of the effective electron-positron Hamiltonian in the nonrelativistic limit. For more complicated theories as QCD the hint to choose $H^{(0)}$ comes from phenomenological models.

In the next section we define explicitly bound state perturbation theory for positronium system. The calculation of Bohr spectrum and the ground state spin-splittings is given further. In analytical calculations of singlet-triplet spin-splitting we follow the work [39].

## 5.1 Bound state perturbative theory (BSPT)

First introduce instead of the light front parameterization fig.(3), used before for the single-particle momenta, the instant form. We express the variable $(x, \vec{\kappa}_\perp)$ in terms of the equal-time variable $\vec{p} = (p_z, \vec{\kappa}_\perp)$ as

$$x = \frac{1}{2}\left(1 + \frac{p_z}{\sqrt{\vec{p}^2 + m^2}}\right) \tag{5.1}$$

$$\vec{p}^2 = p_z^2 + \vec{\kappa}_\perp^2 \tag{5.2}$$

and similarly for $x'$ and $\vec{p}'^2$ as function of $p_z'$.

The Jacobian of this transformation, $J(p)$, is

$$J(p) = \frac{dx}{dp_z} = \frac{\kappa_\perp^2 + m^2}{2(\vec{p}^2 + m^2)^{3/2}} \; . \tag{5.3}$$

The instant form is used for practical purposes: it is simpler to recover the rotational symmetry there, the symmetry that is not manifest in the light-front frame.

We choose the leading order Hamiltonian operator for positronium

$$H^{(0)} = h + \hat{V}_{coul} \; , \tag{5.4}$$

where $h$ is the free part (sum of corresponding kinetic terms) and $\hat{V}_{coul}$ is the Coulomb interaction

$$V_{coul} = -\frac{16e^2m^2}{(\kappa_\perp - \kappa'_\perp)^2 + (p_z - p'_z)^2} = -\frac{16e^2m^2}{(\vec{p} - \vec{p'})^2}\ . \tag{5.5}$$

Let us solve the corresponding Schrödinger equation on the light-front

$$H^{(0)}|\psi_N(P)>= E_N|\psi_N(P)>\ , \tag{5.6}$$

where $P$ is the positronium momentum. The eigenvalues and eigenfunctions for positronium bound state on the light-front are defined in a standard way

$$\begin{gathered} E_N = \tfrac{P_\perp^2 + M_N^2}{P^+} \\ |\psi_N(P)>= \textstyle\sum_{s_1s_2} \int_{p_1p_2} \sqrt{p_1^+p_2^+}\, 2(2\pi)^3\, \delta^{(3)}(P - p_1 - p_2)\, \tilde{\Phi}_N(x\kappa_\perp s_1s_2)\, b^+_{s_1}(p_1)\, d^+_{s_2}(p_2)|0> \\ \textstyle\sum_{s_1s_2} \frac{\int d^2\kappa_\perp \int_0^1 dx}{2(2\pi)^3}\, \tilde{\Phi}^*_N(x\kappa_\perp s_1s_2)\, \tilde{\Phi}'_N(x\kappa_\perp s_1s_2) = \delta_{NN'} \end{gathered} \tag{5.7}$$

$M_N$ stands here for the leading order mass of positronium. Combining the definitions for the wave function and the energy together with the light-front Schrödinger equation, one has

$$\left[M_N^2 - \frac{\kappa_\perp'^2 + m^2}{x'(1-x')}\right]\tilde{\Phi}_N(x'\kappa'_\perp s_3s_4) = \sum_{s_1s_2} \frac{\int d^2\kappa_\perp \int_0^1 dx}{2(2\pi)^3}\, V_{coul}\, \tilde{\Phi}_N(x\kappa_\perp s_1s_2)\ , \tag{5.8}$$

or, after change of coordinates according to eq. (5.2),

$$\left(M_N^2 - 4(\vec{p'}^2 + m^2)\right)\Phi_N(\vec{p'}s_3s_4) = \sum_{s_1s_2} \frac{\int d^3p\sqrt{J(p)J(p')}}{2(2\pi)^3}\, V_{coul}(\vec{p},\vec{p'})\, \Phi_N(\vec{p}s_1s_2)\ , \tag{5.9}$$

where the wave functions are redefined to have the norm

$$\sum_{s_1s_2} \int d^3p\, \Phi^*_N(\vec{p}s_1s_2)\, \Phi'_N(\vec{p}s_1s_2) = \delta_{NN'}\ . \tag{5.10}$$

Our aim is to obtain the nonrelativistic Schrödinger equation for positronium. Note, that in the nonrelativistic limit $\vec{p}^2/m^2 \ll 1$ we have

$$\begin{aligned} \sqrt{J(p)J(p')} &\approx \tfrac{1}{2m}\left(1 - \tfrac{\vec{p}^2 + (p_z^2 + {p'_z}^2)}{2m^2}\right) \\ M_N &= (2m + B_N)^2 \approx 4m^2 + 4mB_N^{(0)} \quad , \end{aligned} \tag{5.11}$$

where the leading order binding energy $B_N^{(0)}$ is introduced. Then in the leading order the bound state equation for positronium is

$$\left(\frac{\vec{p'}^2}{m} - B_N\right)\Phi_N(\vec{p'}s_3s_4) = -\sum_{s_1s_2}\int d^3p \left(\frac{1}{2m}\frac{1}{2(2\pi)^3}\frac{1}{4m}\, V_{coul}\right)\Phi_N(\vec{p}s_1s_2)$$

$$. \tag{5.12}$$

Using the explicit form for the Coulomb potential, eq. (5.5), we get the equation that determines the leading order bound state wave function:

$$\left(\frac{\vec{p'}^2}{m} - B_N\right)\Phi_\mu(\vec{p'}) = \frac{\alpha}{2\pi^2}\int \frac{d^3p}{(\vec{p} - \vec{p'})^2}\,\Phi_\mu(\vec{p}) \tag{5.13}$$

with

$$\Phi_N \;=\; \Phi_{\mu,s_e,s_{\bar{e}}}(\vec{p'}s_3s_4) \;=\; \Phi_\mu(\vec{p'})\,\delta_{s_es_3}\,\delta_{s_{\bar{e}}s_4}\;. \tag{5.14}$$

This is the standard nonrelativistic Schrödinger equation for positronium. The solution is characterized by $\mu=(n,l,m)$, the usual principal and angular momentum quantum numbers. The wave functions are given through the hyperspherical harmonics

$$\begin{aligned}
Y_\mu(\Omega) \;&=\; \frac{(e_n^2+\vec{p}^2)^2}{4\,e_n^{5/2}}\,\Phi_\mu\\
Y_\mu \;=\; Y_{n,l,m} \;&=\; f_{n,l}(\omega)\,Y_{l,m}(\theta,\phi)\\
B_N \;&=\; -\frac{m\alpha^2}{4n^2},\qquad e_n \;=\; \frac{m\alpha}{2n}
\end{aligned} \tag{5.15}$$

and for the binding energy one has the standard nonrelativistic expression for positronium bound state to $O(e^2)$. We write for completeness the coordinates used in the solution

$$\begin{aligned}
(e_n^2=-mB_N,\vec{p}) \;&\longrightarrow\; (u_0,\vec{u})\\
u_0 \;=\; \cos\omega \;&=\; \frac{e_n^2-\vec{p}^2}{e_n^2+\vec{p}^2}\\
\vec{u} \;=\; \frac{\vec{p}}{|\vec{p}|}\sin\omega \;&=\; \frac{2e_n\vec{p}}{e_n^2+\vec{p}^2}\;,
\end{aligned} \tag{5.16}$$

but, for details, refer to [39].

Now we define BSPT to solve positronium bound state problem. We introduce the potential, arising in the nonrelativistic Schrödinger equation, eq. (5.13),

$$\begin{aligned}
&V'(\vec{p'}s_3s_4;\vec{p}s_1s_2) = \lim_{\frac{\vec{p}^2}{m^2}<<1}\frac{\sqrt{J(p)J(p')}}{2(2\pi)^3}\frac{1}{4m}V^{eff}\\
&\approx \frac{1}{2(2\pi)^3}\frac{1}{2m}\frac{1}{4m}\lim_{\frac{\vec{p}^2}{m^2}<<1}(\tilde{V}_{exch}+\tilde{V}_{ann})\;.
\end{aligned} \tag{5.17}$$

where $\tilde{V}^{eff}_{LC}=\tilde{V}_{exch}+\tilde{V}_{ann}$ is the effective electron-positron interaction, obtained in the previous chapter. The leading order solution is given in eq. (5.15). We perform perturbative bound state calculations with respect to the difference

$$\delta V = V'(\vec{p'}s_3s_4;\vec{p}s_1s_2) - (-\frac{\alpha}{2\pi^2})\frac{1}{(\vec{p}-\vec{p'})^2}\delta_{s_1s_3}\delta_{s_2s_4}\;, \tag{5.18}$$

Note, that, in order to define the Coulomb potential, i.e. the $e\bar{e}$ interaction in the leading order of BSPT, we take only the first term of nonrelativistic expansion of the Jacobian $J(p)$.

Further we use the matrix elements of $\delta V$, that are defined as

$$<\Phi_{nlm}|\delta V|\Phi_{nlm}>=\int d^3p d^3p'\Phi^*_{nlm}(\vec{p})\delta V\,\Phi_{nlm}(\vec{p'})\;, \tag{5.19}$$

where $\Phi_{nlm}$ are the Coulomb wave functions.

## 5.2 Effective electron-positron interaction in light-front and instant frames

We summarize together all the terms defining the electron-positron interaction $V^{eff}$, eq. (4.39)

$$V^{eff} = \tilde{V}_{exch} + \tilde{V}_{ann} = \sum_{channel} (\tilde{V}^{gen} + \tilde{V}^{inst}) \tag{5.20}$$

we remind that *tilde* above the interaction terms denotes the rescaled potential ($V = \tilde{V}/P^{+2}$), that does not depend on the total momentum $P^+$, i.e. is invariant under the light-front boosts.

In the **light-front frame** the generated interaction and instantaneous term are given resp. in the **exchange channel**

$$\begin{aligned} \tilde{V}^{gen} &= -e^2 N_1 \left( \frac{\tilde{\Delta}_1 + \tilde{\Delta}_2}{\tilde{\Delta}_1^2 + \tilde{\Delta}_2^2} \right) \\ \tilde{V}^{inst} &= -\frac{4e^2}{(x-x')^2}\, \delta_{s_1 s_3}\, \delta_{s_2 s_4} \end{aligned} \tag{5.21}$$

in the **annihilation channel**

$$\begin{aligned} \tilde{V}^{gen} &= e^2 N_2 \left( \frac{M_0^2 + M_0'^2}{M_0^4 + M_0'^4} \right) \\ \tilde{V}^{inst} &= 4e^2\, \delta_{s_1 \bar{s}_3}\, \delta_{s_2 \bar{s}_4}\ , \end{aligned} \tag{5.22}$$

The functions $N_1, N_2$ (current-current terms) and the energy denominators $\tilde{\Delta}_i, i = 1, 2, 3$, $M_0^2, M_0'^2, M_n^2$ are defined in the light-front dynamics [24] as follows (see Appendix A) fig.(3)

$$\begin{aligned} N_1 &= \delta_{s_1 s_3}\delta_{s_2 s_4} T_1^\perp \cdot T_2^\perp - \delta_{s_1 \bar{s}_2}\delta_{s_1 \bar{s}_3}\delta_{s_2 \bar{s}_4} 2m^2 \frac{(x-x')^2}{xx'(1-x)(1-x')} \\ &\quad + im\sqrt{2}(x'-x) \left[ \delta_{s_1 \bar{s}_3}\delta_{s_2 s_4} \frac{s_1}{xx'} T_1^\perp \cdot \varepsilon_{s_1}^\perp + \delta_{s_1 s_3}\delta_{s_2 \bar{s}_4} \frac{s_2}{(1-x)(1-x')} T_2^\perp \cdot \varepsilon_{s_2}^\perp \right] \\ N_2 &= \delta_{s_1 \bar{s}_2}\delta_{s_3 \bar{s}_4} T_3^\perp \cdot T_4^\perp + \delta_{s_1 s_2}\delta_{s_3 s_4}\delta_{s_1 s_3} 2m^2 \frac{1}{xx'(1-x)(1-x')} \\ &\quad + im\sqrt{2} \left[ \delta_{s_3 \bar{s}_4}\delta_{s_1 s_2} \frac{s_1}{x(1-x)} T_3^\perp \cdot \varepsilon_{s_1}^\perp - \delta_{s_3 s_4}\delta_{s_1 \bar{s}_2} \frac{s_3}{x'(1-x')} T_4^\perp \cdot \varepsilon_{s_4}^{\perp *} \right] \\ &\quad \varepsilon_s^i = -\frac{1}{\sqrt{2}}(s, i) \end{aligned} \tag{5.23}$$

and

$$\begin{aligned} T_1^i &= -\left[ 2\frac{(\kappa_\perp - \kappa'_\perp)^i}{(x-x')} + \frac{\kappa_\perp^i(s_2)}{(1-x)} + \frac{\kappa_\perp'^i(\bar{s}_2)}{(1-x')} \right] ; \qquad T_2^i = 2\frac{(\kappa_\perp - \kappa'_\perp)^i}{(x-x')} - \frac{\kappa_\perp^i(s_1)}{x} - \frac{\kappa_\perp'^i(\bar{s}_1)}{x'} \\ T_3^i &= -\frac{\kappa_\perp'^i(\bar{s}_3)}{x'} + \frac{\kappa_\perp'^i(s_3)}{(1-x')} ; \qquad T_4^i = \frac{\kappa_\perp^i(\bar{s}_1)}{(1-x)} - \frac{\kappa_\perp^i(s_1)}{x} \\ &\quad \kappa_\perp^i(s) = \kappa_\perp^i + is\varepsilon_{ij}\kappa_\perp^j\ ; \qquad \varepsilon_{ij} = \varepsilon_{ij3}\ ; \qquad \bar{s} = -s \end{aligned}$$

with the definitions

$$\tilde{\Delta}_1 = \frac{(x\kappa'_\perp - x'\kappa_\perp)^2 + m^2(x-x')^2}{xx'} ; \qquad \tilde{\Delta}_2 = \tilde{\Delta}_1|_{x\to(1-x),x'\to(1-x')}$$

$$
\begin{aligned}
&\Delta_1 = \frac{\tilde{\Delta}_1}{x'-x}\;; \qquad \Delta_2 = \frac{\tilde{\Delta}_2}{x'-x} \\
&M_0^2 = \frac{\kappa_\perp^2 + m^2}{x(1-x)}\;; \qquad M_0^{'2} = \frac{\kappa_\perp^{'2} + m^2}{x'(1-x')} \\
&P^- = \frac{(P^\perp)^2 + M_N^2}{P^+}\;; \qquad P = (P^+, P^\perp)\;; \qquad M_N = 2m + B_N\;. \qquad (5.24)
\end{aligned}
$$

Here $x$ is the light front fraction of the electron momentum, $P$ is the total momentum of positronium and $B_N$ the binding energy of the positronium. The effective interaction eq. (5.20), generated by the flow equations, is defined in the whole parameter region, (except maybe for the Coulomb singularity point $\vec{q} = \vec{p} - \vec{p'} = 0$, where we are not able to eliminate the electron-photon vertex) as follows

$$
\begin{aligned}
V^{eff} &= \tilde{V}_{exch} + \tilde{V}_{ann} \\
&= -e^2 N_1 \left( \frac{\tilde{\Delta}_1 + \tilde{\Delta}_2}{\tilde{\Delta}_1^2 + \tilde{\Delta}_2^2} \right) + \left( -\frac{4e^2}{(x-x')^2}\, \delta_{s_1 s_3}\, \delta_{s_2 s_4} \right) \\
&\quad + e^2 N_2 \left( \frac{M_0^2 + M_0^{'2}}{M_0^4 + M_0^{'4}} \right) + \left( 4e^2\, \delta_{s_1 \bar{s}_3}\, \delta_{s_2 \bar{s}_4} \right)\;, \qquad (5.25)
\end{aligned}
$$

To get the effective interaction in the **instant frame** the substitutions $x(p_z), x'(p_z^{'})$ eq. (5.2) are to be done, also in the instant frame holds

$$
M_0^2 = 4(\vec{p}^{\,2} + m^2)\;; \qquad M_0^{'2} = 4(\vec{p'}^{\,2} + m^2)\;; \qquad (5.26)
$$

At the end of this section we illustrate, that the effective interaction eq. (5.25) gives in the leading order of nonrelativistic expansion $|\vec{p}|/m \ll 1$ the Coulomb interaction. In the leading order one has (for the exchange channel, that gives the dominant contribution)

$$
\begin{aligned}
&\tilde{\Delta}_1 \sim \tilde{\Delta}_2 = \tilde{\Delta} = (\vec{p} - \vec{p'})^2 \\
&V^{gen} \approx -e^2 \frac{N_1}{(\vec{p} - \vec{p'})^2} \\
&\Delta = \frac{(\vec{p} - \vec{p'})^2}{x'-x} \qquad (5.27)
\end{aligned}
$$

and the electron-positron interaction is

$$
V^{|e\bar{e}>} \approx -e^2 \frac{N_1}{(\vec{p} - \vec{p'})^2} - \frac{4e^2}{(x-x')^2} \delta_{s_1 s_3} \delta_{s_2 s_4} \qquad (5.28)
$$

Using the following expressions

$$
\begin{aligned}
&N_1^{diag} \approx -4 \frac{(\vec{\kappa}_\perp - \vec{\kappa}_\perp^{'})^2}{(x-x')^2} \delta_{s_1 s_3} \delta_{s_2 s_4} \\
&(\vec{p} - \vec{p'})^2 = (\vec{\kappa}_\perp - \vec{\kappa}_\perp^{'})^2 + (p_z - p_z^{'})^2 \approx (\vec{\kappa}_\perp - \vec{\kappa}_\perp^{'})^2 + 4m^2 (x-x')^2 \qquad (5.29)
\end{aligned}
$$

one obtains in leading order of the nonrelativistic approximation the 3-dimensional Coulomb interaction ($e^2 = 4\pi\alpha$)

$$
V^{|e\bar{e}>} \approx 16 m^2 \left( -\frac{e^2}{(\vec{p} - \vec{p'})^2} \right) \delta_{s_1 s_3} \delta_{s_2 s_4} \qquad (5.30)
$$

Hence the rotational invariance is restored in this order. This result eq. (5.30) does not depend on the details of the similarity function $f_\lambda(\Delta)$.

## 5.3 Positronium's ground state spin splitting

In this section we use the effective electron-positron interaction eq. (5.25) to calculate the ground state singlet-triplet splitting for positronium. We follow the work [39], where the similarity renormalization scheme was used to get an effective electron-positron interaction.

There is an important difference between the two approaches, flow equations and similarity transformation. Flow equations eliminate the matrix elements between states with large energy differences ($|E_i - E_j| > \lambda$, where $\lambda$ is an effective UV-cutoff), but only for those blocks that change the number of quasiparticles. The value of $\lambda = \Lambda \to \infty$ corresponds to the initial bare Hamiltonian, a finite $\lambda$ determines the effective Hamiltonian at an intermediate stage, for $\lambda = 0$ the elimination of the particle number changing sectors is complete and the effective Hamiltonian is block-diagonal in particle number. One can work then in a few (or even one) lowest Fock sectors.

The effective Hamiltonian, obtained by the similarity transformation, is band-diagonal in the 'energy space'. [1] The width of the band $\lambda$ (namely $\lambda^2/P^+$) introduces the artificial parameter in the procedure, which must be adjusted from the physical reasoning. The effective UV-cutoff must be low enough to neglect the contribution of high Fock states, but is restricted from below to stay in perturbation theory region. In the case of positronium the "window of opportunity" is simple to choose, since there are two dynamical energy scales in QED, $\frac{m^2\alpha^2}{P^+}$ and $\frac{m^2\alpha}{P^+}$, that is one of the reasons why QED calculations have been always so successful. Namely one chooses $m^2\alpha^2 << \lambda^2 << m^2\alpha$, and the effective electron-positron interaction does not depend on $\lambda$ and is defined on the energy scale of positronium bound state formation [39]. In the case of QCD, unfortunately, there is no such 'window', and the procedure of fitting the cutoff seems to be nontrivial [20]. In the case of flow equations elimination of particle number changing sectors can be performed completely, so that there is no artificial parameter (as effective UV-cutoff) left in the effective Hamiltonian.

We use the potential eq. (5.17), that appears in the nonrelativistic Schrödinger equation for positronium eq. (5.13), and defines the nonrelativistic binding energy $B_N$ ($M_N^2 \approx 4m^2 + 4mB_N$). The effective electron-positron interaction eq. (5.25) has the following form in the nonrelativistic limit

$$\begin{aligned} V' &= \frac{1}{2(2\pi)^3}\frac{1}{4m}\frac{1}{2m}\left(1 - \frac{\vec{p}^2}{2m^2}\right) V^{eff} \\ V^{eff} &= \tilde{V}_{exch} + \tilde{V}_{ann} \\ &= -\frac{e^2 N_1}{(\vec{p}-\vec{p}')^2} - \frac{4e^2}{(x-x')^2}\,\delta_{s_1 s_3}\,\delta_{s_2 s_4} \\ &\quad + \frac{e^2 N_2}{4m^2} + 4e^2\,\delta_{s_1 \bar{s}_3}\,\delta_{s_2 \bar{s}_4}\ , \end{aligned} \tag{5.31}$$

where the energy denominators were simplified as

$$x - x' = \frac{p_z - p_z^{'}}{2m}\left[1 + \frac{\vec{p}^2}{2m^2}\right] + O\left(m^2\left(\frac{p}{m}\right)^5\right)$$

$$\tilde{\Delta}_1 = \tilde{\Delta}_2 = (\vec{p}-\vec{p}')^2 + O\left(m^2\left(\frac{p}{m}\right)^5\right)$$

$$\Delta_1 = \Delta_2 = \frac{2m(\vec{p}'-\vec{p})^2}{(p_z^{'} - p_z)}\left[1 + O\left(\left(\frac{p}{m}\right)^2\right)\right]\ ; \qquad \Delta = \frac{2m(\vec{p}'-\vec{p})^2}{(p_z' - p_z)}$$

---

[1] Under the 'energy space' we understand the basis of the free Hamiltonian $H_0$.

$$M_0^2 = M_0'^2 = 4m^2 + O\left(m^2 \left(\frac{p}{m}\right)^2\right) \ , \tag{5.32}$$

The expression for Jacobian of the coordinate change is given

$$\sqrt{J(p)J(p')} = \frac{1}{2m}\left[1 - \frac{\vec{p}^2}{2m^2} + O\left(\frac{p_z^2}{m^2}, \frac{p_z'^2}{m^2}\right)\right] \ , \tag{5.33}$$

Combining all together, we have

$$\begin{aligned} V'(\vec{p},\vec{p'}) \;\; = \;\; & \frac{1}{2(2\pi)^3}\frac{1}{4m}\frac{1}{2m}\left(1 - \frac{\vec{p}^2}{2m^2}\right) \\ & \times\Big[-\frac{e^2 N_1}{(\vec{p}-\vec{p'})^2} \;\; - \frac{16e^2m^2}{(p_z - p_z')^2}\left(1 + \frac{\vec{p}^2}{m^2}\right)\, \delta_{s_1 s_3}\, \delta_{s_2 s_4} \\ & \qquad + \frac{e^2 N_2}{4m^2} \qquad\qquad\qquad\qquad\quad + \; 4e^2 \, \delta_{s_1 \bar{s}_2}\, \delta_{s_3 \bar{s}_4}\Big] \ . \end{aligned} \tag{5.34}$$

We expand the factors $N_1$ and $N_2$, appearing in the interaction, in the nonrelativistic limit. The term $N_1$ contributes in $V'$ in the order

$\underline{O(1), O\left(\left(\frac{p}{m}\right)^2\right)}$:

$$\begin{aligned} - T_1^{\perp} T_2^{\perp} \;\; = \;\; & 16m^2 \frac{q_\perp^2}{q_z^2}\left(1 + \frac{\vec{p}^2}{m^2}\right) + 16\frac{q_\perp^i}{q_z}\left(\kappa_\perp^i p_z + \kappa_\perp^{'i} p_z^{'}\right) \\ & -16i(s_1+s_2)[\kappa_\perp^{'}\kappa_\perp] - 4(\kappa_\perp + \kappa_\perp^{'})^2 + 4s_1 s_2 q_\perp^2 \ , \end{aligned}$$

$\underline{O\left(\frac{p}{m}\right), O\left(\left(\frac{p}{m}\right)^2\right)}$ :

$$\begin{aligned} & im\sqrt{2}(x'-x)\left(\frac{s_1}{xx'}\,\varepsilon_{s_1}^{\perp}\cdot T_1^{\perp}\,\delta_{\bar{s}_1 s_3}\,\delta_{s_2 s_4} \;+ \frac{s_2}{(1-x)(1-x')}\,\varepsilon_{s_2}^{\perp}\cdot T_2^{\perp}\,\delta_{\bar{s}_4 s_2}\,\delta_{s_1 s_3}\right) \\ & \quad = 8\,\delta_{\bar{s}_1 s_3}\,\delta_{s_2 s_4}\,\left[m\,(iq_\perp^x - s_1 q_\perp^y)\left(1 - \frac{p_z + p_z^{'}}{m}\right) + q_z\,(i\tilde{p}_\perp^x - s_1\tilde{p}_\perp^y) + \frac{1}{2}s_2 q_z (q_\perp^y - is_1 q_\perp^x)\right] \\ & \qquad - \delta_{\bar{s}_4 s_2}\,\delta_{s_1 s_3}\left[m\,(iq_\perp^x - s_2 q_\perp^y)\,\left(1 + \frac{p_z + p_z'}{m}\right) - q_z\,(i\tilde{p}_\perp^x - s_2\tilde{p}_\perp^y) - \frac{1}{2}s_1 q_z (q_\perp^y - is_2 q_\perp^x)\right] \ , \end{aligned}$$

$\underline{O\left(\left(\frac{p}{m}\right)^2\right)}$ :

$$2m^2 \frac{(x-x')^2}{xx'(1-x)(1-x')} = 8q_z^2 \ .$$

The term $N_2$ contributes to $V'$ in the order

$\underline{O\left(\left(\frac{p}{m}\right)^2\right)}$ :

$$2m^2 \frac{1}{xx'(1-x)(1-x')} = 32m^2 \ . \tag{5.35}$$

In these formulas we have used $[\kappa_\perp^{'}, \kappa_\perp] = \varepsilon_{ij}\kappa_\perp^{'i}\kappa_\perp^{j}$, $\varepsilon_{ij} = \varepsilon_{ij3}$ and $\varepsilon_s^i = -\frac{1}{\sqrt{2}}(s,i)$; also the following variables have been introduced

$$\begin{aligned} & q_\perp = \kappa_\perp^{'} - \kappa_\perp \ , \qquad (\perp = x,y) \ , \ q_z = p_z^{'} - p_z \\ & \tilde{p}_\perp = \frac{\kappa_\perp + \kappa_\perp^{'}}{2} \ . \end{aligned} \tag{5.36}$$

We do not analyse here the expressions for $N_1$ and $N_2$, where also in this form some terms can be identified as spin-orbit and spin-spin interactions in the transverse plane and in longitudinal (z) direction.

Instead we follow [39], where an analogous calculation of singlet-triplet ground state mass splitting of positronium was performed in the similarity renormalization scheme. We therefore can drop in $N_1$, except for the leading order term $O(1)$, the diagonal part in spin space. Also the terms of the type $f = \kappa_\perp^{x,y} p_z$ , $\kappa_\perp^{x,y} p_z^{'}$ , $\kappa_\perp^x \kappa_\perp^y$ do not contribute to the ground state mass splitting, since

$$\int d^3p d^3p' \, \Phi_{100}^*(\vec{p}) \, \frac{f}{\vec{q}^2} \, \Phi_{100}(\vec{p'}) \; , \tag{5.37}$$

average over directions, gives zero.

In the **leading order** $O(1)$ of nonrelativistic expansion we obtain the following $e\bar{e}$-potential

$$\begin{aligned} V^{'(0)}(\vec{p'},\vec{p}) &= \frac{1}{2(2\pi)^3} \frac{1}{4m} \frac{1}{2m} \left(1 - \frac{\vec{p}^2}{2m^2}\right) \\ &\quad \times \left[ \frac{16e^2m^2}{\vec{q}^2} \frac{q_\perp^2}{q_z^2} \left(1 + \frac{\vec{p}^2}{m^2}\right) - \frac{16e^2m^2}{q_z^2} \left(1 + \frac{\vec{p}^2}{m^2}\right) \right] \delta_{s_1s_3} \, \delta_{s_2s_4} \\ &= -\frac{\alpha}{2\pi^2} \frac{1}{\vec{q}^2} \left(1 + \frac{\vec{p}^2}{2m^2}\right) \delta_{s_1s_3} \, \delta_{s_2s_4} \\ &\longrightarrow \quad V(r) \left(1 + \frac{\vec{p}^2}{2m^2}\right) \; . \end{aligned} \tag{5.38}$$

where $\vec{q} = \vec{p'} - \vec{p}$, and we have done in the last expression the Fourier transformation with respect to $\vec{q}$ to the coordinate space. In the leading order of nonrelativistic expansion we have reproduced the Coulomb potential, defined before as the leading order term in BSPT.

We combine this expression with the kinetic term from the Schrödinger equation, eq. (5.13), and write it in the form

$$\frac{1}{m} \left(1 + \frac{V(r)}{2m}\right) \vec{p}^2 + V(r) \; . \tag{5.39}$$

Here the potential $V(r)$ plays a different role in the two terms. In the first term, corresponding to kinetic energy, it generates an effective mass of the electron, which depends on the relative position and manifests the non-locality of the interaction. The second term is the usual potential energy, in our case, the Coulomb interaction.

The energy of the Coulomb level for positronium with quantum numbers $(nlm)$ is the standard one

$$B^{(0)} =< \Phi_{nlm} | V^{'(0)} | \Phi_{nlm} >= \int d^3p d^3p' \Phi_{nlm}^*(\vec{p}) \left( -\frac{\alpha}{2\pi^2} \frac{1}{(\vec{p} - \vec{p'})^2} \right) \Phi_{nlm}(\vec{p'}) = -\frac{m\alpha^2}{4n^2} \; , \tag{5.40}$$

where the Coulomb wave function $\Phi_{nlm}$ is defined in eq. (5.14),eq. (5.15). We have used in eq. (5.40) the following representation

$$\begin{aligned} (\vec{p} - \vec{p'})^2 &= \frac{(e_n^2 + \vec{p}^2)\,(e_n^2 + \vec{p'}^2)}{4e_n^2} \,(u - u')^2 \\ \frac{1}{(u - u')^2} &= \sum_\mu \frac{2\pi^2}{n} \, Y_\mu(\Omega_p) \, Y_\mu^*(\Omega_{p'}) \\ d^3p &= d\Omega_p \left( \frac{e_n^2 + \vec{p}^2}{2e_n} \right)^3 \end{aligned} \tag{5.41}$$

and also orthogonality of the hyperspherical harmonics

$$\int d\Omega \, Y^*_\mu \, Y_{\mu'} = \delta_{\mu\mu'} \ . \tag{5.42}$$

More details can be found in [39].

Now the result of the first and the second order bound state perturbation theory for positronium ground state ($n = 1$) is presented. These are the corrections to the leading order binding energy $B_n^{(0)}$ eq. (5.40), defined by the nonrelativistic Schrödinger equation for positronium eq. (5.13).

**The next to leading order** $O\left(\frac{p}{m}\right)$

$$\begin{aligned} \delta V^{(1)} &= \frac{1}{2(2\pi)^3} \frac{1}{4m} \frac{1}{2m} \left( -\frac{e^2}{\vec{q}^{\,2}} \right) \\ &\times \left( 8m(iq_\perp^x - s_1 q_\perp^y)\delta_{s_1\bar{s}_3}\delta_{s_2 s_4} - 8m(iq_\perp^x - s_2 q_\perp^y)\delta_{s_1 s_3}\delta_{s_2\bar{s}_4} \right) \end{aligned} \tag{5.43}$$

contributes (because of the spin structure) to the second order of BSPT:

$$\delta^{(2)} B = \sum_{\mu \neq (1,0,0), s_i} \frac{< \Phi_{100} | \delta V^{(1)} | \Phi_{\mu, s_i} > < \Phi_{\mu, s_i} | \delta V^{(1)} | \Phi_{100} >}{B_1^{(0)} - B_n^{(0)}} \ . \tag{5.44}$$

Recall, that $\mu = (n, l, m)$, the usual principal and angular momentum quantum numbers of nonrelativistic positronium. **The order** $O\left(\left(\frac{p}{m}\right)^2\right)$ (cf. remark after eq. (5.36)) is

$$\delta V^{(2)} = \frac{1}{2(2\pi)^3} \frac{1}{4m} \frac{1}{2m} \left( 8e^2 \frac{q_z^2}{\vec{q}^{\,2}} \delta_{s_1\bar{s}_2}\delta_{s_1\bar{s}_3}\delta_{s_2\bar{s}_4} + 8e^2 \delta_{s_1 s_2}\delta_{s_3 s_4}\delta_{s_1 s_3} + 4e^2 \delta_{s_1\bar{s}_3}\delta_{s_2\bar{s}_4} \right) \tag{5.45}$$

and contributes to the first order of BSPT:

$$\delta^{(1)} B = < \Phi_{100} | \delta V^{(2)} | \Phi_{100} > \ . \tag{5.46}$$

Both contributions were calculated in [39] with the result

$$\begin{aligned} \delta B &= \delta^{(1)} B + \delta^{(2)} B \\ < 1 | \delta B | 1 > &= -\frac{5}{12} m\alpha^4 \\ < 2 | \delta B | 2 > &= < 3 | \delta B | 3 > = < 4 | \delta B | 4 > = \frac{1}{6} m\alpha^4 \ , \end{aligned} \tag{5.47}$$

where the eigenvectors in spin space are defined as follows:

$$\begin{aligned} &|1> = \frac{1}{\sqrt{2}} \left( |+-> - |-+> \right) \ , \\ &|2> = \frac{1}{\sqrt{2}} \left( |+-> + |-+> \right) \ , \qquad |3> = |--> \ , \qquad |4> = |++> \ . \end{aligned} \tag{5.48}$$

Using the relation between Coulomb energy units and Ryd $= \frac{1}{2} m\alpha^2$, we get the standard result for the singlet-triplet mass splitting of positronium

$$B_{triplet} - B_{singlet} = \frac{7}{6} \alpha^2 \mathrm{Ryd} + O(m\alpha^5) \tag{5.49}$$

The degeneracy of the triplet ground state $n = 1$ signals the rotational invariance, that is not-manifest symmetry on the light-front.

Brisudova and Perry [42] tried to bring the effective light-front Hamiltonian of positronium, obtained in the second order in coupling by similarity transformation, to the rotational invariant form. They succeeded to get the correct spin-spin interactions, namely they obtained the familiar Breit-Fermi spin-spin and tensor terms. They failed to reproduce the standard (equal-time) spin-orbit interaction using the effective Hamiltonian in the order $O(e^2)$. The reason can be the following.

Each spin enters the electron-positron interaction with a factor of order $q/m$ as compared to the leading Coulomb interaction, that is of order $q^{-2}$. Thus the two-spin interaction enters only in the order $q^0$ or higher. The only contribution to fine structure splitting, $\alpha^4$, comes from order $e^2$ (from the terms $e^2q^0$). The same holds for the spin-triplet splitting (which is quadratic in the spin), discussed above. The contributions to the spin-orbit coupling are of the order $q^{-1}$. In the order $\alpha^4$ also term $e^4q^{-2}$ is important, its contribution to the mass spectrum in order $\alpha^4$ must be considered together with the contribution of $e^2q^{-1}$ term. To get the correct spin-orbit splittings one has to derive the effective interaction to the order $e^4$.

Spin independent interaction is of order $q^{-2}$ and contain also subleading terms in $q$ $(q^{-1}, q^0)$. The spin-independent term $e^2q^0$ contribute to the fine structure splitting, in the order $\alpha^4$. In this order also terms of order $e^4q^{-1}$ and $e^6q^{-2}$ are important. Thus to obtain all contributions of order $\alpha^4$ one has to consider the effective interaction in order $e^2$, $e^4$ and $e^6$.

# Chapter 6

# Positronium spectrum (numerically)

This part of the work is done in collaboration with Dr. U.Trittmann. In this chapter we suggest the form of the effective electron-positron interaction, that preserves the rotational symmetry (at least on the level of the mass spectrum). Using this interaction the light-front integral equation for positronium bound states is solved numerically[1].

## 6.1 Light-front bound state equation

The effective light-front eigenvalue equation for positronium bound states reads (see subsection 4.3.2)

$$\tilde{H}^{eff}|(e\bar{e})_n>=M_n^2|(e\bar{e})_n> . \tag{6.1}$$

where $n$ labels all quantum numbers, and the effective light-front Hamiltonian consists of the free (noninteracting) part and the effective electron-positron interaction

$$\tilde{H}^{eff}=H^{(0)}+V^{eff} \tag{6.2}$$

Note, that the rescaled value (that does not depend on $P^+$) of the effective electron-positron interaction, obtained in the chapter 4, stands in eq. (6.1),eq. (6.2). The integral light-front equation in the momentum space, corresponding to eq. (6.1), is given

$$\left(M_n^2-\frac{m^2+\vec{k}_\perp^2}{x(1-x)}\right)\psi_n(x,\vec{k}_\perp;\lambda_1,\lambda_2)$$

$$=\sum_{\lambda_1',\lambda_2'}\int_D\frac{dx'd^2\vec{k}_\perp'}{2(2\pi)^3}<x,\vec{k}_\perp;\lambda_1,\lambda_2|V^{eff}|x',\vec{k}_\perp';\lambda_1',\lambda_2'>\psi_n(x',\vec{k}_\perp';\lambda_1',\lambda_2') \tag{6.3}$$

where the wave function is normalized

$$\sum_{\lambda_1,\lambda_2}\frac{dxd^2\vec{k}_\perp}{2(2\pi)^3}\psi_n^*(x,\vec{k}_\perp;\lambda_1,\lambda_2)\psi_{n'}(x,\vec{k}_\perp;\lambda_1,\lambda_2)=\delta_{nn'} \tag{6.4}$$

For practical purposes we have chosen Jacobi momenta as depicted on fig.(4). The integration domain $D$ is restricted by the covariant cutoff condition [45]

$$\frac{m^2+\vec{k}_\perp^2}{x(1-x)}\leq\Lambda^2+4m^2 \tag{6.5}$$

---

[1] All numerical calculations were performed by Dr.U.Trittmann. The calculations are preliminary.

which allows for states to have the kinetic energy below the bare cutoff $\Lambda$.

In order to introduce the spectroscopic notation for positronium mass spectrum we integrate out the angular degree of freedom $\varphi$, where $\vec{k}_\perp = k_\perp(\cos\varphi, \sin\varphi)$, by substituting it with the discrete quantum number $J_z = n$, $n \in \mathbf{Z}$ (actually for the annihilation channel only $|J_z| \leq 1$ is possible)

$$\begin{aligned} &< x, k_\perp; J_z, \lambda_1, \lambda_2|\tilde{V}^{eff}|x', k'_\perp; J'_z, \lambda'_1, \lambda'_2 > \\ &\quad = \frac{1}{2\pi}\int_0^{2\pi} d\varphi \mathrm{e}^{-iL_z\varphi}\int_0^{2\pi} d\varphi' \mathrm{e}^{iL'_z\varphi'}(-\frac{1}{2(2\pi)^3}) < x, k_\perp, \varphi; \lambda_1, \lambda_2|V^{eff}|x', k'_\perp, \varphi'; \lambda'_1, \lambda'_2 > \end{aligned} \tag{6.6}$$

where $L_z = J_z - S_z$; $S_z = \frac{\lambda_1}{2} + \frac{\lambda_2}{2}$ and the states can be classified (strictly speaking only for rotationally invariant systems, that is the case in the nonrelativistic limit considered in the chapter 5) according to their quantum numbers of total angular momentum $J$, orbit angular momentum $L$, and total spin $S$. It should be noted that the definition of angular momentum operators in light-front dynamics is problematic because they include the interaction (see introduction in the chapter 3).

We proceed now to solve for the positronium spectrum in all sectors of $J_z$. We formulate therefore the light-front integral equation eq. (6.3) in the form where the integral kernel is given by the effective interaction for the total momentum $J_z$ eq. (6.6). After the change of variables eq. (5.2) $(\vec{k}_\perp; x) = (k_\perp, \varphi; x) \to \vec{p} = (\vec{k}_\perp, k_z) = (\mu\sin\theta\cos\varphi, \mu\sin\theta\sin\varphi, \mu\cos\theta)$

$$x = \frac{1}{2}\left(1 + \frac{\mu\cos\theta}{\sqrt{\mu^2 + m^2}}\right) \tag{6.7}$$

where the Jacobian reads

$$J = \frac{\mu^2}{2}\frac{m^2 + \mu^2(1 - \cos^2\theta)}{(m^2 + \mu^2)^{3/2}}\sin\theta \tag{6.8}$$

one has the following integral equation

$$\begin{aligned} &(M_n^2 - 4(m^2 + \mu^2))\tilde{\psi}_n(\mu, \cos\theta; J_z, \lambda_1, \lambda_2) + \sum_{J'_z, \lambda'_1, \lambda'_2}\int_D d\mu' \int_{-1}^{+1} d\cos\theta' \frac{\mu'^2}{2}\frac{m^2 + \mu'^2(1 - \cos^2\theta')}{(m^2 + \mu'^2)^{3/2}} \\ &\quad \times < \mu, \cos\theta; J_z, \lambda_1, \lambda_2|\tilde{V}^{eff}|\mu', \cos\theta'; J'_z, \lambda'_1, \lambda'_2 > \tilde{\psi}_n(\mu', \cos\theta'; J'_z, \lambda'_1, \lambda'_2) = 0 \end{aligned} \tag{6.9}$$

The integration domain $D$ eq. (6.5) is given now by $\mu \in [0; \frac{\Lambda}{2}]$. Neither $L_z$ nor $S_z$ are good quantum numbers; therefore we set $L_z = J_z - S_z$.

The wave function is normalized

$$\sum_{J_z, \lambda_1, \lambda_2}\int d\mu \; d\cos\theta \tilde{\psi}_n^*(\mu, \cos\theta; J_z, \lambda_1, \lambda_2)\tilde{\psi}_{n'}(\mu, \cos\theta; J_z, \lambda_1, \lambda_2) = \delta_{nn'} \tag{6.10}$$

where $n$ labels all quantum numbers.

The integral equation eq. (6.9) is used further to calculate the positronium mass spectrum numerically.

## 6.2 Brodsky-Lepage prescription of the light-front dynamics: effective electron-positron interaction

In this section we write the effective electron-positron interaction, using the light-front prescription as formulated by Brodsky and Lepage [45]. The problem in the light-front field theory is, that parity and rotational invariance are not manifest symmetries, leaving the possibility that approximations or incorrect renormalization (in our case not gauge invariant regularization) might lead to violations of these symmetries for physical observables. The formulation for light-front field theory of Brodsky, Lepage is for practical use, since it enables to pick up the rotation violating part in the electron-positron interaction and to cancel its contribution in the mass spectrum.

In what follows we write the second order solution of the flow equations in a useful for our calculations form (subsection 6.2.1) and exploit it below to calculate the effective electron-positron interaction, using Brodsky-Lepage prescription of light-front QED (subsection 6.2.2).

### 6.2.1 First and second order solutions of the flow equations

In this section we express the solutions of the flow equations in the first and second orders of perturbation theory through the similarity function. The similarity function defines the 'rate' how fast the 'rest' sectors are eliminated with the flow parameter $l$ (or effective UV-cutoff $\lambda$); exact definition is given below.

We consider the flow equations, written in the form eq. (2.31)

$$\begin{aligned}
\frac{dH_{ij}}{dl} &= [\eta, H_d + H_r]_{ij} - (E_i - E_j)[H_d, H_r]_{ij} + \frac{du_{ij}}{dl}\frac{H_{ij}}{u_{ij}} \\
\eta_{ij} &= [H_d, H_r]_{ij} + \frac{1}{E_i - E_j}\left(-\frac{du_{ij}}{dl}\frac{H_{ij}}{u_{ij}}\right)
\end{aligned} \tag{6.11}$$

where the following conditions on the cutoff function in 'diagonal' and 'rest' sectors, resp., are imposed

$$\begin{aligned}
u_{dij} &= 1 \\
u_{rij} &= u_{ij}
\end{aligned} \tag{6.12}$$

In the perturbative frame we break the Hamiltonian as

$$H = H_{0d} + \sum_n (H_d^{(n)} + H_r^{(n)}) \tag{6.13}$$

where $H^{(n)} \sim e^n$, $e$ is the bare coupling constant (here we do not refer to the definite field theory). To the order of $n$ in coupling constant the flow equations in both sectors are given

$$\begin{aligned}
\frac{dH_{dij}^{(n)}}{dl} &= \sum_k [\eta^{(k)}, H_r^{(n-k)}]_{dij} \\
\eta_{dij}^{(n)} &= 0 \\
\frac{dH_{rij}^{(n)}}{dl} &= \sum_k [\eta^{(k)}, H_d^{(n-k)} + H_r^{(n-k)}]_{rij} - (E_i - E_j)\sum_k [H_d^{(k)}, H_r^{(n-k)}]_{rij} + \frac{du_{ij}}{dl}\frac{H_{rij}^{(n)}}{u_{ij}} \\
\eta_{rij}^{(n)} &= \sum_k [H_d^{(k)}, H_r^{(n-k)}]_{rij} + \frac{1}{E_i - E_j}\left(-\frac{du_{ij}}{dl}\frac{H_{rij}^{(n)}}{u_{ij}}\right) \\
\eta^{(n)} &= \eta_d^{(n)} + \eta_r^{(n)}
\end{aligned} \tag{6.14}$$

We solve these equations in the leading order for the Fock state conserving sector.

$$\begin{aligned}
&\frac{dH^{(2)}_{dij}}{dl} = [\eta^{(1)}_r, H^{(1)}_r]_{dij} \\
&\eta^{(1)}_{rij} = -\frac{1}{E_i - E_j}\frac{dH^{(1)}_{rij}}{dl} \\
&\frac{dH^{(1)}_{rij}}{dl} = \frac{du_{ij}}{dl}\frac{H^{(1)}_{rij}}{u_{ij}}
\end{aligned} \tag{6.15}$$

and $H^{(1)}_{rij} = H^{(1)}_{rji}$. Explicitly one has

$$\begin{aligned}
&\frac{dH^{(2)}_{dij}}{dl} = -\sum_k \left( \frac{1}{E_i - E_k}\frac{dH^{(1)}_{rik}}{dl} H^{(1)}_{rjk} + \frac{1}{E_j - E_k}\frac{dH^{(1)}_{rjk}}{dl} H^{(1)}_{rik} \right)_d \\
&H^{(1)}_{rij}(l) = H^{(1)}_{rij}(l=0)\frac{f_{ij}(l)}{f_{ij}(l=0)}
\end{aligned} \tag{6.16}$$

where we have introduced the function $f_{ij}$ defining the leading order solution for the 'rest' part. Further we refer to it as similarity function. Here

$$f_{ij}(l) = u_{ij}(l) = \mathrm{e}^{-(E_i - E_j)^2 l} \tag{6.17}$$

The similarity function $f_\lambda(\Delta)$ has the same behavior (when $\lambda \to \infty \quad f_\lambda(\Delta) = 1$, and when $\lambda \to 0 \quad f_\lambda(\Delta) = 0$) as the cutoff function $u_\lambda(\Delta)$.

Making use of the connection $l = 1/\lambda^2$, we get

$$\begin{aligned}
&\frac{dH^{(2)}_{dij}}{d\lambda} = -\sum_k \left( \frac{1}{E_i - E_k}\frac{dH^{(1)}_{rik}}{d\lambda} H^{(1)}_{rjk} + \frac{1}{E_j - E_k}\frac{dH^{(1)}_{rjk}}{d\lambda} H^{(1)}_{rik} \right)_d \\
&H^{(1)}_{rij}(\lambda) = H^{(1)}_{rij}(\Lambda \to \infty)\frac{f_{ij}(\lambda)}{f_{ij}(\Lambda \to \infty)}
\end{aligned} \tag{6.18}$$

Neglecting the dependence of the energy $E_i$ on the cutoff, one has

$$\begin{aligned}
&H^{(2)}_{dij}(\lambda) = H^{(2)}_{dij}(\Lambda \to \infty) + \sum_k \left( H^{(1)}_{rik}(\Lambda \to \infty) H^{(1)}_{rjk}(\Lambda \to \infty) \right)_d \\
&\times \left( \frac{1}{E_i - E_k}\int_\lambda^\infty \frac{df_{ik}(\lambda')}{d\lambda'} f_{jk}(\lambda') d\lambda' + \frac{1}{E_j - E_k}\int_\lambda^\infty \frac{df_{jk}(\lambda')}{d\lambda'} f_{ik}(\lambda') d\lambda' \right)_d
\end{aligned} \tag{6.19}$$

where $\Lambda$ is the bare cutoff; the sum $\sum_k$ is over all intermediate states; and the label 'd' denotes the 'diagonal' sector.

In the case of other unitary transformations, eq. (2.33),eq. (2.34), the similarity functions $f(\lambda)$ are given

$$\begin{aligned}
&\frac{dH_{ij}}{d\lambda} = u_{ij}[\eta, H_d + H_r]_{ij} + r_{ij}\frac{du_{ij}}{d\lambda}\frac{H_{ij}}{u_{ij}} \\
&\eta_{ij} = \frac{r_{ij}}{E_i - E_j}\left( [\eta, H_d + H_r]_{ij} - \frac{du_{ij}}{d\lambda}\frac{H_{ij}}{u_{ij}} \right) \\
&f_{ij}(\lambda) = u_{ij}(\lambda)\mathrm{e}^{r_{ij}(\lambda)} \\
&u_{ij} + r_{ij} = 1
\end{aligned} \tag{6.20}$$

and

$$
\begin{aligned}
&\frac{dH_{ij}}{d\lambda} = u_{ij}[\eta, H_d + H_r]_{ij} + \frac{du_{ij}}{d\lambda}\frac{H_{ij}}{u_{ij}} \\
&\eta_{ij} = \frac{1}{E_i - E_j}\left(r_{ij}[\eta, H_d + H_r]_{ij} - \frac{du_{ij}}{d\lambda}\frac{H_{ij}}{u_{ij}}\right) \\
&f_{ij}(\lambda) = u_{ij}(\lambda)
\end{aligned}
\tag{6.21}
$$

where $u(\lambda)$ is the cutoff function. One can choose $u_{ij} = \theta(\lambda - |\Delta_{ij}|)$, where $\Delta_{ij} = \sum_{k=1}^{n_2} E_{i,k} - \sum_{k=1}^{n_1} E_{j,k}$.

The equations eq. (6.19) are the same for all unitary transformations, given above up to the choice of the similarity function $f(\lambda)$. Specifying the function $f(\lambda)$ we get the interaction $H_d^{(2)}$, generated by different unitary transformations.

### 6.2.2 Effective electron-positron interaction

The exchange channel brings the dominant contribution to the mass spectrum. We focus therefore on the electron-positron interaction in the exchange channel. We use eq. (6.19) to calculate the generated electron-positron interaction in the second order in $e$. In this case the 'diagonal' sector (denoted 'd') is $|e\bar{e}>$ sector, and the matrix element is given fig.(4) $< p_1, \lambda_1; p_2, \lambda_2|...|p_1', \lambda_1'; p_2', \lambda_2' >$; $H_r^{(1)}(\Lambda \to \infty)$ is the electron-photon coupling term with the bare coupling constant $e$; the initial value of generated interaction is given $H_d^{(2)}(\Lambda \to \infty) = 0$. The generated interaction is given

$$
\begin{aligned}
V_\lambda^{gen} &= -e^2 < \gamma^\mu\gamma^\nu > \Big[\frac{\theta_\varepsilon(q^+)}{q^+}D_{\mu\nu}(q)\left(\frac{\Theta_\lambda(D_1, D_2)}{D_1} + \frac{\Theta_\lambda(D_2, D_1)}{D_2}\right) \\
&\quad + \frac{\theta_\varepsilon(-q^+)}{-q^+}D_{\mu\nu}(-q)\left(\frac{\Theta_\lambda(-D_1, -D_2)}{-D_1} + \frac{\Theta_\lambda(-D_2, -D_1)}{-D_2}\right)\Big] \\
\Theta_\lambda(D_1, D_2) &= \int_\lambda^\infty \frac{df_{\lambda'}(D_1)}{d\lambda'}f_{\lambda'}(D_2)d\lambda'
\end{aligned}
\tag{6.22}
$$

where we sum ($\sum_k$ in eq. (6.19)) the two terms corresponding to the two time-ordered diagrams with $q^+ > 0$ and $q^+ < 0$; $\lambda$ is the 'running' cutoff, that defines the continuous step of the unitary transformation; $f_\lambda(\Delta)$ is the similarity function, arising from the unitary transformation; the function $\theta_\varepsilon(q^+)$ restricts the longitudinal momentum of intermediate photon. The similarity function $f_\lambda(\Delta)$ and the cutoff function $\theta_\varepsilon(q^+)$ are specified below.[2] $D_{\mu\nu}(q) = \sum_\lambda \epsilon_\mu(\lambda, q)\epsilon_\nu^\star(\lambda, q)$ is the polarization sum; the null vector $\eta_\mu = (0, \eta_+, 0, 0)$, $\eta^\mu\eta_\mu = 0$ is given below; the energy denominators in the exchange channel are given (fig.(4)) $D_1 = p_1^{'-} - p_1^- - q^-$ and $D_2 = p_2^- - p_2^{'-} - q^-$; $q = p_1' - p_1$ is the exchanged photon momentum, with $q^- = \frac{q_\perp^2}{q^+}$. The notation $< \gamma^\mu\gamma^\nu >$ is introduced for the current-current term. In the exchange channel this matrix element is given fig.(4)

$$
< \gamma^\mu\gamma^\nu > |_{exch} = \frac{\bar{u}(p_1, \lambda_1)}{\sqrt{p_1^+}}\gamma^\mu\frac{u(p_1', \lambda_1')}{\sqrt{p_1^{'+}}}\frac{\bar{v}(p_2', \lambda_2')}{\sqrt{p_2^{'+}}}\gamma^\nu\frac{v(p_2, \lambda_2)}{\sqrt{p_2^+}}P^{+2}
\tag{6.23}
$$

---

[2] The similarity function $f_\Lambda$ plays the role of transverse UV regulator (see the chapter 7), and the function $\theta_\varepsilon$ regulates the longitudinal IR divergences. On a tree level there is no UV divergences in four fermion interaction, but the longitudinal IR divergences are present.

where $p_i, p_i^{'}$ are light-front three-momenta carried by the constituents, $\lambda_i, \lambda_i^{'}$ are their light-front helicities, $u(p_1, \lambda_1), v(p_2, \lambda_2)$ are their spinors (see below); index $i = 1, 2$ refers to electron and positron, respectively; $P = (P^+, P^\perp)$ is light-front positronium momentum.

Below we use the light-front conventions formulated by Lepage and Brodsky [45] (see also [22]). The polarization sum is given

$$D_{\mu\nu}(q) = \sum_\lambda \epsilon_\mu(q, \lambda)\epsilon_\nu^\star(q, \lambda) = -g_{\mu\nu} + \frac{\eta_\mu q_\nu + \eta_\nu q_\mu}{q^+} \tag{6.24}$$

where the metric tensor(s)

$$g^{\mu\nu} = \begin{pmatrix} 0 & 2 & 0 & 0 \\ 2 & 0 & 0 & 0 \\ 0 & 0 & -1 & 0 \\ 0 & 0 & 0 & -1 \end{pmatrix} \quad \text{and} \quad g_{\mu\nu} = \begin{pmatrix} 0 & \frac{1}{2} & 0 & 0 \\ \frac{1}{2} & 0 & 0 & 0 \\ 0 & 0 & -1 & 0 \\ 0 & 0 & 0 & -1 \end{pmatrix} . \tag{6.25}$$

and the null vector is $\eta^\mu = (0, 2, \vec{0})$. The Dirac spinors are given

$$u(p, \lambda) = \frac{1}{\sqrt{p^+}} \left(p^+ + \beta m + \vec{\alpha}_\perp \vec{p}_\perp\right) \times \begin{cases} \chi(\uparrow), & \text{for } \lambda = +1, \\ \chi(\downarrow), & \text{for } \lambda = -1, \end{cases} \tag{6.26}$$

$$v(p, \lambda) = \frac{1}{\sqrt{p^+}} \left(p^+ - \beta m + \vec{\alpha}_\perp \vec{p}_\perp\right) \times \begin{cases} \chi(\downarrow), & \text{for } \lambda = +1, \\ \chi(\uparrow), & \text{for } \lambda = -1. \end{cases} \tag{6.27}$$

Here $\beta = \gamma^0$, $\vec{\alpha} = \gamma^0\vec{\gamma}$; and the two $\chi$-spinors are

$$\chi(\uparrow) = \frac{1}{\sqrt{2}} \begin{pmatrix} 1 \\ 0 \\ 1 \\ 0 \end{pmatrix} \quad \text{and} \quad \chi(\downarrow) = \frac{1}{\sqrt{2}} \begin{pmatrix} 0 \\ 1 \\ 0 \\ -1 \end{pmatrix} . \tag{6.28}$$

These conventions are used in Appendix B to calculate the matrix elements of the effective interactions [3].

Using the symmetry

$$\begin{aligned} &f_\lambda(-D) = f_\lambda(D) \\ &D_{\mu\nu}(-q) = D_{\mu\nu}(q) \end{aligned} \tag{6.31}$$

---

[3] In the chapters 3 and 4 we have used the prescription of the light-front field theory as formulated by Zhang and Harindranath [24]. They have used the following conventions: the polarization sum is

$$D_{\mu\nu}(q) = \frac{q^{\perp 2}}{q^{+2}}\eta_\mu\eta_\nu + \frac{1}{q^+}(\eta_\mu q_\nu^\perp + \eta_\nu q_\mu^\perp) - g_{\mu\nu}^\perp \tag{6.29}$$

with the null vector $\eta_\mu = (0, 1, \vec{0})$; the four-component spinors $u(p, \lambda)$, $v(p, \lambda)$ are given through the two-component spinors $\chi_\lambda$ in eq. (**??**) and eq. (3.10), chapter 3.

Using the above equations, we get

$$< \gamma^\mu\gamma^\nu > |_{exch} D_{\mu\nu}(q) = M_{2ii}^{ex} \tag{6.30}$$

where $M_{2ij}^{(ex)} = [\chi_{\lambda_1}^+ \Gamma^i(p_1', p_1, p_1' - p_1)\chi_{\lambda_1'}]\,[\chi_{\bar{\lambda}_2'}^+ \Gamma^j(-p_2, -p_2', -(p_1' - p_1))\chi_{\bar{\lambda}_2}]$ is the matrix element, obtained in the chapter 4 eq. (4.29) direct from the two-component field theory eq. (3.3)-eq. (3.7). We reproduce then the form of generated interaction, obtained in the chapter 4 eq. (4.30).

we have the following generated interaction in the electron-positron sector

$$V_\lambda^{gen} = -e^2 < \gamma^\mu \gamma^\nu > \frac{\theta_\varepsilon(q^+) + \theta_\varepsilon(-q^+)}{q^+} D_{\mu\nu}(q) \left( \frac{\Theta_\lambda(D_1, D_2)}{D_1} + \frac{\Theta_\lambda(D_2, D_1)}{D_2} \right) \tag{6.32}$$

We specify the cutoff function $\theta_\varepsilon$ in a form [50]

$$\theta_\varepsilon = \theta(q^+ - \varepsilon) F(q^+, q_\perp) \tag{6.33}$$

where $\varepsilon$ is 'small', say $\varepsilon \sim \frac{m^2}{\Lambda}$ and $\Lambda$ is the bare cutoff. For our purposes we do not need the explicit form of the function $F(q^+, q_\perp)$, it defines the upper boundary for $|q^+|$. The combination $(\theta_\varepsilon(q^+) + \theta_\varepsilon(-q^+))$ restricts $|q^+|$ to be above $\varepsilon$. In the integral in $dq^+$ this ensures the symmetric cutoff for longitudinal photon momentum

$$\int_{-\infty}^{+\infty} dq^+ \to \int_{-\infty}^{-\varepsilon} dq^+ + \int_{\varepsilon}^{+\infty} dq^+ \tag{6.34}$$

The resulting generated interaction is given at the value $\lambda = 0$, $V^{gen} = V_{\lambda=0}^{gen}$. To get the effective electron-positron interaction in the light-front dynamics we sum the resulting generated interaction and instantaneous photon exchange arising in the light-front QED

$$V^{eff} = V^{gen} + V^{inst} \tag{6.35}$$

where each term is defined

$$V^{gen} = -e^2 < \gamma^\mu \gamma^\nu > \frac{1}{q^+} D_{\mu\nu}(q) \left( \frac{\Theta(D_1, D_2)}{D_1} + \frac{\Theta(D_2, D_1)}{D_2} \right)$$

$$V^{inst} = -e^2 < \gamma^\mu \gamma^\nu > \frac{1}{q^{+2}} \eta_\mu \eta_\nu \tag{6.36}$$

$$\Theta(D_1, D_2) = \Theta_{\lambda=0}(D_1, D_2) = \int_0^\infty \frac{df_{\lambda'}(D_1)}{d\lambda'} f_{\lambda'}(D_2) d\lambda' \tag{6.37}$$

For both interactions the prescription eq. (6.33) (eq. (6.34)) to treat infrared divergences, small $q^+$, is imposed. We combine all the terms together with the result

$$\begin{aligned} V^{eff} &= e^2 < \gamma^\mu \gamma^\nu > g_{\mu\nu} \frac{1}{q^+} \left( \frac{\Theta(D_1, D_2)}{D_1} + \frac{\Theta(D_2, D_1)}{D_2} \right) \\ &- e^2 < \gamma^\mu \gamma^\nu > \eta_\mu \eta_\nu \frac{1}{2q^{+2}} (D_1 - D_2) \left( \frac{\Theta(D_1, D_2)}{D_1} - \frac{\Theta(D_2, D_1)}{D_2} \right) \end{aligned} \tag{6.38}$$

This equation does not depend on the explicit form of $\Theta$-factor. The generated interaction has two types of infrared singularities: $\frac{1}{q^{+2}}$ and $\frac{1}{q^+}$ types. We see that the $\frac{1}{q^{+2}}$ singularity of generated term is cancelled exactly by the instantaneous term in the effective electron-positron interaction. Further we show that the cutoff condition eq. (6.33) ensures the cancellation of $\frac{1}{q^+}$ type singularity in the physical observables, calculated from the effective electron-positron interaction.

We introduce

$$2d = D_1 - D_2 \; ; \quad D = \frac{D_1 + D_2}{2} \tag{6.39}$$

that gives

$$D_1 = D + d \; ; \quad D_2 = D - d \tag{6.40}$$

As $q^+ \to 0$ we expand the effective interaction eq. (6.38) in the series in terms of $\frac{d}{D} << 1$ $(d \sim (M_0'^2 - M_0^2)/P^+;\ D \sim (-q^-))$

$$\begin{aligned}
V^{eff} &= e^2 < \gamma^\mu \gamma^\nu > g_{\mu\nu} \frac{1}{q^+ D} \\
&\quad \times \left(1 - \frac{d}{D}[\Theta(D_1, D_2) - \Theta(D_2, D_1)] + (\frac{d^2}{D^2}) - (\frac{d^3}{D^3})[\Theta(D_1, D_2) - \Theta(D_2, D_1)]\right) \\
&+ e^2 < \gamma^\mu \gamma^\nu > \eta_\mu \eta_\nu \frac{1}{q^{+2}} \\
&\quad \times \left(-\frac{d}{D}[\Theta(D_1, D_2) - \Theta(D_2, D_1)] + (\frac{d^2}{D^2}) - (\frac{d^3}{D^3})[\Theta(D_1, D_2) - \Theta(D_2, D_1)]\right) \\
&+ O\left(m^2 \frac{d^4}{D^4}\right) \\
&= V_0^{eff} + \sum_i \Delta V_{g_{\mu\nu}}^{(i)} + \sum_i \Delta V_{\eta_\mu \eta_\nu}^{(i)} \qquad (6.41)
\end{aligned}$$

where we have used the identities

$$\begin{aligned}
&\frac{\Theta(D_1, D_2)}{D_1} + \frac{\Theta(D_2, D_1)}{D_2} = \frac{1}{2}\left(\frac{1}{D_1} + \frac{1}{D_2}\right) + \frac{1}{2}\left(\frac{1}{D_1} - \frac{1}{D_2}\right)(\Theta(D_1, D_2) - \Theta(D_2, D_1)) \\
&\Theta(D_1, D_2) + \Theta(D_2, D_1) = 1 \qquad (6.42)
\end{aligned}$$

index $(i)$ denotes the order with respect of $\frac{d}{D}$. The leading order term is given

$$V_0^{eff} = e^2 < \gamma^\mu \gamma^\nu > g_{\mu\nu} \frac{1}{q^+ D} \qquad (6.43)$$

In the leading order of nonrelativistic approximation $|\vec{p}|/m << 1$ this term eq. (6.43) gives the 3-dimensional Coulomb interaction [53]

$$V_0^{eff} \approx -\frac{16 e^2 m^2}{\vec{q}^2} \qquad (6.44)$$

where $\vec{q}(q_z, \vec{q}_\perp) = \vec{p'} - \vec{p}$ is the exchanged momentum. Hence the effective electron-positron interaction eq. (6.38) produces Bohr energy levels [53]. The nonrelativistic expansion of the term eq. (6.43) up to the second order $O\left(\frac{\vec{p}^2}{m^2}\right)$ gives the familiar Breit-Fermi spin-spin and tensor interactions [42], that insures the correct spin-splittings for the positronium ground state [39].

Corrections $\Delta V_{g_{\mu\nu}}^{(i)}$ and $\Delta V_{\eta_\mu \eta_\nu}^{(i)}$ arise due to the unitary transformation performed, i.e. that are the corrections due to the energy denominators in the "$g_{\mu\nu}''$ term and the "$\eta_\mu \eta_\nu''$ term. The first order corrections $O(d/D)$ were estimated in [42],[55], using the explicit form for similarity function $f_\lambda(D)$. We are interested here in general properties (independent on the choice of $f_\lambda(D)$) of the effective interaction, particularly in the origin of infrared divergences.

In eq. (6.41) the product of $''\eta_\mu \eta_\nu''$ term with the term $\sim (\frac{d}{D})$ gives the singularity of $\frac{1}{q^+}$ type (when $(\Theta(D_1, D_2) - \Theta(D_2, D_1)) \sim const$ with respect to $(d/D)$). To find the corresponding infrared counterterm we integrate the singular term over 'external legs' (that correspond in QED to physical particles) with the wave packet function, $\int dq^+ d^2 q_\perp \phi(p + q)$, where $p \sim p_1, p_2$. The integration of $\frac{1}{q^+}$ type term leads to logarithmic infrared divergences, that are cancelled from small positive and negative longitudinal momenta due to the symmetric cutoff condition eq. (6.34). Therefore, there are no infrared counterterms to be introduced in the second order

$O(e^2)$ in the effective interaction. Moreover, this is true in the order $O(e^2)$ for all tree level diagrams in QED.

The same cancellation of the infrared divergent contribution from $''\eta_\mu\eta_\nu''$ term occurs, due to the symmetric cutoff, in the spectrum of masses for positronium.

What about the finite corrections from $''\eta_\mu\eta_\nu''$ term? The leading order finite correction from $''\eta_\mu\eta_\nu''$ term eq. (6.41) is $\sim \eta_\mu\eta_\nu \frac{1}{q^{+2}}(\frac{d}{D})^2$, which is of the order $e^2q^0$. The interaction of light-front field theory $V^{PT}$ eq. (6.52) and the effective interaction $V^{eff}$ eq. (6.38), generated by the unitary transformation, have both a leading Coulomb behavior, but they differ by spin-independent $''\eta_\mu\eta_\nu''$ term (excluding the divergent part) in the order $e^2q^0$, which contributes to the mass in the order $\alpha^4$. In the order of fine structure splitting $\alpha^4$ also terms of order $e^4q^{-1}$ and $e^6q^{-2}$ are important. These terms arise from the next orders transformation of both electron-photon vertex and also instantaneous term. Since the Coulomb interaction, that is the only spin-independent part of electron-positron interaction, arise from $''g_{\mu\nu}''$ term in the effective interaction $V^{eff}$, we expect that the spin-independent $''\eta_\mu\eta_\nu''$ term in the order $e^2q^0$ will be compensated in the mass spectrum by the corresponding terms of the order $e^4$ and $e^6$.

Compare effective electron-positron interaction eq. (6.38), generated in the second order in $e$ by flow equations, with the electron-positron interaction arising from perturbative photon exchange. The electron-positron interaction in the light-front perturbation theory is given by a sum of dynamical photon exchange $V^{phot}$ and the instantaneous interaction, $V^{PT} = V^{phot} + V^{inst}$. The instantaneous term is given by eq. (6.37), and the $V^{phot}$ term, defined by the diagram with one photon exchange, is [45]

$$V^{phot} = -e^2 < \gamma^\mu\gamma^\nu > \left( \frac{\theta_\varepsilon(q^+)}{q^+} D_{\mu\nu}(q) \frac{1}{\tilde{D}_+} + \frac{\theta_\varepsilon(-q^+)}{-q^+} D_{\mu\nu}(-q) \frac{1}{\tilde{D}_-} \right) \tag{6.45}$$

where the energy denominators are given $\tilde{D}_\pm = \sum_{inc} p^- - \sum_{interm} p^-$, with the sums over the light-front energies, $p^-$, of incident (inc) and intermediate (interm) particles; and ± denotes two different time orderings of the photon. For the process depicted on fig.(4) we have $\tilde{D}_+ = P^- - p_1^- - p_2^{'-} - q^-$ and $\tilde{D}_- = P^- - p_1^{'-} - p_2^- + q^-$, where $q = p_1' - p_1$, $P^- = M_n^2/P^+$ (let $P^\perp = 0$). One can rewrite eq. (6.45) in the form [53] (also see Appendix B)

$$V^{phot} = -e^2 < \gamma^\mu\gamma^\nu > \frac{\theta_\varepsilon(q^+) + \theta_\varepsilon(-q^+)}{q^+} D_{\mu\nu}(q) \frac{1}{\tilde{D}} \tag{6.46}$$

where

$$\theta_\varepsilon(q^+)\tilde{D}_+ = -\theta_\varepsilon(-q^+)\tilde{D}_- = \tilde{D} \tag{6.47}$$

Combining instantaneous eq. (6.37) and one photon exchange eq. (6.46) terms together, we have

$$V^{PT} = e^2 < \gamma^\mu\gamma^\nu > g_{\mu\nu} \frac{1}{q^+\tilde{D}} - e^2 < \gamma^\mu\gamma^\nu > \eta_\mu\eta_\nu \frac{1}{q^{+2}} \left(1 - \frac{D}{\tilde{D}}\right) \tag{6.48}$$

where the prescription eq. (6.33) (eq. (6.34)) to treat infrared divergences is imposed.

The $''\eta_\mu\eta_\nu''$ term carries the infrared divergent part of the interaction $V^{PT}$. We approximate the positronium mass as average over the masses of initial and final free (not bound) states

$$M_n^2 = \frac{M_0^2 + M_0^{'2}}{2} \tag{6.49}$$

where $p_1^- + p_2^- = M_0^2/P^+$, $p_1^{'-} + p_2^{'-} = M_0^{'2}/P^+$, $P^- = M_n^2/P^+$, and $P(P^+, P_\perp = 0)$ is the positronium momentum. In this approximation the energy denominator of perturbative photon exchange diagram is

$$\tilde{D} \to D = \frac{D_1 + D_2}{2} \tag{6.50}$$

It is obvious, when one notes (see also Appendix B)

$$\begin{aligned} D &= \frac{D_1 + D_2}{2} = \frac{p_1^{'-} - p_1^- + p_2^- - p_2^{'-}}{2} - q^- = \frac{p_1^{'-} + p_2^{'-} + p_1^- + p_2^-}{2} - p_1^- - p_2^{'-} - q^- \\ &= -\left(\frac{p_1^{'-} + p_2^{'-} + p_1^- + p_2^-}{2} - p_1^{'-} - p_2^- + q^-\right) \end{aligned} \tag{6.51}$$

Given the eq. (6.50), the instantaneous interaction $V^{inst}$ eq. (6.37), which is the source of infrared divergences, is precisely canceled by the part in $V^{phot}$ corresponding to emission and absorption of longitudinal photons. The resulting electron-positron interaction, obtained in the light-front perturbation theory, is given in this approximation eq. (6.49)

$$V^{PT} = e^2 < \gamma^\mu \gamma^\nu > g_{\mu\nu} \frac{1}{q^+ D} \tag{6.52}$$

By the special choice of similarity function this answer eq. (6.52) can be generated by the flow equations. When the similarity function is

$$\begin{aligned} &f_\lambda(D) = \mathrm{e}^{-\frac{DD'}{\lambda}} \\ &D' = sign D \end{aligned} \tag{6.53}$$

the $\Theta$-factor eq. (6.37) is $\Theta_1 = \frac{D_1}{D_1 + D_2}$, and $''\eta_\mu \eta_\nu''$ term is equal to zero in eq. (6.38). The effective electron-positron interaction eq. (6.38) is given by the result of perturbation theory eq. (6.52)

$$V^{eff}|_{f_\lambda(D)} = V^{PT} \tag{6.54}$$

where the condition eq. (6.49) (eq. (6.50)) is imposed. This is the remarkable result, that shows that specifying the unitary transformation in a proper way one can get rid of $''\eta_\mu \eta_\nu''$ term in the effective interaction eq. (6.38), the term that causes the infrared divergences in longitudinal direction. In all other cases we need to introduce the symmetric cutoff condition eq. (6.33) (eq. (6.34)) on $q^+$ to cancel the divergent contribution in physical observables.

What is the status of $''\eta_\mu \eta_\nu''$ term in the effective electron-positron interaction $V^{eff}$ eq. (6.38)? The $''\eta_\mu \eta_\nu''$ term describes instant emission and absorption of 'longitudinal' photon and is specific in the light-front gauge computations. As was discussed above, this term is not desirable in the electron-positron interaction and can be considered as a consequence of the unitary transformation performed. The physical reason for its appearance is the violation of Lorenz and gauge symmetries by the derivation of the effective, renormalized Hamiltonian. The first problem in the light-front field theory is that whenever the generator of a symmetry is dynamical (contains interactions) it is somewhere between very difficult and impossible to monitor and maintain that symmetry at each step of a calculation - unless of course one can solve the theory exactly. This concerns parity and rotational invariance, that are not manifest symmetries on the light-front. The second problem is that whenever we use the Hamiltonian technique, the naive regularization by introducing the cutoffs breaks the gauge invariance (and also Lorenz covariance), and forces the bare Hamiltonian to contain a larger than normal suite of counterterms to enable a finite limit as the cutoffs are removed. One way is, that the counterterms are then adjusted to reproduce physical observables and to restore the symmetries broken by cutoffs. The other way is to find the gauge invariant procedure for regularization of Hamiltonians. The attempt in the latter direction was made by Brodsky, Hiller, and McCartor [47]. Solving the Yukawa theory they have tried to preserve more symmetries by using Pauli-Villars procedure for regularization.

In the next section we use the effective electron-positron interaction $V^{eff}$ eq. (6.38), namely its $"g''_{\mu\nu}$ part, to calculate mass spectrum and wave functions for positronium.

## 6.3 Mass spectrum and wave functions of positronium

We start with the effective electron-positron interaction, generated in the second order in coupling by flow equations, eq. (6.38)

$$\begin{aligned} V^{eff} &= e^2 < \gamma^\mu \gamma^\nu > g_{\mu\nu} \frac{1}{q^+} \left( \frac{\Theta(D_1, D_2)}{D_1} + \frac{\Theta(D_2, D_1)}{D_2} \right) \\ &- e^2 < \gamma^\mu \gamma^\nu > \eta_\mu \eta_\nu \frac{1}{2q^{+2}} (D_1 - D_2) \left( \frac{\Theta(D_1, D_2)}{D_1} - \frac{\Theta(D_2, D_1)}{D_2} \right) \end{aligned} \tag{6.55}$$

where we impose the prescription eq. (6.33) (eq. (6.34)) to treat infrared divergences, small $q^+$.

We use Jacobi momenta, depicted on fig.(4)

$$\begin{aligned} & p_1(xP^+, x\vec{P}_\perp + \vec{k}_\perp) \\ & p_2((1-x)P^+, (1-x)\vec{P}_\perp - \vec{k}_\perp) \end{aligned} \tag{6.56}$$

and corresponding for the momenta $p'_1, p'_2$; here $x$ is the light-front fraction of electron momentum and $P(P^+, \vec{P}_\perp)$ is the total momentum of positronium. For convenience we introduce

$$D_1 = \frac{\Delta_1}{P^+} = -\frac{\tilde{\Delta}_1}{q^+}; \quad D_2 = \frac{\Delta_2}{P^+} = -\frac{\tilde{\Delta}_2}{q^+} \tag{6.57}$$

and from now on we use the rescaled value of the cutoff $\lambda \to \lambda^2/P^+$. The effective electron-positron interaction is written then

$$\begin{aligned} V^{eff} = &- e^2 < \gamma^\mu \gamma^\nu > g_{\mu\nu} \left( \frac{\Theta(\Delta_1, \Delta_2)}{\tilde{\Delta}_1} + \frac{\Theta(\Delta_2, \Delta_1)}{\tilde{\Delta}_2} \right) \\ &- e^2 < \gamma^\mu \gamma^\nu > \eta_\mu \eta_\nu \frac{1}{2q^{+2}} (\tilde{\Delta}_1 - \tilde{\Delta}_2) \left( \frac{\Theta(\Delta_1, \Delta_2)}{\tilde{\Delta}_1} - \frac{\Theta(\Delta_2, \Delta_1)}{\tilde{\Delta}_2} \right) \\ \Theta(\Delta_1, \Delta_2) &= \int_0^\infty \frac{df_{\lambda'}(\Delta_1)}{d\lambda'^2} f_{\lambda'}(\Delta_2) d\lambda'^2 \end{aligned} \tag{6.58}$$

where the energy denominators in eq. (6.58) read

$$\begin{aligned} \tilde{\Delta}_1 &= \frac{(x\vec{k}'_\perp - x'\vec{k}_\perp)^2 + m^2(x-x')^2}{xx'}; \qquad \tilde{\Delta}_2 = \tilde{\Delta}_1|_{x \to (1-x), x' \to (1-x')} \\ & \Delta_1 = \frac{\tilde{\Delta}_1}{x - x'}; \qquad \Delta_2 = \frac{\tilde{\Delta}_2}{x - x'} \end{aligned} \tag{6.59}$$

Note $\tilde{\Delta}_1, \ \tilde{\Delta}_2$ are positive definite.

To perform the angular integration eq. (6.6) analytically we choose the similarity function as follows

$$f_\lambda(\Delta) = u_\lambda(\Delta) = \theta(\lambda^2 - |\Delta|) \tag{6.60}$$

where for simplicity we use the sharp cutoff function $u_\lambda(\Delta)$. Then the effective interaction reads

$$\begin{aligned} V^{eff} = & - e^2 < \gamma^\mu \gamma^\nu > g_{\mu\nu} \left( \frac{\theta(\tilde{\Delta}_1 - \tilde{\Delta}_2)}{\tilde{\Delta}_1} + \frac{\theta(\tilde{\Delta}_2 - \tilde{\Delta}_1)}{\tilde{\Delta}_2} \right) \\ & - e^2 < \gamma^\mu \gamma^\nu > \eta_\mu \eta_\nu \frac{1}{2q^{+2}} |\tilde{\Delta}_1 - \tilde{\Delta}_2| \left( \frac{\theta(\tilde{\Delta}_1 - \tilde{\Delta}_2)}{\tilde{\Delta}_1} + \frac{\theta(\tilde{\Delta}_2 - \tilde{\Delta}_1)}{\tilde{\Delta}_2} \right) \end{aligned} \tag{6.61}$$

where we have used $\theta(x) - \theta(-x) = sign(x)$ [4].

The general matrix elements for the effective interaction eq. (6.61) depending on the angles $\varphi, \varphi'$ (actually on the difference $(\varphi - \varphi')$) $< x, k_\perp, \varphi; \lambda_1, \lambda_2 | V^{eff} | x', k'_\perp, \varphi'; \lambda'_1, \lambda'_2 >$ and also the matrix elements of the effective interaction after the angular integration eq. (6.6) for the total momentum $J_z$ $< x, k_\perp; J_z, \lambda_1, \lambda_2 | \tilde{V}^{eff} | x', k'_\perp; J'_z, \lambda'_1, \lambda'_2 >$ are given in Appendix B.

The positronium spectrum is calculated numerically, using the integral equation eq. (6.9) with the matrix elements given in Appendix B. We use for the numerical integration the

---

[4] In this particular case, when the similarity function is given by eq. (6.60), the divergence arising is of the $\frac{1}{|q^+|}$ type, that prevents from the first glance the cancellation of logarithmic divergences in the integral

$$\int_{|q^+|>\varepsilon} dq^+ \tag{6.62}$$

We have chosen the sharp cutoff for simplicity, but generally the smooth cutoffs are preferred to avoid non-analyticities in the structure of counterterms [50]. We demand only, that the cutoff function $u(x)$ with $x = \frac{|D|}{\lambda} \to \frac{|\Delta|}{\lambda^2}$ is 1 for small arguments and vanishes for large arguments. Explicit one can choose

$$\begin{aligned} & u(x) = 1 \;\; for \;\; 0 \le x \le \frac{1}{3} \\ & u(x) \; monoton \; falls \; from \; 1 \; to \; 0 \; for \; \frac{1}{3} \le x \le \frac{2}{3} \\ & u(x) = 0 \;\; for \;\; \frac{2}{3} \le x \le 1 \end{aligned} \tag{6.63}$$

and to simplify the calculation of the integral eq. (6.58), we assume $\frac{du(x)}{d\lambda^2} \sim \delta(1-x)$. Then, when the similarity function (the function that defines the first order solution in the perturbation theory of the flow equation) is equal to the cutoff function $f(x) = u(x)$, the effective electron-positron interaction reads

$$\begin{aligned} V^{eff} = & - e^2 < \gamma^\mu \gamma^\nu > g_{\mu\nu} \left( \frac{u(\tilde{\Delta}_1/\tilde{\Delta}_2)}{\tilde{\Delta}_1} + \frac{u(\tilde{\Delta}_2/\tilde{\Delta}_1)}{\tilde{\Delta}_2} \right) \\ & - e^2 < \gamma^\mu \gamma^\nu > \eta_\mu \eta_\nu \frac{1}{2q^{+2}} (\tilde{\Delta}_1 - \tilde{\Delta}_2) \left( \frac{u(\tilde{\Delta}_1/\tilde{\Delta}_2)}{\tilde{\Delta}_1} - \frac{u(\tilde{\Delta}_2/\tilde{\Delta}_1)}{\tilde{\Delta}_2} \right) \end{aligned} \tag{6.64}$$

In this case the prescription eq. (6.62) ensures the cancellation of logarithmic divergences, and one does not need to introduce counterterms. In the integral equation eq. (6.3) we have the following restriction of the integration domain

$$\int dx' \to \int_{|x'-x|>\varepsilon/P^+} d(x'-x) \tag{6.65}$$

resulting, that the divergent part in $''\eta_\mu \eta''_\nu$ term of the effective interaction eq. (6.64) does not contribute to mass spectrum.

Gauss-Legendre algorithm (Gaussian quadratures). To improve the numerical convergence the technique of Coulomb counterterms is included. The problem has been solved for all components of the total angular momentum, $J_z$. Since we calculate the values of an invariant mass squared, a strong coupling constant $\alpha = 0,3$ has been chosen. The latter means also, that the method of flow equations is applicable in non-perturbative regime. We get the ionization threshold at $M^2 \sim 4m^2$, the Bohr spectrum, and what is more important, the fine structure. The agreement is quantitative (for the lowest eigenvalues), particularly for the physical value of the fine structure constant $\alpha = \frac{1}{137}$.

The figure (5) is the summary of the spectra for different components of the total angular momentum, $J_z$. As one can see, certain mass eigenvalues at $J_z = 0$ are degenerate with certain eigenvalues at other $J_z$ to a very high degree of numerical precision. As an example, consider the second lowest eigenvalue for $J_z = 0$. It is degenerate with the lowest eigenvalue for $J_z = \pm 1$, and can thus be classified as a member of the triplet with $J = 1$. Correspondingly, the lowest eigenvalue for $J_z = 0$ having no companion can be classified as the singlet state with $J = 0$. Quite in general one can interpret $2J_{z,max} + 1$ degenerate multiplets as members of a state with total angular momentum $J$. One can get the quantum number of total angular momentum $J$ from the number of degenerate states for a fixed eigenvalue $M_n^2$. Such form of spectrum is driven by rotational invariance. It is a remarkable result, we restore the rotational symmetry in the light-front positronium calculations on the level of mass spectrum.

The integral equation is approximated by Gaussian quadratures, and the results are studied as a function of the number of integration points $N$, as displayed in Figures (6) and (7). On the fig.(6) the mass squared eigenvalues $M_n^2$ for $J_z = 0$ are shown as functions of the number of integration points $N = N_1 = N_2$. One sees, that the results stabilize themselves quickly. To find out if the degeneracy obtained is merely a numerical artifact, or a property of the positronium model, consider fig.(7). The mass (squared) discrepancy between the $J_z = 0$ and $J_z = 1$ eigenvalues is plotted versus the number of integration points N for three different states. It is important, that the convergence of the value $\Delta M^2(1^3S_1)$ with N occurs. But the mass gap does not converge to zero, rather to some small value $\sim 10^{-5}$. The mass gap for $2^1P_1$ state vanishes as $N$ increases, while for $2^3P_1$ state $\Delta M^2$ converges again to a finite small number $\sim 10^{-4}$. Kaluza and Pirner [36] and Trittmann and Pauli [30] found that in light-front perturbation theory there is a discrepancy between the case of $J_z = 0$ and $J_z = 1$.

# Chapter 7

# Renormalization in the light-front QED

## 7.1 Introduction.

In this section we consider the renormalization group problem for light-front QED, arising first in the second order in coupling. Renormalization in the light-front field theory is much more complicated than in covariant Feynman perturbation theory, and is nontrivial already in the leading order for QED. Generally, there are three renormalization problems that are signaled by the divergence of the free energy:
(1) $\vec{p}_\perp^{\,2}$;
(2) $p^+ \to 0$;
(3) $p^+ = 0$.

The divergences from (1) are 'ultraviolet' (UV), producing counterterms that are local in the transverse direction. While the counterterm structure is richer than what is required in manifestly covariant perturbation theory, in perturbative regime one has that masses are relevant operators, and other gauge interactions are marginal.

The divergences from (2) are 'infrared' (IR), producing counterterms that are nonlocal at least in the longitudinal direction and which may also be nonlocal in the transverse direction. These infrared divergences do not appear in Feynman perturbation theory in covariant gauges. They must cancel perturbatively for gauge invariant matrix elements in QED. Coupling coherence fixes the infrared divergent part of the Hamiltonian as a power series in the gauge coupling, allowing us to next consider re-summations that preserve cancellation of all infrared divergences.

Finally, (3) is the vacuum problem, that we do not consider here. The light-front vacuum is 'trivial', except for zero modes. The light-front gauge $A^+ = 0$ has a singularity at longitudinal momentum $p^+ = 0$, i.e. the zero-modes $p^+ = 0$ should be treated specially, that is called the problem of zero-modes. One can connect (3) and (2), but we ignore the problem of zero modes in QED (at least here).

In light-front renormalization group transverse and longitudinal directions scale separately, and transverse scaling runs the cutoff. We assume transverse locality and identify relevant and marginal operators using power counting, which is valid in the perturbative regime. The longitudinal scale is not important for the perturbative classification of operators. This means, that entire functions of longitudinal momenta (their dimensionless ratios), including any longitudinal momentum scale introduced by cutoff, appear in the relevant and marginal operators. The simplest way to adjust the new operators is to fix broken by the cutoff covariance (Lorenz covariance) and gauge invariance in physical observables. Generally, infinite number of counteterms must be added to the Hamiltonian to restore these symmetries in observables, and to obtain finite results. As a result, the renormalizability and as a consequence predictive power of the theory seem to be problematic.

Coupling coherence, developed by Perry and Wilson [44], says how to deal in practice with the functions that appear in marginal and relevant light-front operators and how to reduce the number (infinite number) of couplings, that arise by renormalization scaling when the symmetries of the theory (rotational and gauge invariance) are broken by cutoffs. We demand that these additional counterterms required to restore the symmetries run coherently with the "canonical renormalizable couplings" - that is we do not allow them to explicitly depend on the cutoff but only implicitly through the "canonical renormalizable couplings" dependences on the cutoff. In other words, coupling coherence provides the condition under which a finite number of running variables determines the renormalization group trajectory of the renormalized Hamiltonian. Also it is conjectured that coupling coherence restores (or reveal) symmetries broken by the regulator or vacuum.

Coupling coherent Hamiltonian written in terms of dimensionless couplings for $\lambda << \Lambda$ satisfies

$$H_\lambda = U(\lambda,\Lambda) H_\Lambda(\Lambda, e_\Lambda, m_\Lambda, w_\Lambda, c(e_\Lambda, m_\Lambda)) U^+(\lambda,\Lambda) \to H_\Lambda(\lambda, e_\lambda, m_\lambda, w(e_\lambda, m_\lambda), c(e_\lambda, m_\lambda)) \tag{7.1}$$

where $U(\lambda,\Lambda)$ is the unitary transformation defined by flow equations. The additional requirement to eq. (7.1) is that all dependent couplings (represented by '$c$' in the argument of the Hamiltonians) vanish when the independent marginal couplings are set to zero. In eq. (7.1), $e_\Lambda$ and $m_\Lambda$ are independent dimensionless marginal and relevant couplings, respectively; $w_\Lambda$ represents the infinite set of independent dimensionless irrelevant couplings; $c(e_\lambda, m_\lambda)$ represents the infinite set of dependent dimensionless relevant, marginal and irrelevant couplings. More about classification of couplings see [44].

The initial bare Hamiltonian $H_\Lambda$ does not satisfy eq. (7.1) *a priori*, its form changes under the action of transformation $U(\lambda,\Lambda).H_\Lambda$ must be adjusted until its form does not change. This "adjustment" is the process of renormalization. Coupling coherence is a highly nontrivial constraint on the theory and to date has only been solved perturbatively. Further we present the solution of eq. (7.1) for QED in the second order in coupling (we calculate the electron and photon 'mass' operators), that turns out to be simple because coupling constant does not run until the third order.

In the second order in coupling the program we proceed to find renormalized electron and photon masses is the following:

(1) regularize the canonical light-front QED Hamiltonian. In this case, we introduce the bare cutoff $\Lambda$, that regulates the divergences in transverse direction, and introduce the second order mass counterterm $\delta M_\Lambda^{(2)}$. We start with the bare cutoff mass $m_\Lambda^2 = m^2 + \delta M_\Lambda^{(2)}$, where $m$ is the mass term in free Hamiltonian $H_0$;

(2) perform the unitary transformation $U(\lambda,\Lambda)$. The second-order change in the Hamiltonian is given in eq. (4.14) (section 4.2), which gives in one-body sector the shift to the electron (photon) mass

$$\sim \int_\Lambda^\lambda < [\eta^{(1)}, H_{ee\gamma}] >_{one-body} d\lambda' \sim -(\delta\Sigma_\lambda - \delta\Sigma_\Lambda) \tag{7.2}$$

where $\eta^{(1)}$ is the first order generator of transformation, defined by flow equations as $\eta^{(1)} = [H_0, H_{ee\gamma}]$, $H_{ee\gamma}$ is the electron-photon vertex operator, and $\delta\Sigma_\lambda$ is proportional to the value of the integral in eq. (7.2) at the point $\lambda$ and defines mass correction, namely self energy term.

Physically, in the electron sector the energy scales $\Lambda$ down to $\lambda$ from photon emission have been 'integrated out' and placed in effective interactions (the corresponding in the photon sector); (3) renormalize the Hamiltonian, i.e. adjust the Hamiltonian that its form does not change under the unitary transformation eq. (7.1) using coupling coherence. As a result we get the renormalized (in the given order) Hamiltonian $H_\lambda$. In this case, since the electron-photon coupling does not run until third order, the constraint eq. (7.1) is simple to solve: to second order the self-energy must exactly reproduce itself with $\Lambda \to \lambda$

$$\begin{aligned}&[m^2 - (\delta\Sigma_\lambda - \delta\Sigma_\Lambda) + \delta M_\Lambda^{(2)} + O(e^4)] = [m^2 + \delta M_\Lambda^{(2)} + O(e^4)]_{\Lambda\to\lambda} \\ &= [m^2 - \delta\Sigma_\lambda + O(e^4)] \end{aligned} \tag{7.3}$$

this fixes the counterterm

$$\delta M_\Lambda^{(2)} = -\delta\Sigma_\Lambda + O(e^4) \tag{7.4}$$

i.e. in the second order electron (photon) mass squared runs coherently with the cutoff according to eq. (7.1) as

$$m_\lambda^2 = m^2 - \delta\Sigma_\lambda \tag{7.5}$$

(4) using the renormalized Hamiltonian $H_\lambda$ calculate physical observables, that due to the constraint of coupling coherence are cutoff and renormalization scale independent (are finite as $\Lambda \to \infty$ and $\varepsilon \to 0$, where $\Lambda$ is UV regulator in transverse direction and $\varepsilon$ is IR regulator in longitudinal direction (generally, it can be a set of regulators), and are independent of $\lambda$ or any other scale introduced by renormalization), and manifest the symmetries of the theory broken by cutoffs. We calculate the physical mass of electron (photon), that includes the running mass $m_\lambda$ from $H_\lambda$ and in the second order the perturbation theory corrections. In the electron sector these corrections arise from the low-energy photon emission, since $H_\lambda$ still has the photon emission interaction below $\lambda$ of the form $f_\lambda \int d^2x^\perp dx^- H_{ee\gamma}$. (One has in the photon sector the corresponding interaction term, where the energy of $e\bar{e}$ pair is restricted by $\lambda$.) It turns out, that the electron (photon) perturbative mass-squared shift is exactly equal to the self-energy term obtained in (3)

$$\delta m^2 = \delta\Sigma_\lambda + O(e^4) \tag{7.6}$$

therefore the physical mass-squared is given

$$m_{phys}^2 = m_\lambda^2 + \delta m^2 = m^2 - \delta\Sigma_\lambda + \delta\Sigma_\lambda = m^2 \tag{7.7}$$

where $m^2$ is the renormalized electron mass-squared in the free Hamiltonian $H_0$. This result is to be expected, that shows that the renormalization procedure using flow equations and coupling coherence is successful (at least in the second order).

All details of calculation can be found in two sections that follow. The renormalization scheme presented seems to work trivially simple in the second order. But there are difficulties, that one encounters in practical calculations. The integral in eq. (7.2) is infrared singular (in both electron and photon sectors), resulting in infrared divergent self-energy and hence infrared divergent running mass $m_\lambda$, with new types of divergences (the electron mass has both linear and logarithmic infrared divergences). This is in accordance with the discussion presented above. The longitudinal cutoff violates boost invariance and the mass operator, that is a function of a longitudinal momentum scale introduced by the cutoff, is required to restore this symmetry in physical results. Indeed, as shown by Perry [37], the divergent self-energy is exactly canceled by perturbative mixing with small-x photons (see eq. (7.6),eq. (7.7)), resulting in finite mass.

We try to preserve boost invariance, that is manifest symmetry on the light-front, in the second order QED calculations on the level of renormalized Hamiltonian. We take into account the diagrams arising from the normal ordering of instantaneous interactions. The bare light-front QED Hamiltonian contains both the instantaneous interactions and the electron-photon vertex, therefore instantaneous terms must accompany the latter also by scaling from the energies $\Lambda$ down to $\lambda$ eq. (7.1). We get the running electron and photon masses free from infrared divergences, moreover both electron and photon mass conterterms contain the known from the covariant perturbation theory types of divergences. Unfortunately, the electron wave function renormalization constant $Z_2$ contains mixing UV and IR logarithmic divergences and also pure IR logarithmic divergence; the renormalization constant $Z_2$ in photon sector is IR finite. It is argued in [50], that the mixing IR divergences are cancelled in gauge invariant quantities. It is shown in [24], that the mixing divergences are also cancelled completely in the old-fashioned Hamiltonian theory for the coupling constant renormalization. In $x^+$-ordered Hamiltonian theory, the mixing divergences cannot and should not be removed as indicated by the negativity of the second order correction of the wave function renormalization constant, that must result in a physical theory [24].

Zhang and Harindranath [24] performed the similar calculations of self-energy mass operators in light-front QCD, using perturbation theory frame. They have tested different types of regulators to regularize the transverse UV divergences; the regulator for IR divergences was chosen in accordance with the prescription for boundary terms, arising in the light-front Hamiltonian (see chapter 3). In the scheme discussed above the transverse regulator arise automatically at the stage (2), where the unitary transformation, dictated by flow equations, is performed. This is important, since operator classification and renormalization itself are driven by the scaling in transverse direction. The problem, that still remains, is the violation of rotational and gauge symmetries by this regulator, in other words, by the flow equations. We leave this problem for future investigation.

Further the detailed calculations of electron and photon self energies and physical masses, using the program outlined above, are presented.

## 7.2 Flow equations for renormalization issues

As was discussed above and in chapters 3 and 4, the commutator $[\eta^{(1)}, H_{ee\gamma}]$ contributes to the self-energy term, giving rise to the renormalization of fermion and photon masses to the second order. The flow equation for the electron (photon) light-cone energy $p^-$ is

$$\frac{dp^-}{dl} =< [\eta^{(1)}, H_{ee\gamma}] >_{self\ energy} , \tag{7.8}$$

where the matrix element is calculated between the single electron (photon) states $< p', s'|...|p, s >$. We drop the finite part and define $\delta p^-_\lambda = p^-(l_\lambda) - < |H_0| >$. Integration over the finite range gives

$$\delta p^-_\lambda - \delta p^-_\Lambda = \int_{l_\Lambda}^{l_\lambda} < [\eta^{(1)}, H_{ee\gamma}] >_{self\ energy} dl' = -\frac{(\delta\Sigma_\lambda(p) - \delta\Sigma_\Lambda(p))}{p^+} , \tag{7.9}$$

that defines the cutoff dependent self energy $\delta\Sigma_\lambda(p)$. The mass correction and wave function renormalization constant are given correspondingly, cf. [24]

$$\delta m^2_\lambda \;=\; p^+ \delta p^- \Big|_{p^2=m^2} = -\delta\Sigma_\lambda(m^2)$$

$$Z_2 \;=\; 1+\left.\frac{\partial\delta p^-}{\partial p^-}\right|_{p^2=m^2} \quad . \tag{7.10}$$

The on-mass-shell condition is defined through the mass $m$ in the free Hamiltonian $H_0$.

We show further, that to the second order $O(e^2)$ the electron and photon masses and corresponding wave function renormalization constants in the renormalized Hamiltonian vary in accordance with the result of 1-loop renormalization group equations. This can serve as evidence for the equivalence of the flow equations and Wilson's renormalization. Therefore we have rewritten the mass correction $\delta m^2_\lambda$ through the self energy term, arising in 1-loop calculations of ordinary perturbative theory. The negative overall sign stems from our definition of the flow parameter, namely for $\Delta l > 0$ we are lowering the cutoff $dl = -\frac{2}{\lambda^3}d\lambda$.

We start with the bare cutoff mass $m^2_\Lambda = m^2 + \delta M^{(2)}_\Lambda$, where $\delta M^{(2)}_\Lambda$ is the second order mass counterterm. According to eq. (7.9),eq. (7.10) the electron (photon) mass runs

$$m^2_\lambda = m^2_\Lambda - [\delta\Sigma_\lambda(m^2) - \delta\Sigma_\Lambda(m^2)] \tag{7.11}$$

defining, due to renormalizability, the counterterm $\delta M^{(2)}_\Lambda = \delta m^2_\Lambda = -\delta\Sigma_\Lambda(m^2)$ and the dependence of the renormalized mass on the cutoff $\lambda$

$$m^2_\lambda = m^2 + \delta m^2_\lambda = m^2 - \delta\Sigma_\lambda \; . \tag{7.12}$$

We calculate explicitly the self-energy term. The **electron** energy correction contains several terms

$$\delta p^-_\lambda =< p', s'|H - H_0|p, s >= \left(\sum_{n=1}^{3}\delta p^-_{\lambda n}\right)\cdot\delta^{(3)}(p-p')\delta_{ss'} \; . \tag{7.13}$$

The first term is induced by the flow equation in single electron sector, namely comes from the commutator $[\eta(1), H_{ee\gamma}]$

$$\delta p^-_{1\lambda} = -\int_{l_\lambda}^{\infty} < [\eta^{(1)}, H_{ee\gamma}] >_{self\ energy} dl' = -\frac{\delta\Sigma_{1\lambda}(p)}{p^+} \; ; \tag{7.14}$$

it reads, cf. eq. (C.10) in Appendix C,

$$\begin{aligned}\delta p^-_{1\lambda} \;&=\; e^2\int\frac{d^2k^\perp dk^+}{2(2\pi)^3}\frac{\theta(k^+)}{k^+}\theta(p^+-k^+)\\ &\qquad\times\Gamma^i(p-k,p,-k)\Gamma^i(p,p-k,k)\,\frac{1}{p^- - k^- - (p-k)^-}\times(-R) \; .\end{aligned} \tag{7.15}$$

This term explicitly depends on the cutoff $\lambda$ ($l = 1/\lambda^2$) through the similarity function, that plays the role of a regulator in the loop integration

$$R_\lambda = f^2_{p,k,\lambda} = \exp\left\{-2\left(\frac{\Delta_{p,k}}{\lambda}\right)^2\right\} \; . \tag{7.16}$$

Eq. (7.15) corresponds to the first diagram in fig.(9).

Two instantaneous diagrams, the second and third in fig.(9), contribute the cutoff independent (constant) terms. They arise from normal-ordered instantaneous interactions in the single electron sector and can be written as

$$\delta p_{n\lambda} = \delta p_n(l=0) = c_n < \hat{O}\hat{O}^+ > V^{inst}_n(l=0) \tag{7.17}$$

where $n = 2, 3$ corresponds to the second and third diagrams in fig. (8), $c_n$ is the symmetry factor, $< \hat{O}\hat{O}^+ >$ stands for the boson ($n = 2$) and fermion ($n = 3$) contractions (i.e. $< \tilde{a}_k \tilde{a}_k^+ >= \theta(k^+)/k^+$ and $< \tilde{b}_p \tilde{b}_p^+ >= \theta(p^+)$), and $V_n^{inst}(l = 0)$ arises from normal-ordering of $H_{ee\gamma\gamma}$ for $n = 2$ and of $H_{eeee}$ for $n = 3$ (eqs. (3.29) and (3.30)).

These two diagrams $\delta p_n(l = 0)$ define together with the first one $\delta p_1(l = 0)$ the initial condition for the total energy correction, eq. (7.13).

Since the diagrams $n = 2, 3$ come from the normal-ordering canonical Hamiltonian at $l = 0$, they must accompany the first diagram for any flow parameter $l$. In what follows we use for the instantaneous terms the same regulator $R$, eq. (7.16)

$$\begin{aligned} \delta p_{2\lambda}^- &= e^2 \int \frac{d^2k^\perp dk^+}{2(2\pi)^3} \frac{\theta(k^+)}{k^+} \frac{\sigma^i \sigma^i}{[p^+ - k^+]} \times (-R) \\ \delta p_{3\lambda}^- &= e^2 \int \frac{d^2k^\perp dk^+}{2(2\pi)^3} \theta(k^+) \frac{1}{2} \left( \frac{1}{[p^+ - k^+]^2} - \frac{1}{[p^+ + k^+]^2} \right) \times (-R) \ . \end{aligned} \tag{7.18}$$

We define the set of coordinates

$$\begin{aligned} x &= \frac{k^+}{p^+} \\ k &= (xp^+, xp^\perp + \kappa^\perp) \ , \end{aligned} \tag{7.19}$$

where $p = (p^+, p^\perp)$ is the external electron momentum. Then the electron self energy diagrams, fig.(9), eq. (C.14) in Appendix C, contribute

$$\begin{aligned} p^+ \delta p_{1\lambda}^- &= -\frac{e^2}{8\pi^2} \int_0^1 dx \int d\kappa_\perp^2 \\ &\quad \times \left[ \frac{p^2 - m^2}{\kappa_\perp^2 + f(x)} \left( \frac{2}{[x]} - 2 + x \right) - \frac{2m^2}{\kappa_\perp^2 + f(x)} + \left( \frac{2}{[x]^2} + \frac{1}{[1-x]} \right) \right] \times (-R) \\ f(x) &= xm^2 - x(1-x)p^2 \end{aligned} \tag{7.20}$$

and

$$\begin{aligned} p^+ \delta p_{2\lambda}^- &= \frac{e^2}{8\pi^2} \int_0^\infty dx \int d\kappa_\perp^2 \left( \frac{1}{[x][1-x]} \right) \times (-R) \\ &\rightarrow \frac{e^2}{8\pi^2} \int_0^1 dx \int d\kappa_\perp^2 \left( \frac{1}{[x]} \right) \times (-R) \\ p^+ \delta p_{3\lambda}^- &= \frac{e^2}{8\pi^2} \int_0^\infty dx \int d\kappa_\perp^2 \left( \frac{1}{[1-x]^2} - \frac{1}{(1+x)^2} \right) \times (-R) \\ &\rightarrow \frac{e^2}{8\pi^2} \int_0^1 dx \int d\kappa_\perp^2 \left( \frac{2}{[x]^2} \right) \times (-R) \ ; \end{aligned} \tag{7.21}$$

for details we refer to Appendix C. Note, that the transformation in the integrals over $x$ is performed before the regulator is taken into account [24]. (In the second integral the electron momentum is replaced by the gluon one due to momentum conservation). The brackets '[ ]' denote the principle value prescription, defined further in eq. (7.27).

The loop integral over $k$ eqs. (7.20) and (7.21) contains two types of divergences: UV in the transversal coordinate $\kappa^\perp$ and IR in the longitudinal component $k^+$. The physical value of mass must be IR-finite. We show, that the three relevant diagrams together in fact give an IR-finite value for the renormalized mass; this enables to determine counterterms independent of longitudinal momentum. In the wave function renormalization constant, however, the IR-singularity is still present.

Define

$$\delta_1 = \frac{p^+}{P^+} \,, \tag{7.22}$$

where $P = (P^+, P^\perp)$ is the positronium momentum, $p$ the electron momentum. The transversal UV divergence is regularized through the unitary transformation done, i.e. by the regulator $R$, eq. (7.16)

$$R_\lambda = \exp\left\{ -\left( \frac{\tilde{\Delta}_{p,k}}{\lambda^2 \delta_1} \right)^2 \right\} \;\approx\; \theta(\lambda^2 \delta_1 - |\tilde{\Delta}_{p,k}|) \,, \tag{7.23}$$

where the cutoff is rescaled and defined in units of the positronium momentum $P^+$, namely $\lambda \to \sqrt{2}\lambda^2/P^+$, and $\Delta_{p,k} = p^- - k^- - (p-k)^- = \tilde{\Delta}_{p,k}/p^+$. The rude approximation for the exponential through a $\theta$-function changes the numerical coefficient within a few percent; nevertheless it is useful to estimate the integrals in eqs. (7.20) and (7.21) in this way analytically. From eq. (7.23) we have for the sum of intermediate (electron and photon) state momenta (the external electron is on-mass-shell $p^2 = m^2$)

$$\frac{\kappa^{\perp 2}}{[x]} + \frac{\kappa^{\perp 2} + m^2}{[1-x]} \;\leq\; \lambda^2 \delta_1 + m^2 \tag{7.24}$$

giving for the regulator

$$\begin{aligned} R_\lambda &= \theta(\kappa^{\perp 2}_{\lambda max} - \kappa^{\perp 2})\, \theta(\kappa^{\perp 2}_{\lambda max}) \\ \kappa^{\perp 2}_{\lambda max} &= x(1-x)\lambda^2 \delta_1 - x^2 m^2 \end{aligned} \tag{7.25}$$

and $\theta(\kappa^{\perp 2}_{\lambda max})$ leads to the additional condition for the longitudinal momentum

$$\begin{aligned} &0 \leq x \leq x_{max} \\ &x_{max} = \frac{1}{1 + m^2/(\lambda^2 \delta_1)} \end{aligned} \tag{7.26}$$

implying that the singularity of the photon longitudinal momentum for $x \to 1$ is regularized by the function $R_\lambda$. This is the case due to the nonzero fermion mass present in eq. (7.24) for the intermediate state with $(1-x)$ longitudinal momentum. The IR-singularity when $x \to 0$ is still present; it is treated by the principle value prescription [24]

$$\frac{1}{[k^+]} = \frac{1}{2}\left( \frac{1}{k^+ + i\varepsilon P^+} + \frac{1}{k^+ - i\varepsilon P^+} \right) \,, \tag{7.27}$$

where $\varepsilon = 0_+$, and $P^+$ is the longitudinal part of the positronium momentum (used here as typical momentum in the problem). This defines the bracket '[ ]' in eqs. (7.20) and (7.21)

$$\frac{1}{[x]} = \frac{1}{2}\left( \frac{1}{x + i\frac{\varepsilon}{\delta_1}} + \frac{1}{x - i\frac{\varepsilon}{\delta_1}} \right) \,. \tag{7.28}$$

Making use of both regularizations for transversal and longitudinal components, we have for the first diagram, eq. (7.20),

$$
\begin{aligned}
\delta m_{1\lambda}^2 &= p^+\delta p^-|_{p^2=m^2} \\
\delta m_{1\lambda}^2 &= -\frac{e^2}{8\pi^2}\Big[3m^2\ln\left(\frac{\lambda^2\delta_1+m^2}{m^2}\right)+\frac{\lambda^2\delta_1}{\lambda^2\delta_1+m^2}\left(\frac{3}{2}\lambda^2\delta_1+m^2\right) \\
&- 2\lambda^2\delta_1\ln\left(\frac{\lambda^2\delta_1}{\lambda^2\delta_1+m^2}\frac{\delta_1}{\varepsilon}\right)\Big]
\end{aligned}
\tag{7.29}
$$

Note, that the third term has the mixing UV and IR divergences. Combining the three relevant diagrams, fig.(9), and integrating with the common regulator, one obtains for the **electron mass correction**

$$
\begin{aligned}
\delta m_\lambda^2 &= p^+(\delta p_1+\delta p_2+\delta p_3)|_{p^2=m^2} = -\delta\Sigma_\lambda(m^2) \\
\delta m_\lambda^2 &= -\frac{e^2}{8\pi^2}\left\{3m^2\ln\left(\frac{\lambda^2\delta_1+m^2}{m^2}\right)-\frac{\lambda^2\delta_1 m^2}{\lambda^2\delta_1+m^2}\right\}\,.
\end{aligned}
\tag{7.30}
$$

The mass correction is IR-finite (that gives rise to IR-finite counterterms) and contains only a logarithmic UV-divergence. Namely, when $\lambda\delta_1\to\Lambda\gg m$

$$
\delta m_\Lambda^2 = -\frac{3e^2}{8\pi^2}m^2\ln\frac{\Lambda^2}{m^2}\,.
\tag{7.31}
$$

It is remarkable that we reproduce with the cutoff condition of eq. (7.24) the standard result of covariant perturbative theory calculations including its global factor 3/8. As was mentioned above, the difference in sign, as compared with the 1-loop renormalization group result, comes from scaling down from high to low energies in the method of flow equations.

The similar regularization for the intermediate state momenta in the self-energy integrals, called 'global cutoff scheme', was introduced by W. M. Zhang and A. Harindranath [24]. In our approach the UV-regularization, that defines the concrete form of the regulator $R$, arises naturally from the method of flow equations, namely from the unitary transformation performed, where the generator of the transformation is chosen as the commutator $\eta=[H_d,H_r]$. Note also, that the regulator $R$, eq. (7.23), in general is independent of the electron momentum $p^+$ (rescaled cutoff $\lambda\delta_1\longrightarrow\lambda$), and therefore is boost invariant.

For the wave function renormalization constant, eq. (7.10), one has

$$
\left.\frac{\partial\delta p^-}{\partial p^-}\right|_{p^2=m^2} = -\frac{e^2}{8\pi^2}\int_0^1\int d\kappa_\perp^2\left[\frac{2\frac{1}{x}-2+x}{\kappa_\perp^2+f(x)}-\frac{x(1-x)2m^2}{(\kappa_\perp^2+f(x))^2}\right]_{p^2=m^2}\times(-R)\,,
\tag{7.32}
$$

that together with the regulator $R$, eq. (7.23), results

$$
\begin{aligned}
Z_2 &= 1-\frac{e^2}{8\pi^2}\Big[\ln\frac{\lambda^2\delta_1}{m^2}\cdot\left(\frac{3}{2}-2\ln\frac{\delta_1}{\varepsilon}\right)+\ln\frac{\delta_1}{\varepsilon}\cdot\left(2-\ln\frac{\delta_1}{\varepsilon}\right) \\
&+ F\left(\ln\frac{\lambda^2\delta_1}{\lambda^2\delta_1+m^2};\frac{\lambda^2\delta_1}{\lambda^2\delta_1+m^2}\right)\Big] \\
F &= \ln\frac{\lambda^2\delta_1}{\lambda^2\delta_1+m^2}\left(\frac{1}{2}-\ln\frac{\lambda^2\delta_1}{\lambda^2\delta_1+m^2}\right)+\frac{1}{2}\frac{\lambda^2\delta_1}{\lambda^2\delta_1+m^2}-2+2\int_0^{x_{max}}dx\frac{\ln x}{x-1}\,.
\end{aligned}
\tag{7.33}
$$

As $\lambda\delta_1 \to \Lambda \gg m$ the function $F$ tends to a constant

$$F|_{\Lambda\gg m} = C = -\frac{3}{2} + \frac{\pi^2}{3}\,. \tag{7.34}$$

Therefore, by dropping the finite part, we obtain

$$Z_2 \;=\; 1 - \frac{e^2}{8\pi^2}\left\{\ln\frac{\Lambda^2}{m^2}\cdot\left(\frac{3}{2} - 2\ln\frac{1}{\varepsilon}\right) + \ln\frac{1}{\varepsilon}\left(2 - ln\frac{1}{\varepsilon}\right)\right\}\;, \tag{7.35}$$

where we have rescaled $\frac{\varepsilon}{\delta_1} \to \varepsilon$. The electron wave function renormalization constant contains logarithmic UV and IR divergences mixed, together with pure logarithmic IR divergences. We mention, that the value of $Z_2$ is not sensitive to the form of regulator applied; the same result for $Z_2$ was obtained with another choice of regulator [24].

We proceed with renormalization to the second order in the **photon** sector. The diagrams that contribute to the photon self energy are shown in fig.(10). The commutator $[\eta^{(1)}, H_{ee\gamma}]$, corresponding to the first diagram, gives rise to (eq. (C.22) in Appendix C)

$$\begin{aligned}\delta q^-_{1\lambda}\,\delta^{ij} \;&=\; \frac{1}{[q^+]}e^2\int\frac{d^2k^\perp dk^+}{2(2\pi)^3}\,\theta(k^+)\theta(q^+-k^+)\\ &\qquad\times Tr\left[\Gamma^i(k,k-q,q)\Gamma^j(k-q,k,-q)\right]\frac{1}{q^- - k^- - (q-k)^-}\times(-R)\,,\end{aligned} \tag{7.36}$$

where momenta are given in fig.(10), and the regulator is

$$R_\lambda = f^2_{q,k,\lambda} = \exp\left\{-2\left(\frac{\Delta_{q,k}}{\lambda}\right)^2\right\}\,. \tag{7.37}$$

In full analogy with the electron self energy this also defines the regulator for the second diagram with the instantaneous interaction, see fig.(10),

$$\delta q^-_{2\lambda}\,\delta^{ij} = \frac{1}{[q^+]}e^2\int\frac{d^2k^\perp dk^+}{2(2\pi)^3}\theta(k^+)\,Tr(\sigma^i\sigma^j)\left(\frac{1}{[q^+-k^+]} - \frac{1}{[q^++k^+]}\right)\times(-R)\,. \tag{7.38}$$

We define the set of coordinates

$$\begin{aligned}&\frac{(q-k)^+}{q^+} = x\\ &k = ((1-x)q^+, (1-x)q^\perp + \kappa^\perp)\\ &(q-k) = (xq^+, xq^\perp - \kappa^\perp)\,,\end{aligned} \tag{7.39}$$

where $q = (q^+, q^\perp)$ is the external photon momentum. Then two diagrams contribute (for details see Appendix C, eq. (C.26)):

$$\begin{aligned}q^+\,\delta q^-_1 \;&=\; -\frac{e^2}{8\pi^2}\int_0^1 dx\int d\kappa^2_\perp\\ &\qquad\times\left\{\frac{q^2}{\kappa^2_\perp + f(x)}\left(2x^2 - 2x + 1\right) + \frac{2m^2}{\kappa^2_\perp + f(x)} + \left(-2 + \frac{1}{[x][1-x]}\right)\right\}\times(-R)\\ f(x) \;&=\; m^2 - x(1-x)q^2\\ q^+\,\delta q^-_2 \;&=\; \frac{e^2}{8\pi^2}\int_0^\infty dx\int d\kappa^2_\perp\left(\frac{1}{[1-x]} - \frac{1}{1+x}\right)\times(-R)\\ &\to\; -\frac{e^2}{8\pi^2}\int_0^1 dx\int d\kappa^2_\perp\frac{2}{[x]}\times(-R)\,.\end{aligned} \tag{7.40}$$

Note, that the transformation in the second integral is done before the regularization (by regulator the $R$) is performed [24].

Making use of the same approximation for the regulator as in the electron sector, we obtain for the sum of intermediate (two electron) state momenta

$$\begin{aligned} &\frac{\kappa_\perp^2+m^2}{x}+\frac{\kappa_\perp^2+m^2}{1-x}\le\lambda^2\delta_2\\ &\delta_2=\frac{q^+}{P^+}\ , \end{aligned} \tag{7.41}$$

where the photon is put on mass-shell $q^2=0$ and the rescaled cutoff $\lambda\to\sqrt{2}\lambda^2/P^+$ has been used. This condition means for the transversal integration

$$\begin{aligned} R_\lambda &= \theta(\kappa^{\perp 2}_{\lambda max}-\kappa^{\perp 2})\,\theta(\kappa^{\perp 2}_{\lambda max})\\ \kappa^{\perp 2}_{\lambda max} &= x(1-x)\lambda^2\delta_2-m^2\ , \end{aligned} \tag{7.42}$$

and for the longitudinal integration

$$\begin{aligned} &x_1\le x\le x_2\\ &x_1=\frac{1-r}{2}\approx\frac{m^2}{\lambda^2\delta_2}\\ &x_2=\frac{1+r}{2}\approx 1-\frac{m^2}{\lambda^2\delta_2}\\ &r=\sqrt{1-\frac{4m^2}{\lambda^2\delta_2}}\ , \end{aligned} \tag{7.43}$$

where the approximate value is used when $m\ll\lambda$. This shows that the condition of eq. (7.41) for two electrons with masses $m$ removes the light-front infrared singularities from $x\to 0$ and $x\to 1$. Thus, both UV and IR divergences are regularized by the regulator R, eq. (7.42).

The mass correction arising from the first diagram, eq. (7.40), is

$$\delta m^2_{1\lambda}=\frac{e^2}{8\pi^2}\,\frac{2}{3}\,\lambda^2\delta_2\left(1-\frac{4m^2}{\lambda^2\delta_2}\right)^{3/2}\ . \tag{7.44}$$

Combining together both diagrams with the same regulator, eq. (7.40), we obtain

$$\delta m^2_\lambda=\frac{e^2}{8\pi^2}\left(\frac{5}{3}\lambda^2\delta_2\, r-\frac{8}{3}m^2\, r-2m^2\,\ln\frac{1+r}{1-r}\right)\ , \tag{7.45}$$

where $r$ is defined in eq. (7.43). The result shows that the mass correction involves the quadratic and logarithmic UV divergences, i.e. as $\lambda\delta_2\to\Lambda\gg m$

$$\delta m^2_\Lambda=\frac{e^2}{8\pi^2}\left(\frac{5}{3}\Lambda^2-2m^2\,\ln\frac{\Lambda^2}{m^2}\right)\ . \tag{7.46}$$

The wave function renormalization constant is defined through

$$\left.\frac{\partial\delta q^-}{\partial q^-}\right|_{q^2=0}=-\frac{e^2}{8\pi^2}\int_0^1 dx\int d\kappa_\perp^2\left.\left\{\frac{2x^2-2x+1}{\kappa_\perp^2+f(x)}+\frac{2m^2x(1-x)}{(\kappa_\perp^2+f(x))^2}\right\}\right|_{q^2=0}\times(-R)\ , \tag{7.47}$$

that, with the regulator $R$, eq. (7.42), results

$$Z_2=1-\frac{e^2}{8\pi^2}\left(-\frac{2}{3}\ln\frac{1+r}{1-r}+\frac{10}{9}r+\frac{8}{9}\frac{m^2}{\lambda^2\delta_2}r\right)\ . \tag{7.48}$$

The photon wave function renormalization constant contains only logarithmic UV divergence, indeed as $\lambda\delta_2 \to \Lambda \gg m$

$$Z_2 = 1 - \frac{e^2}{8\pi^2}(-\frac{2}{3}\ln\frac{\Lambda^2}{m^2}) \tag{7.49}$$

and is free of IR divergences (as is expected from the form of the regulator $R$, eq. (7.41)).

## 7.3 Mass renormalization

Following light-cone rules the perturbative energy correction of the electron with momentum $p$, coming from the emission and absorption of a photon with momentum $k$, is

$$\delta\tilde{p}^-_{1\lambda} = \int \frac{d^2k^\perp dk^+}{2(2\pi)^3}\frac{\theta(k^+)}{k^+}\theta(p^+ - k^+) g_{p-k,p,\lambda}\Gamma^i_\lambda(p-k,p,-k) g_{p,p-k,\lambda}\Gamma^i_\lambda(p,p-k,k) \\ \times\frac{1}{p^- - k^- - (p-k)^-}\ , \tag{7.50}$$

where $g_{ee\gamma}$-coupling constant restricts the energy of the photon. Making use of the explicit form for the coupling, one has

$$\begin{aligned}\delta\tilde{p}^-_{1\lambda} &= e^2\int \frac{d^2k^\perp dk^+}{2(2\pi)^3}\frac{\theta(k^+)}{k^+}\theta(p^+ - k^+) \qquad (7.51)\\ &\quad \times\Gamma^i_\lambda(p-k,p,-k)\,\Gamma^i_\lambda(p,p-k,k)\frac{1}{p^- - k^- - (p-k)^-}\times(R)\ ,\end{aligned}$$

where $R = f^2_{pk\lambda}$ plays the role of regulator. This expression coincide up to the overall sign with the energy correction obtained in the previous section from the flow equations method.

Two instantaneous diagrams, arising from the normal-ordering Hamiltonian, must be added to the first term with the same regulator $R$. Then the full perturbative energy correction $\delta\tilde{p}^-_\lambda = \delta\tilde{p}^-_{1\lambda} + \delta\tilde{p}^-_{2\lambda} + \delta\tilde{p}^-_{3\lambda}$ is

$$\delta\tilde{p}^-_\lambda = -\delta p^-_\lambda \tag{7.52}$$

where $\delta p^-_\lambda$ is defined in eq. (7.13). This means for the perturbative mass correction

$$\delta m^{PT2}_\lambda = \delta\Sigma_\lambda \tag{7.53}$$

and the self-energy term $\delta\Sigma_\lambda$ is given in eq. (7.30).

We combine the mass operator, renormalized to the second order, eq. (7.12), and the perturbation theory correction, eq. (7.53), to obtain the total physical mass to the order $O(e^2)$

$$m^2_e = m^2_\lambda + \delta m^2 = (m^2 + \delta\Sigma_\lambda) - \delta\Sigma_\lambda = m^2 + O(e^4)\ . \tag{7.54}$$

This means, that to the second order $O(e^2)$ the physical electron mass is, up to a finite part, equal to the electron mass, that stands in the free (canonical) Hamiltonian $H_0$.

Along the same line one can proceed for the photon mass. One finds in the second order in coupling, that the photon mass counterterm, obtained from the flow equations eq. (7.44)-eq. (7.46), is equal up to the overall sign to the perturbative photon mass correction. This means, that in the order $O(e^2)$ the physical photon mass is equal to the photon mass term in the free Hamiltonian, i.e.

$$m^2_{ph} = 0 + O(e^4) \tag{7.55}$$

here the photon mass in the canonical QED Hamiltonian is equal to zero to preserve gauge invariance.

At the end we note, that the similarity function $f_{p_i p_f \lambda}$, restricting the electron-photon vertex, plays the role of UV (and partially IR) regulator in the self energy integrals. This means, that the regularization prescription of divergent integrals follows from the method of flow equations itself. Moreover, the energy correction (i.e. mass correction and wave function renormalization constant), obtained from the flow equations, coincide up to the overall sign with the 1-loop renormalization group result. This is the remarkable result, indicating to the equivalence of flow equations and Wilson's renormalization.

# Chapter 8

# Conclusions and outlook

In this work we applied the method of flow equations to QED on the light-front. We have outlined a strategy to derive an effective low-energy Hamiltonian on the light-front by means of flow equations, considered in the light-front dynamics. Application of the flow equations with the condition, that particle number conserving terms are considered diagonal and those changing the particle number off-diagonal led as in other cases to a useful effective Hamiltonian.

The main advantage of this procedure as compared with the similarity renormalization of Glazek and Wilson [3] is, that finally states of different particle number are completely decoupled, since the particle number violating contributions are eliminated down to $\lambda = 0$. Thus one is able to truncate the Fock space and the positronium problem reduces to a two particle problem, which was analyzed analytically (since in leading order one obtains the nonrelativistic Coulomb problem) in the chapter 4, and numerically in the chapter 5 for positronium bound states.

The effective Hamiltonian, obtained by the similarity transformation, is band-diagonal in the energy space. The width of the band $\lambda$ introduces the artificial parameter in the procedure, which is defined from the physical reasoning ($\lambda$ is low enough to neglect the contribution of high Fock states, but is restricted from below to stay in perturbation theory region). Flow equations as used here with the particle number conserving part of Hamiltonian to be diagonal, have no additional parameter and converge well as $\lambda \to 0$ [2] to the effective Hamiltonian, which is block-diagonal in particle number and are used therefore directly for the numerical calculations of the spectrum.

The procedure of elimination of nondiagonal blocks, that change the number of quasiparticles, is performed not just in one step as in the method of Tamm-Dancoff truncation but rather continuously for the states with different energies in sequence. This is the main advantage of the proposed method as compared with Tamm-Dancoff truncation, the possibility to perform simultaneously the ultraviolet renormalization of the initial Hamiltonian. In general, in the definite order of perturbation theory all counterterms, associated with canonical operators of the theory and also with possible new operators induced by unitary transformation, can be obtained in the procedure [53]. Since different sectors of the effective Hamiltonian are decoupled, one does not encounter the usual difficulties of Tamm-Dancoff truncation and the methods related to it. Namely, the counterterms to be introduced are 'sector-' and 'state-' independent [46].

If one goes beyond the tree approximation then one obtains terms with ultraviolet divergences which have to be renormalized. In the second order in coupling the electron and photon divergent mass corrections are generated by flow equations. There are the same type of UV-divergences as obtained in the covariant perturbation theory, the IR-divergences in the longitudinal direction and mixed UV- and IR-divergences in the mass terms. The two latter types of divergences are specific for the light-front QED calculations. They signal, that the boost invariance is broken, since an explicit dependence on the longitudinal IR-cutoff occur. To preserve boost invariance in the renormalized Hamiltonian we take into account the diagrams arising from the normal ordering of instantaneous interactions. Using then flow equations and coupling coherence we obtain the counterterms for electron and photon masses, that are free from IR-divergences.

Simultaneously also terms describing interactions between more than two particles are generated. In this approach we were not faced with infrared problems, except for the longitudinal IR-divergences, which arise due to the light-front gauge formulation and must be treated properly. These divergences, arising on the level of effective QED Hamiltonian, show that some symmetries of the initial theory, that are not manifest on the light-front, are broken. The first problem in the light-front field theory is that whenever the generator of a symmetry is dynamical (contains interactions) it is practically impossible to monitor and maintain that symmetry at each step of a calculations- unless of course one can solve the theory exactly. This concerns parity and rotational invariance, that are not manifest on the light-front. The second problem is that whenever we use the Hamiltonian technique, the regularization by introducing bare cutoffs breaks the gauge invariance (and also Lorenz covariance), and forces the bare Hamiltonian to contain a larger than normal suite of counterterms to enable a finite limit as the cutoffs are removed. One way is, that the counterterms are then adjusted to reproduce physical observables and to restore the symmetries broken by the cutoffs. The other way is to find the gauge invariant procedure for regularization of Hamiltonians. The attempt in the latter direction was made by Brodsky, Hiller, McCartor [47]. Solving the Yukawa theory they have tried to preserve more symmetries by using Pauli-Villars procedure for regularization.

In our calculations, the effective electron-positron interaction, obtained in the second order in coupling, contains the IR-divergent term, describing instant emission and absorption of 'longitudinal' photon. The physical reason for its appearance is the violation of Lorenz and gauge symmetries by the derivation of the effective, renormalized Hamiltonian. We use the symmetric cutoff condition for IR-divergences in the effective interaction to cancel their contribution to the mass of positronium. We find, that in this case the rotational symmetry is restored on the level of positronium mass spectrum.

In order to solve the flow equations analytically we were forced to apply in this work the perturbation theory expansion. One is able to improve this approach systematically by going to higher orders in the coupling. It is a remarkable result, that the effective electron-positron Hamiltonian, obtained in the second order in coupling, gives the correct Bohr spectrum and hyperfine splitting for positronium.

We consider flow equations as a method which can also be used beyond perturbation theory in a self-consistent way. Examples in solid-state physics are the flow of the tunneling-frequency in the spin-boson model [6] and of the phonon energies in the electron-phonon coupling [10]. Due to the flow the couplings decay even at resonance.

# Appendix A

# Calculation of the commutator $[\eta^{(1)}(l), H_{ee\gamma}]$ in the electron-positron sector

Here we calculate the commutator $[\eta^{(1)}(l), H_{ee\gamma}]$ in the electron-positron sector. The leading order generator $\eta^{(1)}$ is:

$$\begin{aligned}\eta^{(1)}(l) = \sum_{\lambda s_1 s_3} \int d^3p_1 d^3p_3 d^3q (\eta^*_{p_1p_3}(l)\varepsilon^i_\lambda \tilde{a}_q + \eta_{p_1p_3}(l)\varepsilon^{i*}_\lambda \tilde{a}^+_{-q})\,(\tilde{b}^+_{p_3}\tilde{b}_{p_1} + \tilde{b}^+_{p_3}\tilde{d}^+_{-p_1} + \tilde{d}_{-p_3}\tilde{b}_{p_1} + \tilde{d}_{-p_3}\tilde{d}^+_{-p_1}) \\ \times \chi^+_{s_3}\Gamma^i_l(p_1, p_3, -q)\chi_{s_1}\,\delta_{q,-(p_1-p_3)}\ , \qquad \text{(A.1)}\end{aligned}$$

where

$$\eta_{p_1p_3}(l) = -\Delta_{p_1p_3}\cdot g_{p_1p_3} = \frac{1}{\Delta_{p_1p_3}}\cdot\frac{dg_{p_1p_3}}{dl}\ , \qquad \text{(A.2)}$$

$\Delta_{p_1p_3} = p_1^- - p_3^- - (p_1 - p_3)^-$, and the electron-photon coupling

$$\begin{aligned}H_{ee\gamma} = \sum_{\lambda s_2 s_4} \int d^3p_2 d^3p_4 d^3q' (g^*_{p_2p_4}(l)\varepsilon^j_{\lambda'} \tilde{a}_{q'} + g_{p_2p_4}(l)\varepsilon^{j*}_{\lambda'} \tilde{a}^+_{-q'})\,(\tilde{b}^+_{p_4}\tilde{b}_{p_2} + \tilde{b}^+_{p_4}\tilde{d}^+_{-p_2} + \tilde{d}_{-p_4}\tilde{b}_{p_2} + \tilde{d}_{-p_4}\tilde{d}^+_{-p_2}) \\ \times \chi^+_{s_4}\Gamma^i_l(p_2, p_4, -q')\chi_{s_2}\,\delta_{q',-(p_2-p_4)}\ , \qquad \text{(A.3)}\end{aligned}$$

where

$$\Gamma^i_l(p_1, p_2, q) = 2\frac{q^i}{q^+} - \frac{\sigma\cdot p_2^\perp - im_{p_1p_2}(l)}{p_2^+}\sigma^i - \sigma^i\frac{\sigma\cdot p_1^\perp + im_{p_1p_2}(l)}{p_1^+} \qquad \text{(A.4)}$$

and the tilde-fields are defined in eq. (3.31). The mass term $m_{p_1p_2}(l)$ starts to depend on $l$ in the second order in coupling constant. We omit the dependence of $m_{p_1p_2}$ and hence the dependence of vertex matrix element $\Gamma^i(p_1, p_2, q)$ on $l$ in calculation of commutator $[\eta^{(1)}(l), H_{ee\gamma}]$ to the leading (second) order. Further we use the identities for the polarisation vectors and spinors

$$\sum_\lambda \varepsilon^{i*}_\lambda \varepsilon^j_\lambda = \delta^{ij}\ , \qquad \chi^+_s\chi_{s'} = \delta_{ss'}\ . \qquad \text{(A.5)}$$

Using the commutation relations, eq. (3.23), and identities eq. (A.5) we have

$$\begin{aligned}[\eta^{(1)}(l), H_{ee\gamma}] &= \frac{1}{2}\left(-\eta_{p_1p_3}g^*_{p_2p_4}\frac{\theta(p_1^+ - p_3^+)}{p_1^+ - p_3^+} + \eta^*_{p_1p_3}g_{p_2p_4}\frac{\theta(p_3^+ - p_1^+)}{p_3^+ - p_1^+}\right) \qquad \text{(A.6)} \\ &\quad \times\!:(-\tilde{b}^+_{p_3}\tilde{d}^+_{-p_2}\tilde{d}_{-p_4}\tilde{b}_{p_1} - \tilde{b}^+_{p_4}\tilde{d}^+_{-p_1}\tilde{d}_{-p_3}\tilde{b}_{p_2} + \tilde{b}^+_{p_3}\tilde{d}^+_{-p_1}\tilde{d}_{-p_4}\tilde{b}_{p_2} + \tilde{b}^+_{p_4}\tilde{d}^+_{-p_2}\tilde{d}_{-p_3}\tilde{b}_{p_1}): \\ &\quad \times(\chi^+_{s_3}\Gamma^i_l(p_1, p_3, p_1 - p_3)\chi_{s_1})\,(\chi^+_{s_4}\Gamma^i_l(p_2, p_4, p_2 - p_4)\chi_{s_2})\,\delta_{p_1+p_2,p_3+p_4}\ ,\end{aligned}$$

where the first two terms of the field operators contribute to the exchange channel, and the next two to the annihilation channel. We take into account both $s$- and $t$-channel terms to calculate the bound states. The : : stand for the normal ordering of the fermion operators and $(\frac{1}{2})$ is the symmetry factor. The sum over helicities $s_i$ and the 3-dimensional integration over momenta $p_i$, $i = 1, ..4$, according to eq. (3.32) is implied. We rewrite for both channels

$$[\eta, H_{ee\gamma}] = \left\{ \begin{array}{l} M_{2ij}^{(ex)} (\frac{1}{2}) \left\{ \frac{\theta(p_1^+ - p_3^+)}{(p_1^+ - p_3^+)} \left( \eta_{p_1,p_3} g^*_{-p_4,-p_2} - \eta^*_{-p_4,-p_2} g_{p_1,p_3} \right) \right. \\ \qquad \left. + \frac{\theta(-(p_1^+ - p_3^+))}{-(p_1^+ - p_3^+)} \left( \eta_{-p_4,-p_2} g^*_{p_1,p_3} - \eta^*_{p_1,p_3} g_{-p_4,-p_2} \right) \right\} \\ \qquad \times \delta^{ij} \delta_{p_1+p_2,p_3+p_4} \, b^+_{p_3 s_3} d^+_{p_4 \bar{s}_4} d_{p_2 \bar{s}_2} b_{p_1 s_1} \\ \\ -M_{2ij}^{(an)} (\frac{1}{2}) \left\{ \frac{\theta(p_1^+ + p_2^+)}{(p_1^+ + p_2^+)} \left( \eta_{p_1,-p_2} g^*_{-p_4,p_3} - \eta^*_{-p_4,p_3} g_{p_1,-p_2} \right) \right. \\ \qquad \left. + \frac{\theta(-(p_1^+ + p_2^+))}{-(p_1^+ + p_2^+)} \left( \eta_{-p_4,p_3} g^*_{p_1,-p_2} - \eta^*_{p_1,-p_2} g_{-p_4,p_3} \right) \right\} \\ \qquad \times \delta^{ij} \delta_{p_1+p_2,p_3+p_4} \, b^+_{p_3 s_3} d^+_{p_4 \bar{s}_4} d_{p_2 \bar{s}_2} b_{p_1 s_1} \end{array} \right. \tag{A.7}$$

where

$$\begin{aligned} M_{2ij}^{(ex)} &= (\chi^+_{s_3} \Gamma^i (p_1, p_3, p_1 - p_3) \chi_{s_1}) \, (\chi^+_{\bar{s}_2} \Gamma^j (-p_4, -p_2, -(p_1 - p_3)) \chi_{\bar{s}_4}) \\ M_{2ij}^{(an)} &= (\chi^+_{s_3} \Gamma^i (-p_4, p_3, -(p_1 + p_2)) \chi_{\bar{s}_4}) \, (\chi^+_{\bar{s}_2} \Gamma^j (p_1, -p_2, p_1 + p_2) \chi_{s_1}) \; . \end{aligned} \tag{A.8}$$

The first term in the exchange channel with $p_1^+ > p_3^+$ corresponds to the light-front time ordering $x_1^+ < x_3^+$ with the intermediate state $P_k^- = p_3^- + (p_1 - p_3)^- + p_2^-$, the second term $p_1^+ < p_3^+$ and $x_1^+ > x_3^+$ has the intermediate state $P_k^- = p_1^- - (p_1 - p_3)^- + p_4^-$. Both terms can be viewed as the retarded photon exchange. The same does hold for the annihilation channel.

Consider only real couplings and take into account the symmetry

$$\eta_{-p_4,-p_2} = -\eta_{p_4,p_2} \; , \qquad g_{-p_4,-p_2} = g_{p_4,p_2} \; . \tag{A.9}$$

Then $\langle p_3 s_3, p_4 \bar{s}_4 | \, [\eta^{(1)}, H_{ee\gamma}] \, | p_1 s_1, p_2 \bar{s}_2 \rangle$, the matrix element of the commutator between the free states of positronium in the exchange and annihilation channel, reads

$$< [\eta^{(1)}, H_{ee\gamma}] >= \left\{ \begin{array}{l} M_{2ii}^{ex} \frac{1}{(p_1^+ - p_3^+)} \left( \eta_{p_1,p_3} g_{p_4,p_2} + \eta_{p_4,p_2} g_{p_1,p_3} \right) \\ -M_{2ii}^{an} \frac{1}{(p_1^+ + p_2^+)} \left( \eta_{p_1,-p_2} g_{p_4,-p_3} + \eta_{p_4,-p_3} g_{p_1,-p_2} \right) \end{array} \right. \; . \tag{A.10}$$

where the conservation of $'+'$ and $'\perp'$ components of the total momentum is implied, i.e. $p_1^+ + p_2^+ = p_3^+ + p_4^+$ and $p_1^\perp + p_2^\perp = p_3^\perp + p_4^\perp$. We rewrite this expression through the corresponding $f$-functions

$$\begin{aligned} \eta_{p_1,p_3} g_{p_4,p_2} + \eta_{p_4,p_2} g_{p_1,p_3} &= e^2 \left[ \frac{1}{\Delta_{p_1,p_3}} \frac{df_{p_1,p_3}(l)}{dl} f_{p_4,p_2}(l) + \frac{1}{\Delta_{p_4,p_2}} \frac{df_{p_4,p_2}(l)}{dl} f_{p_1,p_3}(l) \right] \\ \eta_{p_1,-p_2} g_{p_4,-p_3} + \eta_{p_4,-p_3} g_{p_1,-p_2} &= e^2 \left[ \frac{1}{\Delta_{p_1,-p_2}} \frac{df_{p_1,-p_2}(l)}{dl} f_{p_4,-p_3}(l) + \frac{1}{\Delta_{p_4,-p_3}} \frac{df_{p_4,-p_3}(l)}{dl} f_{p_1,-p_2}(l) \right] \end{aligned} \tag{A.11}$$

with $\Delta_{p_1,p_2} = p_1^- - p_2^- - (p_1 - p_2)^-$. This form in terms of the $f$-function is universal for all unitary transformations.

We calculate the matrix elements $M_{2ii}$, eq. (188), for both channels. Here we follow the notations introduced in [39].

We make use of the identities

$$\chi_s^+\sigma^i\sigma^j\chi_s=\delta^{ij}+is\varepsilon^{ij}\ ,\qquad \chi_s^+\sigma^j\sigma^i\chi_s=\delta^{ij}+i\bar{s}\varepsilon^{ij} \tag{A.12}$$

with $\bar{s}=-s$ and $\chi_s^+\chi_{s'}=\delta_{ss'}$; also of

$$\chi_{\bar{s}}^+\sigma^i\chi_s=-\sqrt{2}s\varepsilon_s^i\ ,\qquad \chi_s^+\sigma^i\chi_{\bar{s}}=-\sqrt{2}s\varepsilon_s^{i*} \tag{A.13}$$

with $\varepsilon_s^*=-\varepsilon_{\bar{s}}$ and $\varepsilon_s^i\varepsilon_{s'}^i=-\delta_{s\bar{s}'}$.

We use the standard light-front frame, fig.(3),

$$\begin{aligned} p_1&=(xP^+,xP^\perp+\kappa_\perp)\ , & p_2&=((1-x)P^+,(1-x)P^\perp-\kappa_\perp)\ ,\\ p_3&=(x'P^+,x'P^\perp+\kappa'_\perp)\ , & p_4&=((1-x')P^+,(1-x')P^\perp-\kappa'_\perp)\ , \end{aligned} \tag{A.14}$$

where $P=(P^+,P^\perp)$ is the positronium momentum.

Then, to calculate the matrix element $M_{2ii}$ in the **exchange channel**, we find

$$\begin{aligned} P^+[\chi_{s_3}^+\Gamma^i(p_1,p_3,p_1-p_3)\chi_{s_1}] &= \chi_{s_3}^+\left[2\frac{(\kappa_\perp-\kappa'_\perp)^i}{(x-x')}-\frac{\sigma\cdot\kappa'_\perp}{x'}\sigma^i+\sigma^i\frac{\sigma\cdot\kappa_\perp}{x}+im\frac{x-x'}{xx'}\sigma^i\right]\chi_{s_1}\\ &= T_2^i\delta_{s_1s_3}+im\frac{x-x'}{xx'}(-\sqrt{2})s_1\varepsilon_{s_1}^i\delta_{s_1\bar{s}_3}\ , \end{aligned} \tag{A.15}$$

and

$$\begin{aligned} &P^+[\chi_{\bar{s}_2}^+\Gamma^i(-p_4,-p_2,-(p_4-p_2))\chi_{\bar{s}_4}]\\ &\qquad=\chi_{\bar{s}_2}^+\left[2\frac{(\kappa_\perp-\kappa'_\perp)^i}{x-x'}+\left(\frac{\sigma\cdot\kappa_\perp}{1-x}\sigma^i+\sigma^i\frac{\sigma\cdot\kappa'_\perp}{1-x'}\right)-im\frac{x-x'}{(1-x)(1-x')}\sigma^i\right]\chi_{\bar{s}_4}\\ &\qquad=-\left[T_1^i\delta_{s_2s_4}+im\frac{x-x'}{(1-x)(1-x')}(-\sqrt{2})s_2\varepsilon_{s_2}^i\delta_{s_2\bar{s}_4}\right]\ , \end{aligned} \tag{A.16}$$

where we have introduced

$$\begin{aligned} T_1^i &\equiv -\left[2\frac{(\kappa_\perp-\kappa'_\perp)^i}{x-x'}+\frac{\kappa_\perp^i(s_2)}{(1-x)}+\frac{\kappa'^i_\perp(\bar{s}_2)}{(1-x')}\right]\\ T_2^i &\equiv 2\frac{(\kappa_\perp-\kappa'_\perp)^i}{x-x'}-\frac{\kappa_\perp^i(s_1)}{x}-\frac{\kappa'^i_\perp(\bar{s}_1)}{x'} \end{aligned} \tag{A.17}$$

and

$$\kappa_\perp^i(s)\equiv\kappa_\perp^i+is\,\varepsilon_{ij}\,\kappa_\perp^j\ . \tag{A.18}$$

Finaly we result

$$\begin{aligned} P^{+2}\,M_{2ii}^{(ex)} = -\Bigg\{&\delta_{s_1s_3}\delta_{s_2s_4}T_1^\perp\cdot T_2^\perp-\delta_{s_1\bar{s}_2}\delta_{s_1\bar{s}_3}\delta_{s_2\bar{s}_4}2m^2\frac{(x-x')^2}{xx'(1-x)(1-x')}\\ &+im\sqrt{2}(x'-x)\left[\delta_{s_1\bar{s}_3}\delta_{s_2s_4}\frac{s_1}{xx'}T_1^\perp\cdot\varepsilon_{s_1}^\perp+\delta_{s_1s_3}\delta_{s_2\bar{s}_4}\frac{s_2}{(1-x)(1-x')}T_2^\perp\cdot\varepsilon_{s_2}^\perp\right]\Bigg\}\ . \end{aligned} \tag{A.19}$$

Whereas in the **annihilation channel** we calculate

$$\begin{aligned} P^+[\chi_{s_3}^+\Gamma^i(-p_4,p_3,-(p_1+p_2))\chi_{\bar{s}_4}] &= \chi_{s_3}^+\left[-\frac{\sigma\cdot\kappa'_\perp}{x'}\sigma^i+\sigma^i\frac{\sigma\cdot\kappa'_\perp}{1-x'}+im\frac{1}{x'(1-x')}\sigma^i\right]\chi_{\bar{s}_4}\\ &= T_3^i\delta_{s_3\bar{s}_4}+im\frac{1}{x'(1-x')}(-\sqrt{2})s_4\varepsilon_{s_4}^{i*}\delta_{s_3s_4} \end{aligned} \tag{A.20}$$

and

$$P^+[\chi^+_{\bar{s}_2}\Gamma^i(p_1,-p_2,p_1+p_2)\chi_{s_1}] = \chi^+_{\bar{s}_2}\left[\frac{\sigma\cdot\kappa_\perp}{1-x}\sigma^i-\sigma^i\frac{\sigma\cdot\kappa_\perp}{x}-im\frac{1}{x(1-x)}\sigma^i\right]\chi_{s_1}$$
$$= T_4^i\delta_{s_1\bar{s}_2}-im\frac{1}{x(1-x)}(-\sqrt{2})s_1\varepsilon^i_{s_1}\delta_{s_1s_2}\ , \tag{A.21}$$

where we have introduced

$$\begin{aligned} T_3^i &\equiv -\frac{{\kappa'}^i_\perp(\bar{s}_3)}{x'}+\frac{{\kappa'}^i_\perp(s_3)}{1-x'} \\ T_4^i &\equiv \frac{\kappa^i_\perp(\bar{s}_1)}{1-x}-\frac{\kappa^i_\perp(s_1)}{x}\ . \end{aligned} \tag{A.22}$$

We finally have

$$P^{+2}\,M^{(an)}_{2ii} = \delta_{s_1\bar{s}_2}\delta_{s_3\bar{s}_4}T_3^\perp\cdot T_4^\perp+\delta_{s_1s_2}\delta_{s_3s_4}\delta_{s_1s_3}2m^2\frac{1}{xx'(1-x)(1-x')} \tag{A.23}$$
$$+im\sqrt{2}\left[\delta_{s_3\bar{s}_4}\delta_{s_1s_2}\frac{s_1}{x(1-x)}T_3^\perp\cdot\varepsilon^\perp_{s_1}-\delta_{s_3s_4}\delta_{s_1\bar{s}_2}\frac{s_3}{x'(1-x')}T_4^\perp\cdot\varepsilon^{\perp *}_{s_4}\right]\ .$$

# Appendix B

# Matrix elements of the effective interaction.Exchange channel

In this Appendix we follow the scheme of the work [30] to calculate the matrix elements of the effective interaction in the exchange channel. Here, we list the general, angle-dependent matrix elements defining the effective interaction in the exchange channel eq. (6.55) (part I), and the corresponding matrix elements of the effective interaction for arbitrary $J_z$, after integrating out the angles eq. (6.6) (part II). The whole is given for the similarity function $f_\lambda(\Delta) = u_\lambda(\Delta) = \theta(\lambda^2 - |\Delta|)$ eq. (2.34) with the sharp cutoff. The effective interaction generated by the unitary transformation in the exchange channel reads eq. (6.58),eq. (6.61)

$$
\begin{aligned}
V_{LC}^{eff} &= -e^2 < \gamma^\mu \gamma^\nu > g_{\mu\nu} \left( \frac{\theta(a_1 - a_2)}{\tilde{\Delta}_1} + \frac{\theta(a_2 - a_1)}{\tilde{\Delta}_2} \right) \\
&\quad -e^2 < \gamma^\mu \gamma^\nu > \eta_\mu \eta_\nu \frac{1}{2q^{+2}} \left( \frac{(a_1 - a_2)\theta(a_1 - a_2)}{\tilde{\Delta}_1} + \frac{(a_2 - a_1)\theta(a_2 - a_1)}{\tilde{\Delta}_2} \right) \\
&= -e^2 < \gamma^\mu \gamma^\nu > g_{\mu\nu} \left( \frac{\theta(a_1 - a_2)}{\tilde{\Delta}_1} + \frac{\theta(a_2 - a_1)}{\tilde{\Delta}_2} \right) \\
&\quad -e^2 < \gamma^\mu \gamma^\nu > \eta_\mu \eta_\nu \frac{1}{2q^{+2}} |a_1 - a_2| \left( \frac{\theta(a_1 - a_2)}{\tilde{\Delta}_1} + \frac{\theta(a_2 - a_1)}{\tilde{\Delta}_2} \right)
\end{aligned}
\tag{B.1}
$$

where fig.(4)

$$
< \gamma^\mu \gamma^\nu > |_{exch} = \frac{\bar{u}(p_1, \lambda_1)}{\sqrt{p_1^+}} \gamma^\mu \frac{u(p_1^{'}, \lambda_1^{'})}{\sqrt{p_1^{'+}}} \frac{\bar{v}(p_2^{'}, \lambda_2^{'})}{\sqrt{p_2^{'+}}} \gamma^\nu \frac{v(p_2, \lambda_2)}{\sqrt{p_2^+}} P^{+2} \tag{B.2}
$$

$q = p_1' - p_1$ is the momentum transfer. One has in eq. (B.1)

$$
\begin{aligned}
&\tilde{\Delta}_1 = a_1 - 2k_\perp k_\perp^{'} \cos(\varphi - \varphi^{'}) \\
&\tilde{\Delta}_2 = a_2 - 2k_\perp k_\perp^{'} \cos(\varphi - \varphi^{'}) \\
&\tilde{\Delta} = a - 2k_\perp k_\perp^{'} \cos(\varphi - \varphi^{'}) \\
&\vec{k}_\perp = k_\perp(\cos\varphi, \sin\varphi)
\end{aligned}
\tag{B.3}
$$

and

$$
a_1 = \frac{x'}{x} k_\perp^2 + \frac{x}{x'} k_\perp^{'2} + m^2 \frac{(x - x')^2}{xx'}
$$

$$
\begin{aligned}
&= k_\perp^2 + k_\perp^{'2} + (x-x')\left(k_\perp^2(-\frac{1}{x}) - k_\perp^{'2}(-\frac{1}{x'})\right) + m^2\frac{(x-x')^2}{xx'} \\
a_2 &= \frac{1-x'}{1-x}k_\perp^2 + \frac{1-x}{1-x'}k_\perp^{'2} + m^2\frac{(x-x')^2}{(1-x)(1-x')} \\
&= k_\perp^2 + k_\perp^{'2} + (x-x')\left(k_\perp^2\frac{1}{1-x} - k_\perp^{'2}\frac{1}{1-x'}\right) + m^2\frac{(x-x')^2}{(1-x)(1-x')} \\
a &= k_\perp^2 + k_\perp^{'2} + \frac{(x-x')}{2}\left(k_\perp^2(\frac{1}{1-x} - \frac{1}{x}) - k_\perp^{'2}(\frac{1}{1-x'} - \frac{1}{x'})\right) \\
&+ m^2\frac{(x-x')^2}{2}\left(\frac{1}{xx'} + \frac{1}{(1-x)(1-x')}\right) \\
a &= \frac{1}{2}(a_1 + a_2) \qquad \text{(B.4)}
\end{aligned}
$$

The energy denominator ($\tilde{\Delta}$ and $a$ corresponding) in the case of perturbative theory is given for completeness.

It is useful to display the matrix elements of the effective interaction in the form of tables. The matrix elements depend on the one hand on the momenta of the electron and positron, respectively, and on the other hand on their helicities before and after the interaction. The dependence on the helicities occur during the calculation of these functions $E(x,\vec{k}_\perp;\lambda_1,\lambda_2|x',\vec{k}'_\perp;\lambda'_1,\lambda'_2)$ in part I and $G(x,k_\perp;\lambda_1,\lambda_2|x',k'_\perp;\lambda'_1,\lambda'_2)$ in part II as different Kronecker deltas [45]. These functions are displayed in the form of helicity tables. We use the following notation for the elements of the tables

$$F_i(1,2) \;\rightarrow\; E_i(x,\vec{k}_\perp;x',\vec{k}'_\perp);\; G_i(x,k_\perp;x',k'_\perp) \qquad \text{(B.5)}$$

Also we have used in both cases for the permutation of particle and anti-particle

$$F_3^*(x,\vec{k}_\perp;x',\vec{k}'_\perp) = F_3(1-x,-\vec{k}_\perp;1-x',-\vec{k}'_\perp) \qquad \text{(B.6)}$$

one has the corresponding for the elements of arbitrary $J_z$; in the case when the function additionally depends on the component of the total angular momentum $J_z = n$ we have introduced

$$\tilde{F}_i(n) = F_i(-n) \qquad \text{(B.7)}$$

## B.1 The general helicity table.

To calculate the matrix elements of the effective interaction in the exchange channel we use the matrix elements of the Dirac spinors listed in Table B.1 [45]. Also the following holds $\bar{v}_{\lambda'}(p)\gamma^\alpha v_\lambda(q) = \bar{u}_\lambda(q)\gamma^\alpha u_{\lambda'}(p)$.

We introduce for the matrix elements entering in the effective interaction eq. (B.1)

$$
\begin{aligned}
2E^{(1)}(x,\vec{k}_\perp;\lambda_1,\lambda_2|x',\vec{k}'_\perp;\lambda'_1,\lambda'_2) &= <\gamma^\mu\gamma^\nu> g_{\mu\nu} = \\
&= \frac{1}{2}<\gamma^+\gamma^-> + \frac{1}{2}<\gamma^-\gamma^+> - <\gamma_1^2> - <\gamma_2^2> \\
2E^{(2)}(x,\vec{k}_\perp;\lambda_1,\lambda_2|x',\vec{k}'_\perp;\lambda'_1,\lambda'_2) &= <\gamma^\mu\gamma^\nu> \eta_\mu\eta_\nu\frac{1}{q^{+2}} = <\gamma^+\gamma^+> \frac{1}{q^{+2}} \qquad \text{(B.8)}
\end{aligned}
$$

where

$$<\gamma^\mu\gamma^\nu> = \frac{\bar{u}(x,\vec{k}_\perp;\lambda_1)\;\gamma^\mu\;u(x',\vec{k}'_\perp;\lambda'_1)\;\;\bar{v}(1-x',-\vec{k}'_\perp;\lambda'_2)\;\gamma^\nu\;v(1-x,-\vec{k}_\perp;\lambda_2)}{\sqrt{xx'(1-x)(1-x')}} \qquad \text{(B.9)}$$

| $\mathcal{M}$ | $\frac{1}{\sqrt{k^+k'^+}}\bar{u}(k',\lambda')\mathcal{M}u(k,\lambda)$ |
|---|---|
| $\gamma^+$ | $2\delta^{\lambda}_{\lambda'}$ |
| $\gamma^-$ | $\frac{2}{k^+k'^+}\left[\left(m^2+k_\perp k'_\perp e^{+i\lambda(\varphi-\varphi')}\right)\delta^{\lambda}_{\lambda'}-m\lambda\left(k'_\perp e^{+i\lambda\varphi'}-k_\perp e^{+i\lambda\varphi}\right)\delta^{\lambda}_{-\lambda'}\right]$ |
| $\gamma^1_\perp$ | $\left(\frac{k'_\perp}{k'^+}e^{-i\lambda\varphi'}+\frac{k_\perp}{k^+}e^{+i\lambda\varphi}\right)\delta^{\lambda}_{\lambda'}+m\lambda\left(\frac{1}{k'^+}-\frac{1}{k^+}\right)\delta^{\lambda}_{-\lambda'}$ |
| $\gamma^2_\perp$ | $i\lambda\left(\frac{k'_\perp}{k'^+}e^{-i\lambda\varphi'}-\frac{k_\perp}{k^+}e^{+i\lambda\varphi}\right)\delta^{\lambda}_{\lambda'}+im\left(\frac{1}{k'^+}-\frac{1}{k^+}\right)\delta^{\lambda}_{-\lambda'}$ |

Table B.1: Matrix elements of the Dirac spinors.

| **final : initial** | $(\lambda'_1,\lambda'_2)=\uparrow\uparrow$ | $(\lambda'_1,\lambda'_2)=\uparrow\downarrow$ | $(\lambda'_1,\lambda'_2)=\downarrow\uparrow$ | $(\lambda'_1,\lambda'_2)=\downarrow\downarrow$ |
|---|---|---|---|---|
| $(\lambda_1,\lambda_2)=\uparrow\uparrow$ | $E_1(1,2)$ | $E^*_3(1,2)$ | $E_3(1,2)$ | $0$ |
| $(\lambda_1,\lambda_2)=\uparrow\downarrow$ | $E^*_3(2,1)$ | $E_2(1,2)$ | $E_4(1,2)$ | $-E_3(2,1)$ |
| $(\lambda_1,\lambda_2)=\downarrow\uparrow$ | $E_3(2,1)$ | $E_4(1,2)$ | $E_2(1,2)$ | $-E^*_3(2,1)$ |
| $(\lambda_1,\lambda_2)=\downarrow\downarrow$ | $0$ | $-E_3(1,2)$ | $-E^*_3(1,2)$ | $E_1(1,2)$ |

Table B.2: General helicity table defining the effective interaction in the exchange channel.

These functions are displayed in the Table B.2.

The matrix elements $E^{(n)}_i(1,2)=E^{(n)}_i(x,\vec{k}_\perp;x',\vec{k}'_\perp)$ $(n=1,2)$ are the following

$$
\begin{aligned}
E^{(1)}_1(x,\vec{k}_\perp;x',\vec{k}'_\perp) &= m^2\left(\frac{1}{xx'}+\frac{1}{(1-x)(1-x')}\right)+\frac{k_\perp k^{'}_\perp}{xx'(1-x)(1-x')}\mathrm{e}^{-i(\varphi-\varphi^{'})}\\
E^{(1)}_2(x,\vec{k}_\perp;x',\vec{k}'_\perp) &= m^2\left(\frac{1}{xx'}+\frac{1}{(1-x)(1-x')}\right)+k^2_\perp\frac{1}{x(1-x)}+k^{'2}_\perp\frac{1}{x'(1-x')}\\
&+ k_\perp k^{'}_\perp\left(\frac{\mathrm{e}^{i(\varphi-\varphi^{'})}}{xx'}+\frac{\mathrm{e}^{-i(\varphi-\varphi^{'})}}{(1-x)(1-x')}\right)\\
E^{(1)}_3(x,\vec{k}_\perp;x',\vec{k}'_\perp) &= -\frac{m}{xx'}\left(k^{'}_\perp\mathrm{e}^{i\varphi^{'}}-k_\perp\frac{1-x'}{1-x}\mathrm{e}^{i\varphi}\right)\\
E^{(1)}_4(x,\vec{k}_\perp;x',\vec{k}'_\perp) &= -m^2\frac{(x-x')^2}{xx'(1-x)(1-x')}
\end{aligned}
\qquad\text{(B.10)}
$$

and

$$
\begin{aligned}
&E_1^{(2)}(x,\vec{k}_\perp;x',\vec{k}'_\perp) = E_2^{(2)}(x,\vec{k}_\perp;x',\vec{k}'_\perp) = \frac{2}{(x-x')^2} \\
&E_3^{(2)}(x,\vec{k}_\perp;x',\vec{k}'_\perp) = E_4^{(2)}(x,\vec{k}_\perp;x',\vec{k}'_\perp) = 0
\end{aligned}
\tag{B.11}
$$

## B.2 The helicity table for arbitrary $J_z$.

Following the description given in the main text eq. (6.6) we integrate out the angles in the effective interaction in the exchange channel eqs. (6.61) and (B.1). For the matrix elements of the effective interaction for an arbitrary $J_z = n$ with $n \in \mathbf{Z}$ $\quad G(x,k_\perp;\lambda_1,\lambda_2|x',k'_\perp;\lambda'_1,\lambda'_2) =< x,k_\perp;J_z,\lambda_1,\lambda_2|\tilde{V}_{LC}^{eff}|x',k'_\perp;J'_z,\lambda'_1,\lambda'_2 >|_{exch}$ in the exchange channel one obtains the helicity Table B.3.

| **final : initial** | $(\lambda'_1,\lambda'_2)=\uparrow\uparrow$ | $(\lambda'_1,\lambda'_2)=\uparrow\downarrow$ | $(\lambda'_1,\lambda'_2)=\downarrow\uparrow$ | $(\lambda'_1,\lambda'_2)=\downarrow\downarrow$ |
|---|---|---|---|---|
| $(\lambda_1,\lambda_2)=\uparrow\uparrow$ | $G_1(1,2)$ | $G_3^*(1,2)$ | $G_3(1,2)$ | $0$ |
| $(\lambda_1,\lambda_2)=\uparrow\downarrow$ | $G_3^*(2,1)$ | $G_2(1,2)$ | $G_4(1,2)$ | $-\tilde{G}_3(2,1)$ |
| $(\lambda_1,\lambda_2)=\downarrow\uparrow$ | $G_3(2,1)$ | $G_4(1,2)$ | $\tilde{G}_2(1,2)$ | $-\tilde{G}_3^*(2,1)$ |
| $(\lambda_1,\lambda_2)=\downarrow\downarrow$ | $0$ | $-\tilde{G}_3(1,2)$ | $-\tilde{G}_3^*(1,2)$ | $\tilde{G}_1(1,2)$ |

Table B.3: Helicity table of the effective interaction for $J_z = \pm n$, $x > x'$.

Here, the functions $G_i(1,2) = G_i(x,k_\perp;x',k'_\perp)$ are given

$$
\begin{aligned}
G_1(x,k_\perp;x',k'_\perp) &= m^2\left(\frac{1}{xx'}+\frac{1}{(1-x)(1-x')}\right)Int_{a_1a_2}(|1-n|) \\
&+ \frac{k_\perp k'_\perp}{xx'(1-x)(1-x')}Int_{a_1a_2}(|n|) + \frac{|a_1-a_2|}{(x-x')^2}Int_{a_1a_2}(|1-n|) \\
G_2(x,k_\perp;x',k'_\perp) &= (m^2\left(\frac{1}{xx'}+\frac{1}{(1-x)(1-x')}\right) + k_\perp^2\frac{1}{x(1-x)} + k_\perp'^2\frac{1}{x'(1-x')})Int_{a_1a_2}(|n|) \\
&+ k_\perp k'_\perp\left(\frac{1}{xx'}Int_{a_1a_2}(|1-n|) + \frac{1}{(1-x)(1-x')}Int_{a_1a_2}(|1+n|)\right) \\
&+ \frac{|a_1-a_2|}{(x-x')^2}Int_{a_1a_2}(|n|) \\
G_3(x,k_\perp;x',k'_\perp) &= -\frac{m}{xx'}\left(k'_\perp Int_{a_1a_2}(|1+n|) - k_\perp\frac{1-x'}{1-x}Int_{a_1a_2}(|n|)\right) \\
G_4(x,k_\perp;x',k'_\perp) &= -m^2\frac{(x-x')^2}{xx'(1-x)(1-x')}Int_{a_1a_2}(|n|)
\end{aligned}
\tag{B.12}
$$

where we have introduced the functions

$$
\begin{aligned}
&Int_{a_1a_2}(n) = \theta(a_1-a_2)Int_{a_1}(n) + \theta(a_2-a_1)Int_{a_2}(n) \\
&Int_{a_i}(n) = \frac{\alpha}{\pi}(-A(a_i))^{-n+1}\left(\frac{B(a_i)}{k_\perp k'_\perp}\right)^n
\end{aligned}
$$

$$
\begin{aligned}
A(a_i) &= \frac{1}{\sqrt{a_i^2 - 4k_\perp^2 k_\perp'^2}} \\
B(a_i) &= \frac{1}{2}(1 - a_i A(a_i))
\end{aligned}
\tag{B.13}
$$

and the functions $a_i$, $i = 1, 2$ are given in eq. (B.4).

The following integrals were used by the calculation of the matrix elements [30]

$$
\begin{aligned}
\frac{1}{2\pi}\int_0^{2\pi} d\varphi \int_0^{2\pi} d\varphi' \frac{\cos(n(\varphi - \varphi'))}{a_i - 2k_\perp k_\perp' \cos(\varphi - \varphi')} &= 2\pi(-A(a_i))^{-n+1}\left(\frac{B(a_i)}{k_\perp k_\perp'}\right)^n \\
\frac{1}{2\pi}\int_0^{2\pi} d\varphi \int_0^{2\pi} d\varphi' \frac{\sin(n(\varphi - \varphi'))}{a_i - 2k_\perp k_\perp' \cos(\varphi - \varphi')} &= 0
\end{aligned}
\tag{B.14}
$$

The condition on the parameter space $(x, k_\perp)$ due to the $\theta$-function, namely $\theta(a_1 - a_2)$ (i.e. when $a_1 > a_2$) reads

$$
(x - x')\left(x(1-x)(k_\perp'^2 + m^2) - x'(1-x')(k_\perp^2 + m^2)\right) > 0 \tag{B.15}
$$

Making use of the coordinate change eq. (6.7) this is equivalent to

$$
\left(\frac{\mu\cos\theta}{\sqrt{\mu^2 + m^2}} - \frac{\mu'\cos\theta'}{\sqrt{\mu'^2 + m^2}}\right)(\mu - \mu') < 0 \tag{B.16}
$$

# Appendix C

# Fermion and photon self energy terms

We calculate here the fermion and photon self energy terms, arising from the second order commutator $[\eta^{(1)}, H_{ee\gamma}]$.

**I.** We first derive the **electron self energy** terms. Making use of the expressions for the generator of the unitary transformation $\eta^{(1)}$ defined in eq. (4.18) and of $H_{ee\gamma}$, eq. (3.27), we obtain the following expression for the commutator in the electron self energy sector

$$\begin{aligned}\frac{1}{2}(\eta_{p_1p_2}g_{p_2p_1}-\eta_{p_2p_1}g_{p_1p_2})\Big[&\theta(p_1^+)\frac{\theta(p_2^+-p_1^+)}{p_2^+-p_1^+}\theta(p_2^+)\,b_{p_2}^+b_{p_2}\chi_{s_2}^+\chi_{s_2} \\ &-\theta(p_2^+)\frac{\theta(p_1^+-p_2^+)}{p_1^+-p_2^+}\theta(p_1^+)\,b_{p_1}^+b_{p_1}\chi_{s_1}^+\chi_{s_1}\Big]M_{2ij}(p_1,p_2)\delta^{ij}\ ,\end{aligned} \tag{C.1}$$

where

$$M_{2ij}(p_1,p_2)=\Gamma^i(p_1,p_2,p_1-p_2)\Gamma^j(p_2,p_1,p_2-p_1) \tag{C.2}$$

and the momentum integration over $p_1, p_2$ is implied; 1/2 stands as the symmetry factor. The matrix element of the commutator between the free fermion states is

$$\begin{aligned}&< p_1,s_1|[\eta^{(1)},H_{ee\gamma}]|p_1,s_1>_{selfenergy} \\ &\qquad = -\int_{p_2}(\eta_{p_1p_2}g_{p_2p_1}-\eta_{p_2p_1}g_{p_1p_2})\,\theta(p_2^+)\frac{\theta(p_1^+-p_2^+)}{p_1^+-p_2^+}\,M_{2ii}(p_1,p_2)\ ,\end{aligned} \tag{C.3}$$

where the integration $\int_p$ is defined in eq. (3.32). We use the expression for the generator $\eta$ through the coupling, namely

$$\eta_{p_1p_2}g_{p_2p_1}-\eta_{p_2p_1}g_{p_1p_2}=\frac{1}{\Delta_{p_1p_2}}\left(g_{p_1p_2}\frac{dg_{p_2p_1}}{dl}+g_{p_2p_1}\frac{dg_{p_1p_2}}{dl}\right)\ . \tag{C.4}$$

Change of the variables according to

$$\begin{aligned}p_1 &= p \\ p_2 &= p_k \\ p_1-p_2 &= k\end{aligned} \tag{C.5}$$

brings the integral in eq. (C.3) to the standard form of loop integration

$$-\int_k(\eta_{p,p-k}g_{p-k,p}-\eta_{p-k,p}g_{p,p-k})\,\theta(p^+-k^+)\frac{\theta(k^+)}{k^+}\,M_{2ii}(p,p-k)\ . \tag{C.6}$$

According to eq. (7.9), the integral $\int_{l_\lambda}^{l_\Lambda}$ of the commutator $[\eta^{(1)}, H_{ee\gamma}]$ defines the difference between the energies (or energy corrections) $\delta p_{1\lambda}^- - \delta p_{1\Lambda}^-$. Making use of

$$\int_{l_\Lambda}^{l_\lambda} dl' (\eta_{p_1 p_2} g_{p_2 p_1} - \eta_{p_2 p_1} g_{p_1 p_2}) = \frac{1}{p_1^- - p_2^- - (p_1 - p_2)^-} (g_{p_1,p_2,\Lambda} g_{p_2,p_1,\lambda} - g_{p_1,p_2,\lambda} g_{p_2,p_1,\Lambda}) \tag{C.7}$$

we have the following explicit expression:

$$\begin{aligned} \delta p_{1\lambda}^- - \delta p_{1\Lambda}^- = e^2 \int \frac{d^2k^\perp dk^+}{2(2\pi)^3} \frac{\theta(k^+)}{k^+} \theta(p^+ - k^+) \frac{(-1)}{p^- - k^- - (p-k)^-} \\ \times \Gamma^i(p-k, p, -k) \Gamma^i(p, p-k, k) \left[ \exp\left\{ -2 \left( \frac{\Delta_{p,p-k}}{\lambda} \right)^2 \right\} - \exp\left\{ -2 \left( \frac{\Delta_{p,p-k}}{\Lambda} \right)^2 \right\} \right] , \end{aligned} \tag{C.8}$$

where the solution for the $ee\gamma$-coupling constant was used. Therefore the electron energy correction corresponding to the first diagram, fig.(8), is

$$\begin{aligned} \delta p_{1\lambda}^- &= e^2 \int \frac{d^2k^\perp dk^+}{2(2\pi)^3} \frac{\theta(k^+)}{k^+} \theta(p^+ - k^+) \\ &\quad \times \Gamma^i(p-k, p, -k) \Gamma^i(p, p-k, k) \frac{1}{p^- - k^- - (p-k)^-} \times (-R) , \end{aligned} \tag{C.9}$$

where we have introduced the regulator $R$, defining the cutoff condition (see main text),

$$R = \exp\left\{ -2 \left( \frac{\Delta_{p,k}}{\lambda} \right)^2 \right\} \tag{C.10}$$

(note that $\Delta_{p,k} = \Delta_{p,p-k}$). To perform the integration over $k = (k^+, k^\perp)$ explicitly, choose the parametrization

$$\begin{aligned} \frac{k^+}{p^+} &= x \\ k &= (xp^+, xp^\perp + \kappa^\perp) , \end{aligned} \tag{C.11}$$

where $p = (p^+, p^\perp)$ is the external electron momentum. Then the terms occuring in $\delta p_{1\lambda}^-$ are rewritten in the form

$$\begin{aligned} \Gamma^i(p-k, p, -k) \Gamma^i(p, p-k, k) &= \tfrac{1}{(p^+)^2 (1-x)^2} \left( \left( 4\tfrac{1}{x^2} - 4\tfrac{1}{x} + 2 \right) \kappa_\perp^2 + 2m^2 x^2 \right) \\ \Delta_{p,p-k} = p^- - k^- - (p-k)^- &= \tfrac{1}{p^+ x(1-x)} (x(1-x)p^2 - \kappa_\perp^2 - xm^2) = \tfrac{\tilde{\Delta}_{p,p-k}}{p^+} \quad . \end{aligned} \tag{C.12}$$

Therefore the integral for the electron energy correction corresponding to the first diagram of fig.(8) takes the form

$$\begin{aligned} p^+ \delta p_{1\lambda}^- &= -\frac{e^2}{8\pi^2} \int_0^1 dx \int d\kappa_\perp^2 \frac{(\frac{2}{x^2} - \frac{2}{x} + 1)\kappa_\perp^2 + m^2 x^2}{(1-x)(\kappa_\perp^2 + f(x))} \times (-R) \\ &= -\frac{e^2}{8\pi^2} \int_0^1 dx \int d\kappa_\perp^2 \\ &\quad \times \left[ \frac{p^2 - m^2}{\kappa_\perp^2 + f(x)} \left( \frac{2}{[x]} - 2 + x \right) - \frac{2m^2}{\kappa_\perp^2 + f(x)} + \left( \frac{2}{[x]^2} + \frac{1}{[1-x]} \right) \right] \times (-R) , \end{aligned} \tag{C.13}$$

where

$$f(x) = xm^2 - x(1-x)p^2 . \tag{C.14}$$

In the last integral the principal value prescription for $\frac{1}{[x]}$ as $x \to 0$ was introduced (see main text), to regularize the IR divergencies present in the longitudinal direction.

We thus have derived the expression for the energy correction which has been used in the main text.

**II.** We repeat the same procedure for the **photon self energy**. The second order commutator $[\eta^{(1)}, H_{ee\gamma}]$ gives the following expression in the photon self energy sector

$$\begin{aligned}\frac{1}{2}(\eta_{p_1p_2}g_{p_2p_1}-\eta_{p_2p_1}g_{p_1p_2})\cdot\Big[&\theta(p_1^+)\theta(-p_2^+)\frac{\theta(p_1^+-p_2^+)}{(p_1^+-p_2^+)}\,a_{-q}^+a_{-q}\varepsilon_\lambda^{i*}\varepsilon_\lambda^j \\ &-\theta(-p_1^+)\theta(p_2^+)\frac{\theta(p_2^+-p_1^+)}{(p_2^+-p_1^+)}\,a_q^+a_q\varepsilon_\lambda^i\varepsilon_\lambda^{j*}\Big]\cdot TrM_{2ij}(p_1,p_2)\,\delta_{q,-(p_1-p_2)}\;,\end{aligned} \tag{C.15}$$

where $M_{2ij}(p_1, p_2)$ is defined in eq. (C.2) and the trace acts in spin space; the integration over the momenta $q$, $p_1$ and $p_2$ is implied. The matrix element between the free photon states reads

$$\begin{aligned}&< q,\lambda|[\eta^{(1)},H_{ee\gamma}]|q,\lambda>_{selfenergy}\,\delta_{ij} \\ &\qquad= -\frac{1}{q^+}\int_{p_1,p_2}(\eta_{p_1p_2}g_{p_2p_1}-\eta p_2p_1g_{p_1p_2})\,\theta(-p_1^+)\theta(p_2^+)\,TrM_{2ij}(p_1,p_2)\,\delta_{q,-(p_1-p_2)}\;,\end{aligned} \tag{C.16}$$

that can be rewritten after the change of coordinates according to

$$\begin{aligned}p_1 &= -k \\ p_2 &= -(k-q) \\ p_2-p_1 &= q\end{aligned} \tag{C.17}$$

in the following way

$$\frac{1}{q^+}\int_k(\eta_{k,k-q}g_{k-q,k}-\eta_{k-q,k}g_{k,k-q})\,\theta(k^+)\theta(q^+-k^+)\,TrM_{2ij}(k,k-q)\;, \tag{C.18}$$

where the symmetry

$$\begin{aligned}\eta_{-p_1,-p_2} &= -\eta_{p_1,p_2} \\ g_{-p_1,-p_2} &= g_{p_1,p_2}\end{aligned} \tag{C.19}$$

has been used. The integration of the commutator over $l$ in the flow equation gives rise to

$$\begin{aligned}(\delta q_{1\lambda}^- - \delta q_{1\Lambda}^-)\delta^{ij} = \frac{1}{q^+}e^2\int&\frac{d^2k^\perp dk^+}{2(2\pi)^3}\theta(k^+)\theta(q^+-k^+)\,\frac{(-1)}{q^- - k^- - (q-k)^-} \\ \times Tr\left(\Gamma^i(k,k-q,q)\Gamma^j(k-q,k,-q)\right)&\left[\exp\left\{-2\left(\frac{\Delta_{q,q-k}}{\lambda}\right)^2\right\}-\exp\left\{-2\left(\frac{\Delta_{q,q-k}}{\Lambda}\right)^2\right\}\right].\end{aligned} \tag{C.20}$$

This means for the photon energy correction

$$\begin{aligned}\delta q_{1\lambda}^-\delta^{ij} &= \frac{1}{q^+}e^2\int\frac{d^2k^\perp dk^+}{2(2\pi)^3}\theta(k^+)\theta(q^+-k^+) \\ &\quad\times Tr\left(\Gamma^i(k,k-q,q)\Gamma^j(k-q,k,-q)\right)\frac{1}{q^- - k^- - (q-k)^-}\times(-R)\;,\end{aligned} \tag{C.21}$$

where the regulator $R$

$$R = \exp\left\{-2\left(\frac{\Delta_{q,k}}{\lambda}\right)^2\right\} \tag{C.22}$$

has been introduced. Define the new set of coordinates

$$\begin{aligned}\frac{(q-k)^+}{q^+} &= x \\ k &= ((1-x)q^+,(1-x)q^\perp+\kappa^\perp) \\ q-k &= (xq^+,xq^\perp-\kappa^\perp)\;,\end{aligned} \tag{C.23}$$

where $q = (q^+, q^\perp)$ is the photon momentum. Then the terms present in $\delta q^-_{1\lambda}$ are

$$\begin{aligned} \Gamma^i(k, k-q, q)\Gamma^i(k-q, k, -q) &= \tfrac{2}{(q^+)^2 x(1-x)^2} \left( \left( 2x - 2 + \tfrac{1}{x} \right) \kappa^{\perp 2} + \tfrac{m^2}{x} \right) \\ \Delta_{k-q,k} = q^- - k^- - (q-k)^- &= -\tfrac{\kappa^{\perp 2} + m^2}{q^+ x(1-x)} + \tfrac{q^2}{q^+} = \tfrac{\tilde{\Delta}_{k-q,k}}{q^+} \qquad . \end{aligned} \tag{C.24}$$

The integral for the photon energy correction corresponding to the first diagram of fig.(9) takes the form

$$\begin{aligned} q^+ \delta q^-_{1\lambda} &= -\frac{e^2}{8\pi^2} \int_0^1 dx \int d\kappa_\perp^2 \frac{(2x - 2 + \frac{1}{x})\kappa_\perp^2 + \frac{m^2}{x}}{(1-x)(\kappa_\perp^2 + f(x))} \times (-R) \\ &= -\frac{e^2}{8\pi^2} \int_0^1 dx \int d\kappa_\perp^2 \left\{ \frac{q^2}{\kappa_\perp^2 + f(x)} \left( 2x^2 - 2x + 1 \right) + \frac{2m^2}{[1-x]} + \left( -2 + \frac{1}{[x][1-x]} \right) \right\} \times (-R) \end{aligned} \tag{C.25}$$

with

$$f(x) = m^2 - q^2 x(1-x) \ , \tag{C.26}$$

and the principal value prescription, denoted by '[ ]', introduced to regularize the IR divergencies.

This is the form of the photon correction used in the main text.

# Bibliography

[1] See “Sources for Light-Front Physics,” available via anonymous ftp from ftp.physics.ohio-state.edu in the subdirectory pub/infolight in file light.tex.

[2] F. Wegner, Ann.Physik **3**,77 (1994).

[3] S. D. Glazek and K. G. Wilson, Phys. Rev. **D 48**, 5863 (1993);S. D. Glazek and K. G. Wilson, Phys.Rev. **D 49**, 4214 (1994).

[4] K. G. Wilson, T. S. Walhout, A. Harindranath, W.-M. Zhang, R. J. Perry, S. D. Glazek, Phys. Rev. **D 49**, 6720 (1994), hep-th/9401153.

[5] A. Mielke, Lectures ’Flüßgleichungen für Hamiltonoperatoren’, held at the Insitut für theoretische Physik der Universität Heidelberg.

[6] S. K. Kehrein, A. Mielke, con-mat/9701123; S. K. Kehrein, A. Mielke, cond-mat/9607160, to appear in Ann. Physik (Leipzig), 1996; S. K. Kehrein, A. Mielke, cond-mat/9602022; S. K. Kehrein, A. Mielke, P. Neu, HD-TVP-94-25; A. Mielke, quant-ph/9803040.

[7] H. J. Pirner, B. Friman, ’Hamiltonian Flow Equations for the Lipkin Model’, preprint 1998; A. Mielke, quant-ph/9803040.

[8] S. K. Kehrein, A. Mielke, cond-mat/9510145, HD-TVP-95-14; S. K. Kehrein, A. Mielke, cond-mat/9405034.

[9] A. B. Bylev, H. J. Pirner, hep-th/9712203.

[10] P. Lenz, F. Wegner Nucl.Phys. **B482**, 693 (1996), cond-mat/9604087; A. Mielke, cond-mat/9709175, to appear in Europhys.Lett.; A. Mielke, Ann. Phys. **6**, 215 (1997), cond-mat/9609065, TVP-HD-96-9.

[11] P. A. M. Dirac, Rev. Mod. Phys. **21**, 392 (1949).

[12] J. B. Kogut and D. E. Soper, Phys. Rev. **D1** (1970), 2901.

[13] S. J. Chang, R. G. Root, T. M. Yan, Phys. Rev. D7 (1973), 1133; *ibid.* 1147; *ibid.* 1760.

[14] N. E. Ligterink, “Light-front Hamiltonian field theory: covariance and renormalization”, Dissertation, University Amsterdam, 1996; N. E. Ligterink and B. L. G. Bakker, Phys. Rev. **D52** (1995), 5954; S. A. Paston and V. A. Franke, Theoretical and Mathematical Physics, Vol. 112, No.3 (1997), 399.

[15] K. Hornbostel, in “From Fundamental Fields to Nuclear Phenomena”, Eds. J. A. McNeil and C. E. Price, (World Scientific, Singapore, 1991).

[16] K. G. Wilson et al., Phys. Rev. D **49**, 6720 (1994).

[17] K. G. Wilson and M. Brisudova, in *Theory of Hadrons and Light-Front QCD*, Proceedings, Zakopane, 1994, hep-th/9411008.

[18] K. G. Wilson and D. Robertson, in *Theory of Hadrons and Light-Front QCD*, Proceedings, Zakopane, 1994, hep-th/9411007.

[19] S. J. Brodsky and D. G. Robertson, talk presented at the ELFE meeting on Confinement Physics, Cambridge, Eng., July 1995, hep-ph/9511374.

[20] K. G. Wilson, T. S. Walhout, A. Harindranath, W. M. Zhang, R. J. Perry and S. D. Głazek, Phys. Rev. D **49**, 6720 (1994), hep-th/9401153; M. M. Brisudová and R. J. Perry, Phys. Rev. D **54**, 1831 (1996); M. M. Brisudová, R. J. Perry and K. G. Wilson, Phys. Rev. Lett. **78**, 1227 (1997).

[21] A. Bassetto, G. Nardelli and R. Soldati, *Yang-Mills Theories in Algebraic Non-covariant Gauges* (World Scientific, Singapore, 1991); for a fairly complete list of DLCQ references see Reference [1] and S. J. Brodsky and H. C. Pauli, *Light-Cone Quantization and Quantum Chromodynamics*, Recent Aspects of Quantum Fields, H. Mitter and H. Gausterer, Eds., Lecture Notes in Physics, Vol. 396 (Springer-Verlag, Berlin, 1991); B. D. Keister and W. N. Polyzou, Adv. Nucl. Phys. **20**, 225 (1991); S. D. Głazek, Acta Phys. Polon. **B24**, 1315 (1993); R. J. Perry, [37].

[22] S. J. Brodsky, H. C. Pauli and S. S. Pinsky, *Quantum Chromodynamics and Other Field Theories on the Light Cone*, Submitted to Phys. Rept., hep-ph/9705477.

[23] W. M. Zhang, Chin. J. Phys. **32**, 717 (1994), [hep-ph/9412244]; A. Harindranath, *An Introduction to Light-Front Dynamics for Pedestrians*, hep-ph/9612244, [Lectures given at International School on Light-Front Quantization and Non-Perturbative QCD (To be followed by the Workshop 3-14 Jun 1996), Ames, IA, 6 May - 2 Jun 1996].

[24] W. M. Zhang and A. Harindranath, Phys.Rev. **D48**, 4868 (1993), hep-th/9302119; Phys.Rev. **D48** 4881 (1993); *ibid.* 4903.

[25] M. Burkardt, hep-ph/9705224; B. van de Sande and M. Burkardt, hep-th/9510104, MPI H-V38-1995.

[26] B. van de Sand and S. Dalley, hep-ph/9604268; B. van de Sand and S. Dalley, hep-ph/9602291.

[27] W. A. Bardeen and R. B. Pearson, Phys.Rev. **D14**, 547 (1976); W. A. Bardeen, R. B. Pearson, and E. Rabinovici, Phys.Rev. **D21**, 1037 (19980).

[28] H. C. Pauli, preprint MPI H-V26-1997, hep-ph/9707361; S. J. Brodsky, H. C. Pauli, and S. S. Pinsky, hep-ph/9705477 and references within.

[29] H. C. Pauli and S. J. Brodsy, Phys.Rev. **D32**, 1993 (1985); H. C. Pauli and S. J. Brodsy, Phys.Rev. **D32**, 2001 (1985).

[30] U.Trittmann and H. C. Pauli, hep-th/9705021; U.Trittmann and H. C. Pauli, hep-th/9704215 (Dissertation, Heidelberg 1997).

[31] H.C.Pauli, hep-th/9706053.

[32] A. C. Tang, S. J. Brodsky, and H. C. Pauli, Phys.Rev. **D44**, 1842 (1991); A. Tang, Dissertation, SLAC-Report-351, Juni 1990.

[33] I. Tamm, J.Phys. (USSR) **9**, 449 (1945); S. M. Dancoff, Phys.Rev **78**, 382 (1950); R. J. Perry, A. Harindranath and K. G. Wilson, Phys.Rev.Lett. **65**, 2959 (1990).

[34] M. Krautgärtner, H. C. Pauli, and F. Wölz, Phys.Rev. **D45**, 3755 (1992).

[35] M. Kaluza and H. C. Pauli, Phys.Rev. **D45**, 2968 (1992); M .Kaluza, Dissertation, Heidelberg 1991.

[36] M. Kaluza and H. J. Pirner, Phys.Rev. **D47**, 1620 (1993).

[37] R. J. Perry, in *Proceedings of Hadrons 94*, edited by V. Herscovitz and C. Vasconcellos (World Scientific, Singapore, 1995), hep-th/9407056.

[38] R. J. Perry, hep-ph/9604318.

[39] B. D. Jones, R. G. Perry and S. D. Glazek, Phys.Rev. **D 55**, 6561 (1997), hep-th/9605231; B. D. Jones and R. G. Perry hep-th/9703106.

[40] B. D. Jones and R. G. Perry, Phys.Rev. **D55**, 7715 (1997).

[41] F. Wölz, Dissertation (unpublished), Heidelberg 1995.

[42] M. Brisudova and R. Perry, Phys.Rev. **D 54**, 6453 (1996), hep-ph/9605363.

[43] A. C. Kalloniatis and D. G. Robertson, Phys.Rev. **D50**, 5262 (1994).

[44] R. J. Perry and K. G. Wilson, Nucl.Phys. **B403**, 587 (1993).

[45] G. P. Lepage and S. J. Brodsky, Phys. Rev. **D22** 2157 (1980).

[46] K. Harada and A. Okazaki, Phys.Rev. **D55**, 6198 (1997), KYUSHU-HET-35, hep-th/9610020.

[47] S. J. Brodsky, J. R. Hiller, G. McCartor, hep-th/9802120.

[48] A. S. Mueller, A. C. Kalloniatis, H.-C. Pauli, hep-th/9803204.

[49] M. Burkardt, Advances Nucl. Phys. **23** (1996), 1; nucl-th/9802049; hep-ph/9709421; S. J. Brodsky, hep-ph/9706236.

[50] the first reference from [20].

[51] J. Kogut and L. Susskind, Phys. Rep. **8**, 75–172 (1973).

[52] H. Fröhlich, Proc.Roy.Soc. **A215**, 291 (1952).

[53] E. L. Gubankova, F. Wegner, HD-TVP-97-09, hep-th/9702162.

[54] E. L. Gubankova, F. Wegner, HD-TVP-97-11, hep-th/9708054; Phys. Rev. **D58**, 025012, 1998, hep-th/9710233.

[55] E. L. Gubankova, hep-th/9801018.

Figure 1: Flow equations perform the block-diagonalization of the bare Hamiltonian of the canonical theory $H_B(\Lambda)$ into a Hamiltonian consisting of blocks with equal number of particles. For a finite value of $\lambda$ the matrix elements of the 'particle number changing' sectors are squeezed into an energy band with roughly $|E_i - E_j| < \lambda$ (left hand side picture) and are eliminated completely as $\lambda \to 0$ (right hand side picture).

Table 1: The effective light front QED Hamiltonian matrix up to second order in $e$ in the Fock space representation. The matrix elements of the 'diagonal' (Fock state conserving) sectors are unrestricted in the energy differences; the 'rest' (Fock state changing) sectors are squeezed roughly in an energy band of width $\lambda$. Black dots correspond to zero matrix elements in order $O(e^2)$. Instantaneous and disconnected diagrams are not included.

Figure 2: The matrix elements of the effective Hamitonian, obtained by the flow equations in the second order in coupling, with corresponding diagrams. The diagrams $2-5$ belong to the 'diagonal' sector; the $1, 6, 7$ correspond to the 'rest' sector (the $6, 7$ diagrams are drawn schematically, namely the corresponding momentum change must be performed to get the real 'rest' diagrams, depicted in Table 1.) The photon momenta are $x^+$-ordered, from left to right. The similarity function is chosen $f_{p_ip_f,\lambda}=\exp(-\Delta^2_{p_ip_f\lambda}/\lambda^2)$, where $\Delta_{p_ip_f\lambda}=\Sigma p_i^- - \Sigma p_f^-$ (the index '$i$' denotes initial and '$f$' final states) and $\Delta_{p_1p_2\lambda}=p_1^- - p_2^- - (p_1-p_2)^-$, $p^-=(p_\perp^2+m_\lambda^2)/p^+$.

Figure 3 : The effective electron-positron interaction in the exchange channel; the diagrams correspond to the generated and the instantaneous interactions.

Figure 4: Another choice of the coordinates in the effective electron-positron interaction, that are used in the light-front integral equation.

Figure 5: Positronium spectrum for $-3 \leq J_z \leq 3$, $\alpha = 0.3$ and $\Lambda = 1$. The annihilation channel is not included. For an easier identification of the spin-parity multiplets, the corresponding non-relativistic notation $L_J^{J_z}$ is inserted. Masses are given in units of the electron mass.

Figure 6: Stability of positronium spectrum for $J_z = 0$, without annihilation interaction. Eigenvalues $M_i^2$ for $\alpha = 0.3$ and $\Lambda = 1$ are plotted versus $N$, the number of Gaussian points. Masses are in units of the electron mass.

Figure 7: Deviation of corresponding eigenvalues for $J_z = 0$ and $J_z = 1$ ($\alpha = 0.3$ and $\Lambda = 1$) with growing number of integration points $N$. The graphs shown $\Delta M^2 = M_n^2(J_z = 0) - M_n^2(J_z = 1)$ for the states $1^3S_1$ (triagles), $2^3P_1$ (squares), and $2^1P_1$ (circles).

Figure 8: Electron self energy term includes the diagram arising from the commutator term $[\eta^{(1)}, H_{ee\gamma}]$ in the electron sector, and also two diagrams, the second and the third on the figure 5, coming from the normal ordering of instantaneous interactions $H_{ee\gamma\gamma}$ and $H_{eeee}$, resp.

Figure 9: Photon self energy term includes the diagram coming from the commutator $[\eta^{(1)}, H_{ee\gamma}]$ in the photon sector, and also the diagram from the normal ordering of the instantaneous interaction $H_{ee\gamma\gamma}$.

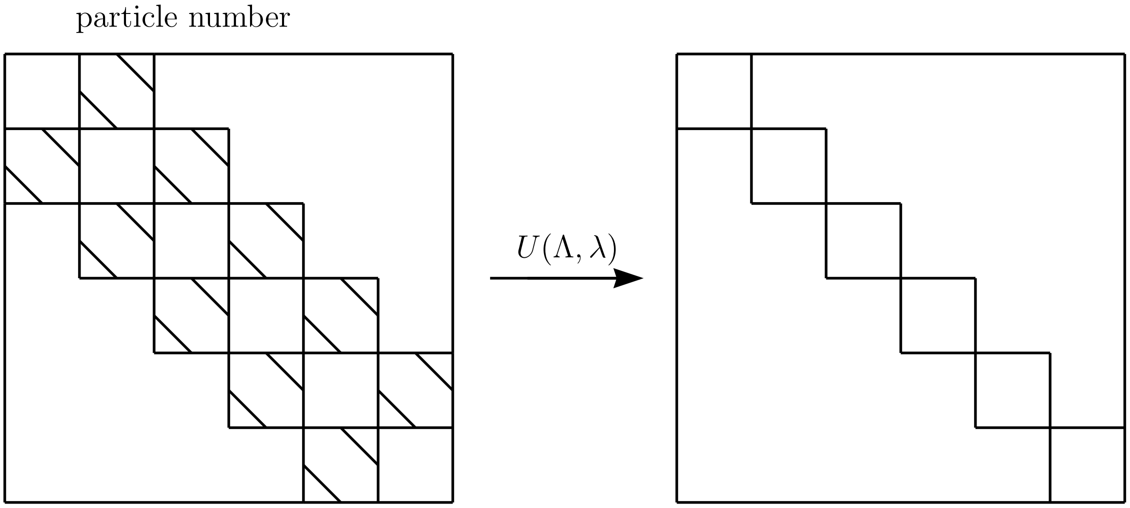

Figure 1

|  | $\|\gamma >$ | $\|e\bar{e} >$ | $\|\gamma\gamma >$ | $\|e\bar{e}\gamma >$ | $\|e\bar{e}e\bar{e} >$ |
|---|---|---|---|---|---|
| $\|\gamma >$ | 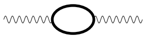 | 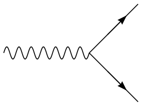 | ● | 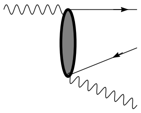 | ● |
| $\|e\bar{e} >$ | 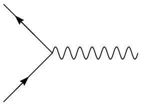 | 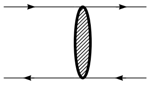 | 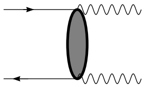 | 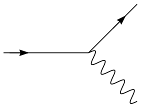 | 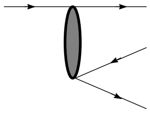 |
| $\|\gamma\gamma >$ | ● | 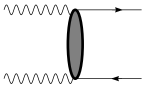 | ● | 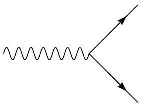 | ● |
| $\|e\bar{e}\gamma >$ | 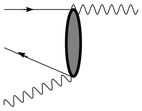 | 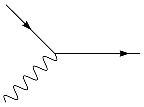 | 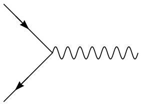 | 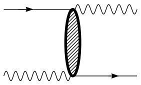 | 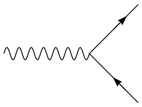 |
| $\|e\bar{e}e\bar{e} >$ | ● | 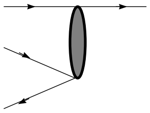 | ● | 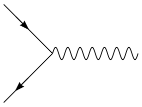 | 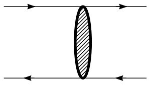 |

Table 1

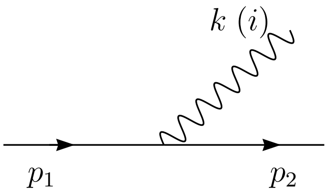

$$-e_\lambda \exp\left\{-\frac{\Delta^2_{p_1p_2}}{\lambda^2}\right\}\chi_2^+\Gamma^i_\lambda(p_1,p_2,k)\chi_1\varepsilon^{i*}$$

$$\Gamma^i_\lambda(p_1,p_2,k) = 2\frac{k^i}{[k^+]} - \frac{\sigma\cdot p_2^\perp - im_\lambda}{[p_2^+]}\sigma^i - \sigma^i\frac{\sigma\cdot p_1^\perp + im_\lambda}{[p_1^+]}$$

$$i = 1,2$$

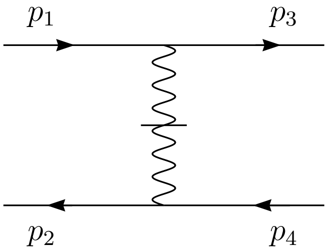

$$e_\lambda^2\ \chi_3^+\chi_{\bar 4}^+\frac{4}{[p_1^+-p_3^+]^2}\chi_1\chi_{\bar 2}$$

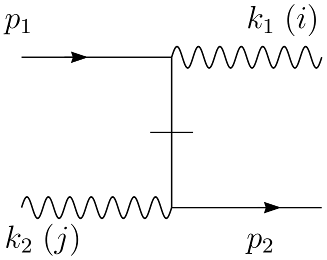

$$e_\lambda^2\chi_2^+\frac{\sigma^j\sigma^i}{[p_1^+-k_1^+]}\chi_1\varepsilon^{i*}\varepsilon^j$$

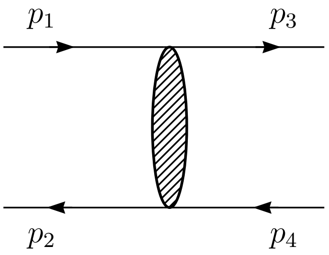

$$-e_\lambda^2 M_{2ij,\lambda}\,\delta^{ij}\frac{1}{[p_1^+-p_3^+]}$$
$$\times\left(\frac{\Delta_{p_1p_3\lambda}+\Delta_{p_4p_2\lambda}}{\Delta^2_{p_1p_3\lambda}+\Delta^2_{p_4p_2\lambda}}\right)\left(1-\exp\left\{-\frac{\Delta^2_{p_1p_3\lambda}+\Delta^2_{p_4p_2\lambda}}{\lambda^2}\right\}\right)$$

$$M_{2ij,\lambda} = \left(\chi_3^+\Gamma^i_\lambda(p_1,p_3,p_1-p_3)\chi_1\right)$$
$$\times\left(\chi_{\bar 2}^+\Gamma^j_\lambda(-p_4,-p_2,-(p_1-p_3))\chi_{\bar 4}\right)$$

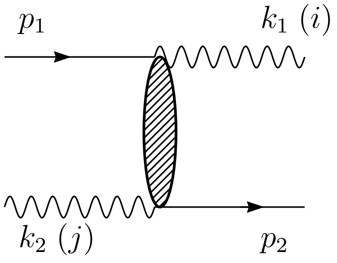

$$e_\lambda^2\widetilde{M}_{2ij,\lambda}\,\varepsilon^{i*}\varepsilon^j$$
$$\times\left(\frac{\Delta_{p_1k_1\lambda}+\Delta_{p_2k_2\lambda}}{\Delta^2_{p_1k_1\lambda}+\Delta^2_{p_2k_2\lambda}}\right)\left(1-\exp\left\{-\frac{\Delta^2_{p_1k_1\lambda}+\Delta^2_{p_2k_2\lambda}}{\lambda^2}\right\}\right)$$

$$\widetilde{M}_{2ij,\lambda} = \chi_2^+\Gamma^i_\lambda(p_1,p_1-k_1,k_1)\,\Gamma^j_\lambda(p_1-k_1,p_2,k_2)\chi_1$$

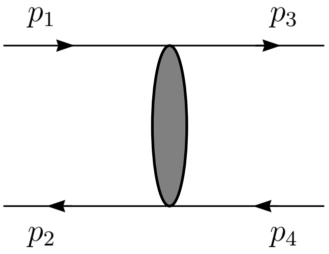

$$-e_\lambda^2 \exp\left\{-\frac{\Delta^2_{p_i p_f}}{\lambda^2}\right\} M_{2ij,\lambda}\,\delta^{ij}\frac{1}{[p_1^+ - p_3^+]}$$
$$\times\frac{1}{2}\left(\frac{1}{\Delta_{p_1p_3\lambda}}+\frac{1}{\Delta_{p_4p_2\lambda}}\right)\left(1-\exp\left\{-2\,\frac{\Delta_{p_1p_3\lambda}\cdot\Delta_{p_4p_2\lambda}}{\lambda^2}\right\}\right)$$
$$M_{2ij,\lambda} = \left(\chi_2^+\Gamma^i_\lambda(p_1,p_2,p_1-p_2)\chi_1\right)$$
$$\times\left(\chi_4^+\Gamma^j_\lambda(p_3,p_4,-(p_1-p_2))\chi_3\right)$$

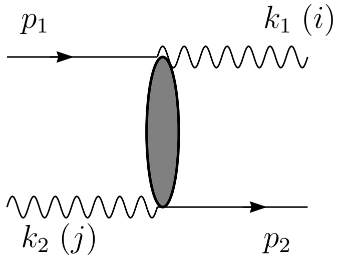

$$e_\lambda^2 \exp\left\{-\frac{\Delta^2_{p_i p_f}}{\lambda^2}\right\}\widetilde{M}_{2ij,\lambda}\,\varepsilon^{i*}\varepsilon^j$$
$$\times\frac{1}{2}\left(\frac{1}{\Delta_{p_1k_1\lambda}}+\frac{1}{\Delta_{p_2k_2\lambda}}\right)\left(1-\exp\left\{-2\,\frac{\Delta_{p_1k_1\lambda}\cdot\Delta_{p_2k_2\lambda}}{\lambda^2}\right\}\right)$$
$$\widetilde{M}_{2ij,\lambda} = \chi_2^+\Gamma^i_\lambda(p_1,p_1-k_1,k_1)\,\Gamma^j_\lambda(p_1-k_1,p_2,k_2)\chi_1$$

Figure 2

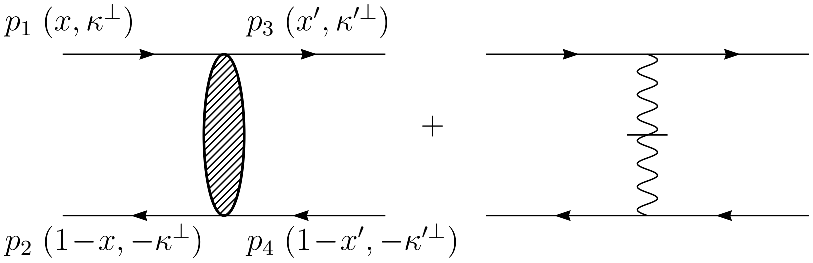
$p_1\ (x, \kappa^\perp)$
$p_3\ (x', \kappa'^\perp)$
$+$
$p_2\ (1-x, -\kappa^\perp)$
$p_4\ (1-x', -\kappa'^\perp)$

Figure 3

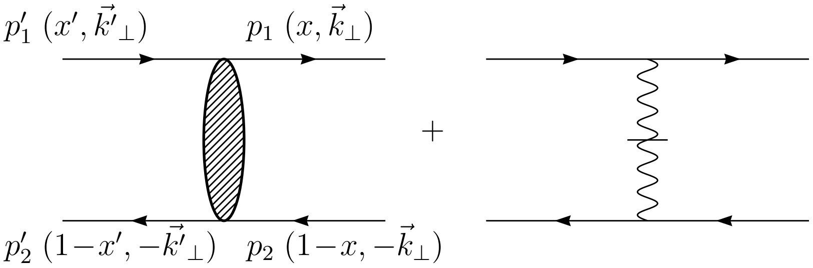
$p_1' \ (x', \vec{k'}_\perp)$
$p_1 \ (x, \vec{k}_\perp)$
$+$
$p_2' \ (1-x', -\vec{k'}_\perp)$
$p_2 \ (1-x, -\vec{k}_\perp)$

Figure 4

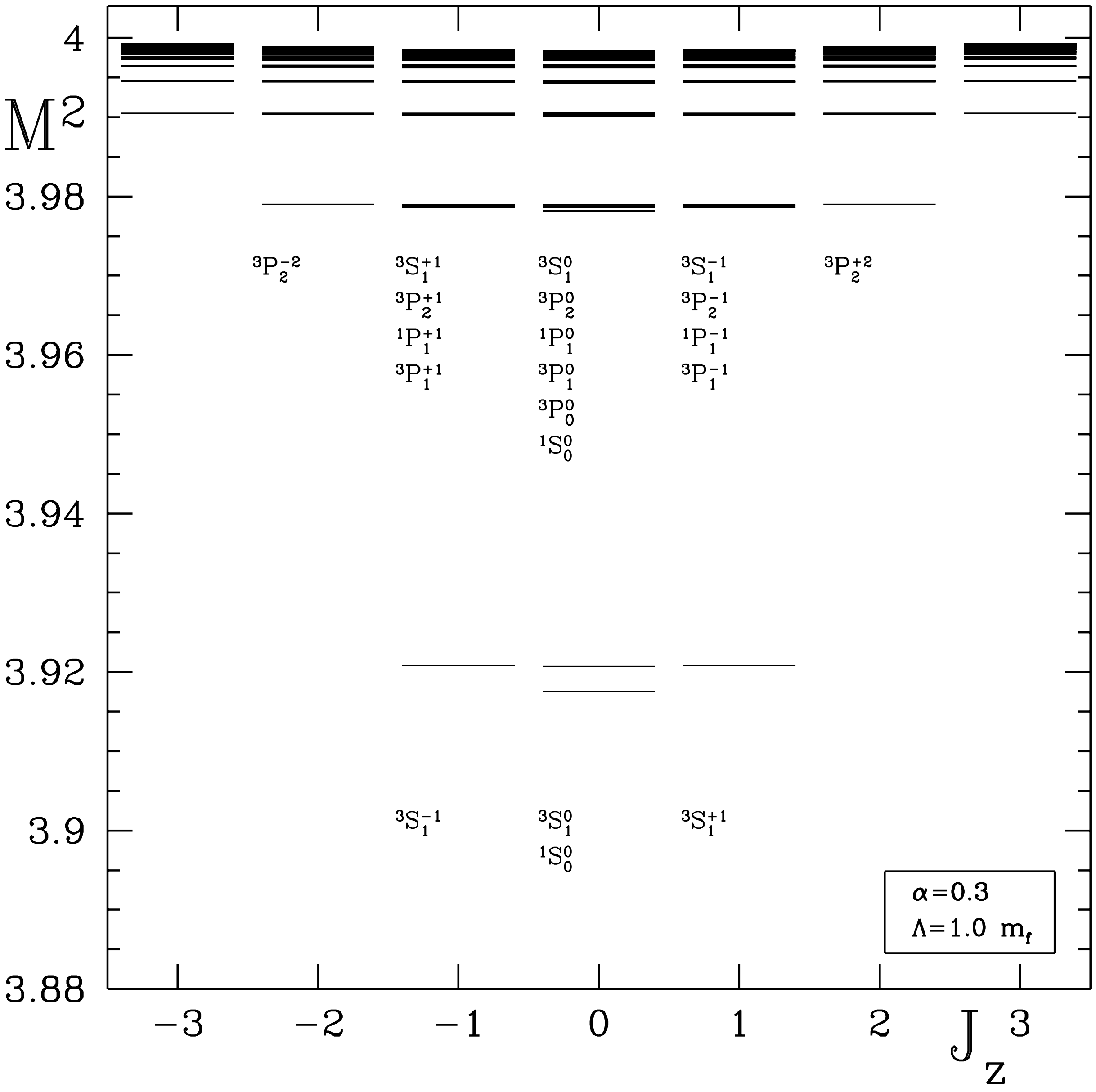
4
M²
3.98
3.96
3.94
3.92
3.9
3.88
−3
−2
−1
0
1
2
3
J_z
³P₂⁻²
³S₁⁺¹
³P₂⁺¹
¹P₁⁺¹
³P₁⁺¹
³S₁⁰
³P₂⁰
¹P₁⁰
³P₁⁰
³P₀⁰
¹S₀⁰
³S₁⁻¹
³P₂⁻¹
¹P₁⁻¹
³P₁⁻¹
³P₂⁺²
³S₁⁻¹
³S₁⁰
¹S₀⁰
³S₁⁺¹
α=0.3
Λ=1.0 m_f

Figure 5

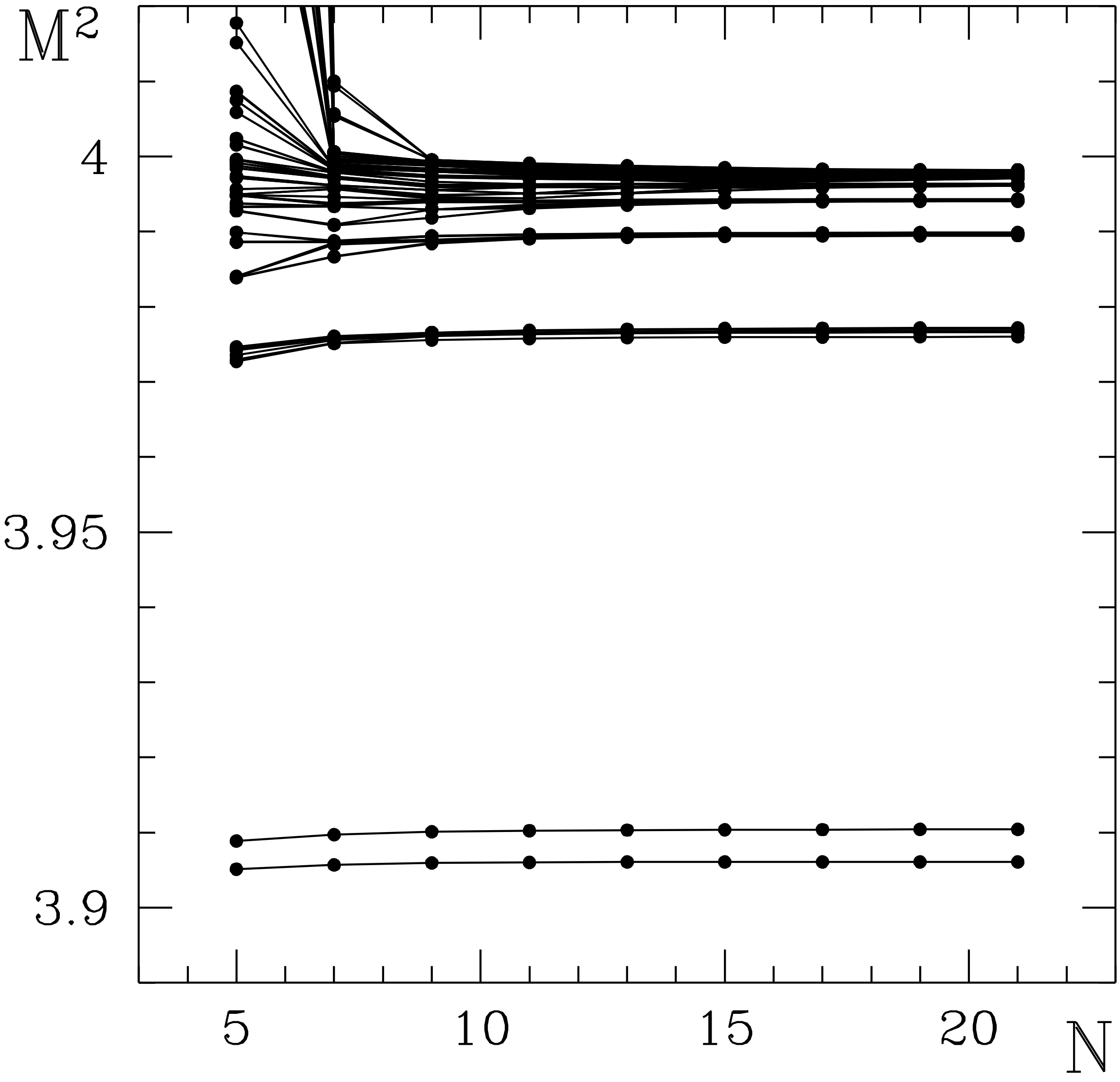

Figure 6

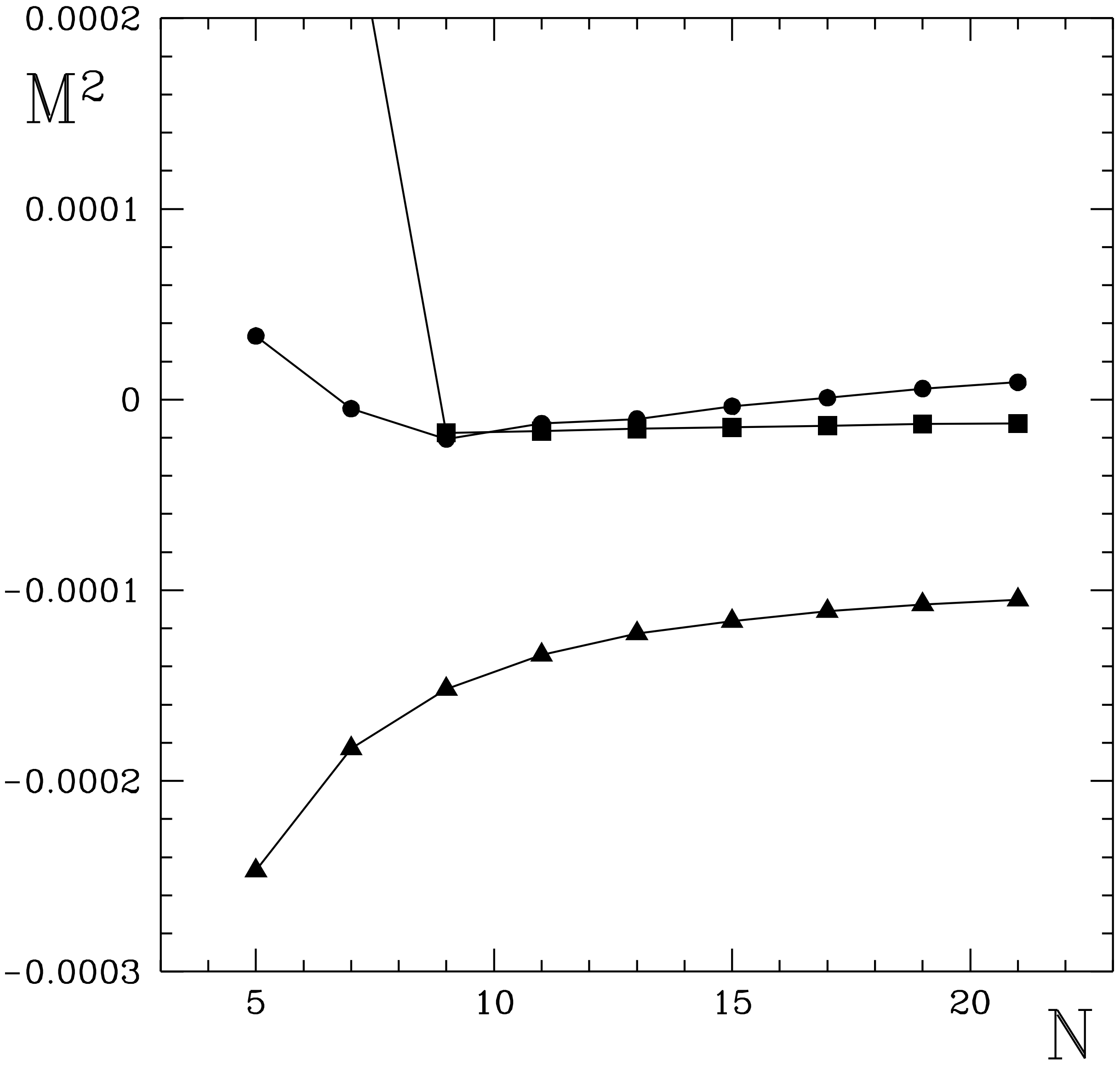

Figure 7

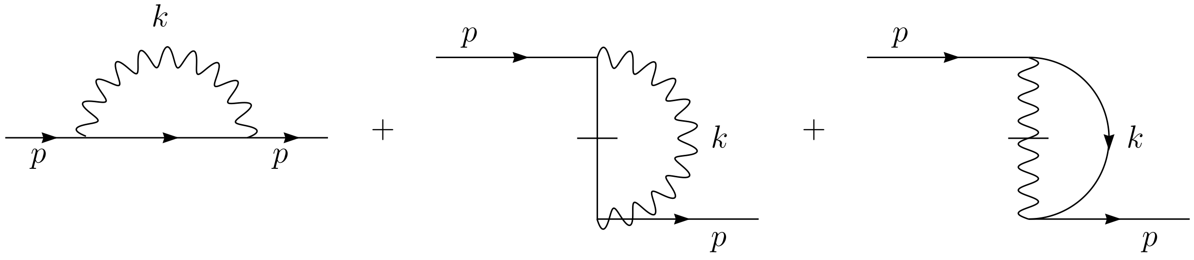

Figure 8

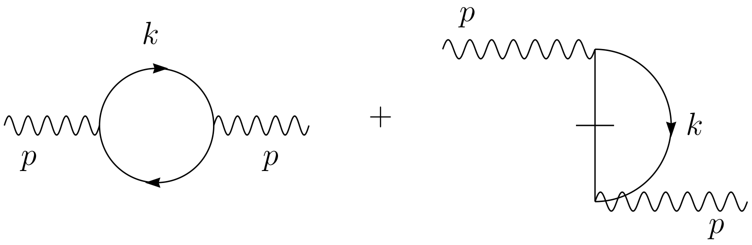

Figure 9

## Acknowledgments

I want to thank my adviser Prof. Franz Wegner for providing me the chance to work on this project under his guidance. I thank him for the guidance and for the help in the work, and also for his warm and considerate attitude to me during the whole time.

I extend warm thanks to Prof. H-C. Pauli for his constant interest in the work and many useful discussions that improved my understanding of the light-front physics. I thank him for his patience and help.

I thank Prof. H.G. Dosch and Prof. H.J. Pirner for the opportunity to perform my Ph.D. study in Heidelberg.

I would like to thank Prof. Yu.A. Simonov for his support and help.

A special thanks to Dr. Brett van de Sande and Dr. Koji Harada for introducing me many ideas.

I would like to thank Dr. Uwe Trittmann for a work in collaboration and for performing the numerical calculations.

I would like to thank Prof. Stan Glazek, Prof. Robert Perry, Prof. John Hiller and also Prof. Matthias Burkardt, Dr. Billy Jones, Dr. Martina Brisudova, Dr. Alex Kalloniatis, Dr. Thomas Heinzl for useful discussions.

I thank Dr. Andreas Mielke and Dr. Stephan Kehrein for the fruitful discussions on the method of flow equations.

I thank Dr. Andreas Metz and Dr. Hilmar Forkel for correction and improving the manuscript, and also Dr. Gabor Papp, Dr. Yong-Bin He and Dr. Umbert D'Alesio for the help with the computer.